



Development of a practical tool to determine the hull damping of modern ship hull forms

Bilel SAAD

Master Thesis

presented in partial fulfillment
of the requirements for the double degree:
"Advanced Master in Naval Architecture" conferred by University of Liege
"Master of Sciences in Applied Mechanics, specialization in Hydrodynamics, Energetic and Propulsion" conferred by Ecole Centrale de Nantes

developed at University of Rostock, Germany
in the framework of the

"EMSHIP"
Erasmus Mundus Master Course
in "Integrated Advanced Ship Design"

Ref. 159652-1-2009-1-BE-ERA MUNDUS-EMMC

Supervisor: Professor. Nikolai Kornev, University of Rostock, Germany
Dipl.Ing. Stefan Winkler, Hoppe Marine

Reviewer: Prof. Dario Boote, University of Genova, Italy

Rostock, February 2014



ABSTRACT

Predicting the roll damping is a crucial step prior to dimensioning the stabilization systems. Therefore, FLUME® Stabilization systems is using the results provided by seakeeping basin model tests in regular seas to determine the behavior of the ship in roll before the stab is designed.

Throughout the decades, FLUME® collected a considerable database that includes general cargo ships, containers, and ships with and without hard chine and ships with various bilge keel aspect ratios etc... That data base was restructured and summarized in a graphical layout $F_{\text{hull}}=f(\text{EWS: effective wave slope})$ that could be used to interpolate the roll damping in a preliminary design stage. Nevertheless, some particular and modern hull forms are not part of the database which makes any attempt of estimation inaccurate.

The aim of this study is, to find a reliable alternative to the basin model test through several validation steps.

First of all, a state of art of the empirical and numerical tools has been established, analyzed and compared. It's obvious that computer programs based on strip theory are widely used in seakeeping analysis and particularly roll motion prediction, while the viscous effect on damping is considered by means of empirical formulas. Therefore, PDstrip, an open source Fortran code has been used to perform a frequency domain strip theory analysis. In order to evaluate the accuracy of this program, two particular ships with detailed roll decay and forced roll results, has been selected from FLUME® database. Another reference ship is the DTMB 5415 (5512) surface combatant model which has been the subject of several CFD and roll model test analysis carried out by the US Naval surface warfare center and by the IIHR—Hydroscience & Engineering lab at the University of IOWA towing tank. The output of PDstrip was post processed and presented in form of roll RAOs in beam seas. Afterwards, 2Droll, a FLUME software extracts the roll damping coefficient from the obtained roll RAO based on a regression between similar hull forms and spring mass system equation with a chosen roll damping coefficient to draw a similar RAO. Once the similarity is established this chosen damping coefficient is adopted.

IKEDA computer program is an up-to-date tool that can give reasonable results and that has taken into account some advanced hull forms. The same ships tested with PDstrip were also tested with IKEDA computer program and Ikeda simple prediction formula. The results were analyzed and compared to experimental results.

Besides, Miller formula with and without forward speed is a preliminary design tool, that have been used in this study in order to analyse its limitations and check the accuracy of the above listed methods.

Finally, a comparison regarding the accuracy and the reliability of all the used methods has been presented and interpreted

TABLE OF CONTENT

ABSTRACT.....	3
LIST OF FIGURES.....	11
LIST OF TABLES.....	13
NOMENCLATURE.....	15
1. INTRODUCTION AND MOTIVATION:.....	19
1.1. Importance Of Roll Motion Studies	19
1.2. Conditions Affecting the Roll Motion and the Factors Contributing to Roll Damping	19
1.3. Objectives Of the Dissertation:	19
2. A REVIEW OF ROLL DAMPING PREDICTION:.....	21
2.1. The Basic Hydrodynamics Of Roll Motion.....	21
2.2. State of the art of the different Approaches used to Analyze the Roll Motion	23
2.2.1. Overview:	23
2.2.2. Experimental Methods:	24
2.2.2.1. Roll Decay Test:	24
2.2.2.2. Forced Roll Test:	25
2.2.3. Watanabe-Inoue-Takahashi-Formula:	26
2.2.4. Tasai-Takaki's table:	28
2.2.5. Component Analysis:	31
2.2.5.1. Skin Friction Damping:	31
2.2.5.2. Eddy Shedding Damping:.....	34
2.2.5.3. Lift Damping Coefficient:	38
2.2.5.4. Wave Damping Coefficient:.....	38
2.2.5.5. Bilge Keel Damping:	39
2.2.6. Blume Method.....	42
2.2.7. Miller method:.....	43
3. THEORY BEHIND THE NUMERICAL TOOLS USED FOR THE ESTIMATION OF ROLL DAMPING:	44
3.1. Overview Of Roll Motion Analysis Models:	44
3.2. Potential Flow Solver Based On Strip Theory: PD strip:	45
3.2.1. Roll Response Prediction With PDstrip:	45
3.2.2. Strip Method in PDStrip:.....	46
3.2.2.1. Fundamental Equations:	46
3.2.2.2. Determination Of the Response Amplitude Operator RAO	47
3.2.3. Inputs:.....	48

3.2.4.	Outputs:	49
3.3.	Component Analysis Programs:	49
3.3.1.	IKEDA Roll Damping Prediction Computer Program: RDPM: (Ikeda 1978).....	49
3.3.2.	Ikeda Simple Formulas Program for the Prediction Of Roll Damping.(Ikeda 2010)....	52
3.4.	“2DRoll Program”: A Flume Software	58
4.	OBSERVATIONS AND ANALYSIS OF THE NUMERICAL SIMULATIONS USED TO PREDICT THE ROLL DAMPING COMPONENT.....	60
4.1.	Overview:	60
4.2.	Numerical Simulations for an 8000-9000 TEU container Ship	60
4.2.1.	Estimation of roll damping using IKEDA simple prediction formula	60
4.2.1.1.	Details and conditions of the computation.	60
4.2.1.2.	Results:	61
4.2.1.3.	Interpretation of the results:.....	62
4.2.2.	Prediction Using Ikeda Computer Program :	63
4.2.2.1.	Details And Conditions Of the computation.	63
4.2.2.2.	Results:	63
4.2.2.3.	Interpretation of the Results	64
4.2.3.	Calculation Using Miller Method:.....	65
4.2.3.1.	Details And Conditions Of the Computation:	65
4.2.3.2.	Results:	66
4.2.3.3.	Interpretation of the Results:	67
4.2.4.	Prediction of Roll Damping from Roll Response Using PDstrip:	67
4.2.4.1.	Details and Conditions Of the Computation:	67
4.2.4.2.	Results:	68
4.2.4.3.	Evaluation Of the Damping Coefficient Using 2DRoll a Flume Software:	69
4.2.4.4.	Interpretation Of the Results:	69
4.3.	Numerical Simulations For an 16000-18000 TEU Container Ship:.....	70
4.3.1.	Prediction of Roll Damping Using IKEDA Simple Prediction Formula	70
4.3.1.1.	Details and Conditions Of the Computation.....	70
4.3.1.2.	Results:	70
4.3.1.3.	Interpretation Of the Results:	71
4.3.2.	Prediction of Roll Damping Using Ikeda Computer Program.....	71
4.3.2.1.	Details and Conditions Of the Computation.....	71
4.3.2.2.	Interpretation Of the Results:	72
4.3.3.	Calculation Using Miller Method :.....	73
4.3.3.1.	Details and Conditions Of the Computation:	73
4.3.3.2.	Results:	74

Development of a practical tool to determine the hull damping of modern ship hull forms	7
4.3.3.3. Interpretation Of the Results:	75
4.3.4. Prediction of Roll Damping from Roll Response Using PDstrip:	75
4.3.4.1. Details and Conditions Of the Computation:	75
4.3.4.2. Evaluation Of the Damping Coefficient Using 2DRoll a Flume Software:	78
4.3.4.3. Interpretation of The results:	79
4.4. Numerical Simulations For DTMB 5415:	79
4.4.1. Post Processing of the Roll Decay Test Measurements Performed by the University of IOWA:	79
4.4.1.1. Roll Decay Test Experimental Conditions	79
4.4.1.2. Roll Decay Test For $\phi_0=15^\circ$	81
4.4.1.3. Roll decay test for $\phi_0=20^\circ$	82
4.4.2. Estimation of Roll Damping of the DTMB 5415 Using Component Analysis Method: Ikeda Program as an Example	84
4.4.2.1. Details and Conditions of the Computation.	84
4.4.2.2. Results of The Simulation:	84
4.4.2.3. Interpretation of the Results:	85
4.4.3. Miller Method Calculation:	86
4.4.3.1. Details and Conditions Of the Calculation.	86
4.4.3.2. Results Of the Calculation:	87
4.4.3.3. Interpretation of the Results:	88
4.4.4. Simulation of Roll Motion Using PDstrip :	88
4.4.4.1. Details and Conditions Of the Simulation.	88
4.4.4.2. Results:	89
4.4.4.3. Evaluation Of the Damping Coefficient Using 2DRoll a Flume Software	89
4.4.4.4. Interpretation Of the Results:	90
4.5. Comparative Analysis Of the Used Simulation Tools:	91
4.5.1. Comparison of the tools used for the 8000-9000 TEU Container Vessel:	91
4.5.2. Comparison of the tools used for the 16000-18000 TEU Container Vessel:	92
4.5.3. Comparison of the tools used for the DTMB 5415:	93
5. CONCLUSION:	94
5.1. Summary:	94
5.2. Areas of Future Work:	96
6. ACKNOWLEDGEMENTS	98
7. REFERENCES:	99
8. APPENDIX	100
8.1. PDstrip Simulation for the 8000-9000 TEU Container Ship:	100
8.2. PDstrip simulation for the 16000-18000 TEU container Ship:	101
8.3. PDstrip simulation for the DTMB 5415:	102

DECLARATION OF AUTHORSHIP

I declare that this thesis and the work presented in it are my own and have been generated by me as the result of my own original research.

Where I have consulted the published work of others, this is always clearly attributed.

Where I have quoted from the work of others, the source is always given. With the exception of such quotations, this thesis is entirely my own work.

I have acknowledged all main sources of help.

Where the thesis is based on work done by myself jointly with others, I have made clear exactly what was done by others and what I have contributed myself.

This thesis contains no material that has been submitted previously, in whole or in part, for the award of any other academic degree or diploma.

I cede copyright of the thesis in favour of the University of Rostock, Germany.

Date: 13.01.2014

Signature

A handwritten signature in blue ink, appearing to be 'S. B. L.', written over a horizontal line.

LIST OF FIGURES:

Figure 1 : Bilge-keel efficiency in Watanabe-Inoue method	28
Figure 2 : Variation of C_f with the Reynolds number	32
Figure 3: Influence of turbulence on the skin friction roll damping	33
Figure 4: comparison between the different methods	34
Figure 5: Effect of advance speed on wave component	39
Figure 6 : Comparison of normal force damping of the bilge keel by Ikeda et al and experiments	40
Figure 7: pressure distribution around the hull due to presence of bilge keel.....	41
Figure 8: Non dimensional Roll damping coefficient VS Roll amplitude obtained with Roll decay test, Forced roll test and Ikeda simple formulas. FW speed=20Kts, GM=2,14m, 90° Beam seas	61
Figure 9: Dimensional roll damping component B44 VS Roll Amplitude, 20Kts, 90° beam seas, GM=2.14m	63
Figure 10 : Miller Nondimensional Damping ratio Vs roll amplitude, 20Kts & T=15m.....	66
Figure 11 : RAO in (°/m) VS Wave frequency in (rad/s), 35°: Stern quartering seas, 20Kts: Forward Speed, GM=2.14m	68
Figure 12 : Sensitivity analysis for the PDstrip RAO regarding the GM value	68
Figure 13 : Non Dimensional Damping Coefficient VS Roll Amplitude	70
Figure 14 : Dimensional roll damping component B44 VS Roll Amplitude	72
Figure 15 : Miller Nondimensional Damping ratio Vs roll amplitude, 20Kts & T=15m.....	74
Figure 16 : RAO in (°/m) VS Wave frequency in (rad/s).....	76
Figure 17 : Sensitivity analysis regarding the value of GM	76
Figure 18: RAO in (°/m) VS Wave frequency in (rad/s).....	78
Figure 19: Roll RAO obtained from 2DRoll at 90° & 21 Kts.....	78
Figure 20: Model 5512 suspended in air from the IIHR towing tank carriage	80
Figure 21: Roll decay time history for initial inclination angle $\phi_0=15^\circ$	81
Figure 22: Roll decrement curve $\Delta\phi/\phi_m$ VS ϕ_m	81
Figure 23: Roll decay time history for $\phi_0=20$	82
Figure 24: Roll decrement curve $\Delta\phi/\phi_m$ VS ϕ_m	83
Figure 25: Comparison of Ikeda original method results for DTMB 5415 with roll decay test results for two different initial inclination angles at Fn=0.28.....	84
Figure 26: Nondimensional damping coefficient for DTMB 5415 Compared to the roll decay test results	87
Figure 27: Roll RAO (η_{44}/kA) VS (λ/L) for the DTMB 5415 at 0 Forward speed & T=6.15 m.....	89
Figure 28: Roll RAO obtained by 2DRoll FLUME Software.....	90
Figure 29: Shape of the bottom of the DTMB 5415	91
Figure 30: Comparison of the nondimensional roll damping coefficient obtained with the different numerical tools used for the 8000-9000 TEU Container ship: FwSpeed= 20Kts, GM=2.14m.....	91
Figure 31: Comparison of the nondimensional roll damping coefficient obtained with the different numerical tools used for the 16000-18000 TEU Container ship: FWS= 21Kts, GM=2.9m	92
Figure 32: Comparison of the nondimensional roll damping coefficient obtained with the different numerical tools used for the 16000-18000 TEU Container ship: FW= 20Kts, T=2.9m	93
Figure 33: Comparison of Ikeda methods for different center of gravity positions.	96

LIST OF TABLES:

Table 1: The main characteristics of the four ships tested by Tasai-Takaki	29
Table 2: Results for the coefficients B_1 , B_2 and B_3 for different ship types and Froude numbers	30
Table 3: C_1 as a function of B/KG	35
Table 4 : C_2 as a function of α and re/D	35
Table 5: non dimensional roll damping using forced roll, roll decay test and Ikeda simple formulation	61
Table 6: Ikeda program numerical values:	63
Table 7: Miller method's parameters for the 8000-9000TEU container ship:	65
Table 8 : Roll damping ratio for 8000-9000TEU container at 20 Kts Forward speed, $T=15m$	65
Table 9 : Miller Damping coefficient after Ikeda nondimensionalisation.....	66
Table 10 : IKEDA Simple Prediction Formula numerical values for a 16000-18000 TEU Container Ship.....	71
Table 11 : IKEDA Computer program numerical values for an 16000-18000 TEU Container Ship ..	72
Table 12 : Miller method parameters for the 16000-18000TEU container ship	73
Table 13 : Roll damping ratio for 8000-9000TEU container at 20 Kts Forward speed, $T=15m$	73
Table 14 : Miller damping coefficient after Ikeda nondimensionalisation:	74
Table 15 : Summary of DTMB model 5512 and fullscale particulars:	80
Table 16 : Roll decrement table	81
Table 17 : Roll decay coefficients:.....	82
Table 18 : Roll decrement table:	83
Table 19 : Roll decay coefficients:.....	83
Table 20: Roll damping numerical values for DTMB 5415:.....	85
Table 21: Miller method parameters for the DTMB 5415:	86
Table 22: The values of the zero speed and forward speed damping ratios are presented.....	86
Table 23: Miller damping coefficient after the Ikeda nondimensionalisation.....	87
Table 24: Summary of the experimental wave condition of the stationary beam seas test of the model DTMB 5415	88
Table 25: Table of Roll RAO VS λ/L for the DTMB 5415 :	89

NOMENCLATURE

F_{hull}	Roll damping factor defined in 2Droll FLUME Software.
EWS	Effective wave slope
DTMB	David Taylor Model Basin
TEU	Twenty-foot equivalent unit
VCG	Vertical position of center of gravity
LCG	Longitudinal Position of the center of gravity
FWS	Forward speed
ϕ	Velocity potential
$\rho g \nabla$	Ship displacement
$GZ(\phi)$	Righting arm.
I_{44}	Roll moment of inertia,
a_{44}	Roll added inertia;
b_{44}	Roll damping;
M_{44}	Total roll moment,
B_{44}	Total Roll damping coefficient
C_{44}	Roll Restoring coefficient
I_{44}	Roll moment of inertia
A_{44}	Roll added mass
$B_1, B_2 \text{ and } B_3$	Linear, quadratic and cubic roll damping factors
$\Delta\phi$	Roll decrement
ϕ_m	Mean roll angle
$a, b \text{ and } c$	Extinction coefficients
N	Bertin coefficient
Φ_A	Roll amplitude
C_B	Ship block coefficient.
L	Ship's length
B	Ship's beam
D	Ship's draft
C_w	Waterline area coefficient
A_b	Area of bilge keel

σ_0	Efficiency of the bilge keels
C_f	Friction coefficient
r_e	Effective bilge radius
ρ	Water density
ν	Kinematic viscosity of water
ω	Wave frequency
R_0	Amplitude of roll motion (in radians),
U	Forward speed (or steady current speed).
OG	Vertical distance from O (still water level) to roll axis, G ($OG=D-KG$).
S	Wetted surface area
B_{F0}	Friction damping coefficient for zero forward speed
B_F	Friction damping coefficient at forward speed
C_e	Drag coefficient
R_b	Bilge radius
B_e	Eddy damping coefficient
M_L	Lift damping moment
C_M	Mid-ship cross-section
B_L	Lift Damping
B_W	Wave damping coefficient
C_D	Bilge keel drag
B_{BKN}	Normal force damping of bilge keel
B_{BKH}	Hull pressure damping due to bilge keels
η_{44}	Roll amplitude
β	Non dimensional roll damping coefficient
q_i	Source strengths in PDStrip
M	Real mass matrix of the ship in PDstrip
S	Real matrix due to hydrostatics in PDstrip
B	complex matrix due to ship motions in PDstrip
F_e	excitation forces due to the incident wave
$\hat{\omega}$	Nondimensional circular wave frequency.
L_{pp}	Length between perpendiculars
B	Ship Breadth
T	Ship Draft
GM	Metacentric height

Δ	Ship displacement
ω_n	Natural frequency
T	Roll period
C_g	Center of gravity
g	Gravity acceleration
K_{xx}	Roll gyration ratio
K_{yy}	Pitch gyration ratio
K_{zz}	Yaw gyration ratio
k	Wave number= $2\pi/\lambda$
λ	wave length
L_{BK}	Length of bilge keel
H_{BK}	Breadth of bilge keel
C_y, C_z	Resistance coefficients
ϕ_0	Initial inclination angle in roll decay test
$\bar{\zeta}$	Effective wave slope

1. INTRODUCTION AND MOTIVATION:

1.1.Importance Of Roll Motion Studies

A deep study of roll motion of a ship is very crucial to ensure the safety of the vessel and its dynamic stability in order to comply with IMO intact stability severe wind and rolling criterion. Moreover, a proper estimation of the roll damping of the ship is highly recommended by the seakeeping committee of the International towing tank conference (ITTC).

1.2.Conditions Affecting the Roll Motion and the Factors Contributing to Roll Damping

Roll motions are by far the most difficult motions of a ship to predict. It is therefore appropriate to discuss this motion separately, even though it is strongly coupled with sway and yaw.

Unlike most of the degrees of freedom where the damping is evaluated using the simple diffraction/ radiation theory, this theory is not available in the case of roll where the radiation damping is generally quite small compared to the total damping in the system. In fact, the high nonlinearity of this component due to the effect of fluid viscosity as well as its strong dependence on the forward speed of ship makes it difficult to predict. Moreover, a ship is very likely to roll severely since its roll natural period generally falls within the frequency range of a typical wave energy spectrum that it can experience.

Due to the above listed conditions, an accurate analytical model is necessary to analyze all the physical processes which occur during small and moderate amplitude roll motions and to predict the effect of these motions on the magnitude of roll motion especially in case of severe environment. Any proposed model should include an accurate treatment of roll nonlinearity like for instance the approximate way of considering the equivalent damping coefficients which provides a better understanding of the physical phenomena that alter the roll damping.

1.3.Objectives Of the Dissertation:

The modelling of damping hydrodynamic components, added inertia and damping, for ship roll motion had been previously addressed. This motivated an examination of existing tools that provided a solution for the description and prediction of this component. This study seeks to investigate the limitation of those tools and provide a better way to use them by combining some of the solutions and recommend a field of application for them.

It is important to highlight the fact that this study aims to match the aspirations of the FLUME Stabilization Systems regarding the exploitation of the FLUME database to improve their capability to predict roll damping without the need of model scale experiments. Therefore, among the test cases, two represent newly built container ships with fully detailed seakeeping reports. The main idea was to analyze the roll motion of the test cases using an open source potential flow solver: PDstrip, in order to have access to the details of the analytical model behind it and to the hydrodynamic components matrix where the damping and added mass components are provided. This allows for an easier tuning and a better interpretation of the results. Component analysis method proved its reliability to describe all the features of roll damping. Therefore, Ikeda computer program and Ikeda simple formulation methods are very likely to be suitable not only for the two FLUME test cases but also for the DTMB 5415 model of the DDG-51 ARLEIGH BURKE-class destroyer. A simple tool, generally used in early design stage, is Miller method. It can be a useful means of verification of the validity of the above listed tools.

It is required to show how complementary these methods are. Indeed, PDstrip is able to provide the wave damping component which is needed as input for Ikeda Program. It must be also proven that some damping component can be derived from one method and used in another.

2. A REVIEW OF ROLL DAMPING PREDICTION:

2.1. The Basic Hydrodynamics Of Roll Motion

A spring mass system equation can be applied to the ship roll motion and a 2nd-order differential equation can be derived:

$$a\ddot{\phi} + b\dot{\phi} + c\phi = f(t) \quad (1)$$

Where a is the roll inertia; b is the damping; c is the stiffness; ϕ is the roll angle; and f(t) is the excitation forcing function. The equivalent roll equation for a ship is the following:

$$(I_{44} + a_{44})\ddot{\phi} + b_{44}\dot{\phi} + \rho g \nabla \cdot GZ(\phi) = f(t) \quad (2)$$

$\rho g \nabla$ is the ship displacement

$GZ(\phi)$ is the righting arm.

I_{44} is the roll moment of inertia,

a_{44} is the roll added inertia;

b_{44} is the roll damping;

The hydrostatic term is the only source of nonlinearity and it is generally represented by an odd order polynomial (cubic or quintic) depending on the corresponding GZ curve.

After dividing the former equation by the inertia term, the following equation is obtained.

$$\ddot{\phi} + 2\delta\dot{\phi} + c(\phi) = F(t) \quad (3)$$

Referring to the spring- mass model, the damping can be identified as 2δ

$$2\delta = \frac{b_{44}}{(I_{xx} + a_{44})} \quad (4)$$

The stiffness is identified as $c(\phi)$

$$c(\phi) = \frac{\rho g \nabla \cdot GZ(\phi)}{(I_{xx} + a_{44})} \quad (5)$$

While the forcing function is given by:

$$F(t) = A_w \sin(\omega t) \quad (6)$$

Where A_w is the amplitude of the wave, and ω is the wave frequency. Furthermore, the stiffness, with dependency on roll angle, can also be expressed as

$$c(\phi) = \omega_n^2 \frac{GZ(\phi)}{GM} \quad (7)$$

Where the roll natural frequency, ω_n , is given as

$$\omega_n = \sqrt{\frac{\rho g \nabla \cdot GM}{(I_{xx} + a_{44})}} \quad (8)$$

GM is the metacentric height.

Roll damping is the energy dissipation of the system therefore it is proportional to roll angular velocity $\omega_E \phi_a$ and it can be denoted as B_{44} .

$$B_{44} = \frac{8}{3\pi} M_\phi \phi_a \omega_E$$

In the standard model of single-degree-of-freedom ship roll motion as a spring-mass-damper system, added inertia is proportional to the acceleration and characterizes the additional inertial effect of the fluid that is displaced by the body during motion.

Considering a single degree-of-freedom model for ship roll motion (as denoted by the index 44), due to roll damping.

$$(I_{44} + A_{44}(\omega))\ddot{\phi} + B_{44}(\dot{\phi}) + C_{44}(\phi) = M_{44}(t) \quad (9)$$

It is possible to decompose B_{44} into linear and non linear components as follows:

The linear term is proportional to the viscous component, the quadratic term represents the vortex effect, and higher orders represent the contribution of additional correction factors. Performing a roll decay test is one of the methods used to determine B_1 , B_2 and $B_3 \dots$

Due to the difficulty to deal with the non linearity stated previously, it is more convenient to express B_{44} in function of a linear equivalent roll damping coefficient (*Ikeda et al 1987*).

$$B_{44} = B_e \dot{\phi} \quad (10)$$

This equivalent coefficient is detailed in Ikeda component analysis described later in this thesis. This assumption has some limitations. In fact, linearization is only applicable for small roll angles. It might also lead to an overestimation of the roll damping in case of moderate to heavy seas and the roll motion will be therefore underestimated.

In frequency domain, the equation of motion is written:

$$\left[-\omega_e^2 (\hat{I}_{44} + \hat{A}_{44}) + i\omega_e \hat{B}_{44}^* + \hat{C}_{44}^* \right] \bar{\eta}_4 + \hat{B}_{44}^* \bar{\eta}_2 + \hat{B}_{46} \bar{\eta}_6 = \hat{F}_4 \quad (1.11)$$

In order to characterise the roll behaviour of a ship, the damped oscillatory motion in calm water resulting from a time harmonic pure roll moment will be examined. The coupling terms \hat{B}_{42}^* and \hat{B}_{46} are generally ignored. The equation becomes:

$$\left[-\omega_e^2 (\hat{I}_{44} + \hat{A}_{44}) + i\omega_e \hat{B}_{44}^* + \hat{C}_{44}^* \right] \bar{\eta}_4 = \hat{F}_4 \quad (1.12)$$

The center of roll is chosen in a way that the coupling with sway and yaw is coming only from $\hat{B}_{42}^* \bar{\eta}$ and $\hat{B}_{46}^* \bar{\eta}_6$. Since this coupling is supposed to be low, the origin of reference can be chosen as the roll center. In fact the coordinates of the roll center are:

$$\left[x = \frac{I_{62} + A_{62}}{\Delta + A_{22}} = 0, y = 0, z = \frac{I_{42} + A_{42}}{\Delta + A_{42}} \right]$$

In the rest of this study the damping is supposed to be determined about that center.

If The equation (1.11) is divided by $C44=g\Delta GM$, it gives:

$$\left[-\hat{\omega}_e^2 + 2i\hat{\omega}_e \beta^* (|\bar{\eta}_4|) + \gamma^* (|\bar{\eta}_4|) \right] \bar{\eta}_4 = f_4$$

Where:

$\hat{\omega}_e = \frac{\omega_e}{\omega_{n4}}$ is the non dimensional encounter frequency

$\gamma^* (|\bar{\eta}_4|) = \frac{\hat{C}_{44}^*}{g\Delta GM_T}$ is the non dimensional roll restoring term

$f_4 = \frac{\hat{F}_4}{g\Delta GM_T}$ is the ND roll moment amplitude

$\omega_{n4} = \sqrt{\frac{g\Delta GM_T}{(\hat{I}_{44} + \hat{A}_{44})}}$ Roll resonance frequency

$\beta^* (|\bar{\eta}_4|) = \frac{\hat{B}_{44}^*}{g\Delta GM_T}$ Is the non dimensional roll damping ratio. This form of

nondimensionalization will be used later to compare the roll damping confidents obtained from various estimation methods. (*Principles of naval architecture Volume III*).

2.2. State of the art of the different Approaches used to Analyze the Roll Motion

2.2.1. Overview:

Roll damping is the representation of the physical process of energy dissipation during the roll motion. In the case of a ship in motion, many elements can contribute to this energy dissipation and we can list the hull shape and friction, the bilge keels, the appendages, wave radiation and lift effect.

Many attempts to study all those phenomena separately (*Ikeda et al 1978, Schmitke 1978, Himeno 1981...*) have lead to the establishment of a component analysis method which divides the equivalent roll damping, described earlier, into various physical components.

The importance of the determination of roll damping lays not only in the necessity of the prediction of the roll motion and intact stability in critical conditions like extreme seas or

parametric rolling, but also in the necessity to reduce this roll motion. In fact, there is a tight relation between this parameter and the dimensioning and position of roll stabilization devices.

The aim of this part is to list and classify the existing methods of roll damping prediction methods.

2.2.2. *Experimental Methods:*

2.2.2.1. *Roll Decay Test:*

This kind of test has to satisfy the following conditions:

- Restrained sway and yaw which allows avoiding the influence of the horizontal motion on the roll motion.
- Free heave and pitch.

The free roll test is the fact of rolling the model to a chosen angle then releasing it. Then an extinction curve is fitted, according to Froude and Baker, by a third- degree polynomial:

$$\Delta\phi = a\phi_m + b\phi_m^2 + c\phi_m^3 \quad (11)$$

Where

$$\Delta\phi = \phi_{n-1} - \phi_n$$

$$\phi_m = [\phi_{n-1} - \phi_n] / 2$$

a, b and c are called extinction coefficients. They are obtained by plotting the roll decrement $\Delta\phi$ in function of the mean roll angle ϕ_m . Thus, the cubic polynomial stated in the equation (11) can be fitted from this curve.

Φ_n is the absolute value of roll angle corresponding to the n-th extreme value.

Finally the roll motion equation without external force term is integrated over a time period for half roll cycle and the energy loss due to damping is equated to the work done by restoring moment. Finally, the following equation is obtained:

$$\Delta\phi = \frac{\pi}{2} \frac{\omega_n}{C_\phi} \phi_m (B_1 + \frac{8}{3\pi} \omega_n \phi_m B_2 + \frac{3}{4} \omega_n^2 \phi_m^2 B_3) \text{ in (rad)} \quad (12)$$

A system of equation is derived from Eq. (11) and Eq. (12) in order to provide the relation between the extinction coefficients and the damping coefficients:

$$\left. \begin{aligned} a &= \frac{\pi \omega_n}{2 C_\phi} B_1 \\ \frac{180}{\pi} b &= \frac{4 \omega_n^2}{3 C_\phi} B_2 \\ \left(\frac{180}{\pi}\right)^2 c &= \frac{3\pi \omega_n^3}{8 C_\phi} B_3 \end{aligned} \right\} \quad (13)$$

The equivalent roll damping coefficient could also be determined directly by defining an equivalent extinction coefficient a_e through the following relation:

$$a_e = a + b\varphi_m + c\varphi_m^2 = \frac{\pi \omega_\phi}{2 C_\phi} B_{\phi e} \quad (14)$$

It is also possible to have an idea about the damping of a ship by plotting Bertins coefficient N as a function of different roll angles. Bertin's expression by Matora, (1964), can be written in the form:

$$\Delta\varphi = \frac{\pi N}{180} \varphi_m^2 \quad (15)$$

Bertin coefficient is an equivalent non linear coefficient that can be also called "N coefficient" given by:

$$N = a \frac{180}{\pi\varphi_m} + b + c \frac{\pi\varphi_m}{180} \quad (16)$$

N coefficient is strongly dependent on the mean roll angle.

2.2.2.2. **Forced Roll Test:**

Forced roll tests is ruled by the following equation where all degrees of freedom are constrained except roll.

$$\begin{aligned} (I_{44} + A_{44}(\omega))\ddot{\phi} + B_{44}(\dot{\phi}) + C_{44}(\phi) &= M_{44}(t) \\ B_{44}(\dot{\phi}) &= B_1\dot{\phi} + B_2\dot{\phi}|\dot{\phi}| + B_3\dot{\phi}^3 + \dots \\ B_{44}(\dot{\phi}) &= B_e\dot{\phi} \end{aligned} \quad (17)$$

A relation between the equivalent linear roll coefficient and B_1 , B_2 and B_3 is derived from the equation of the energy loss, E , during one period of roll motion (*Takaki & Tasai, 1973; Himeno, 1981*).

$$\phi(t) = \phi_A \sin(\omega t)$$

$$\begin{aligned} E &= 4 \int_0^{\pi/(2\omega)} B_{44}(\dot{\phi}) d\phi = 4 \int_0^{\pi/(2\omega)} \left[B_1 \omega \phi_A \cos(\omega t) + B_2 \omega \phi_A \cos(\omega t) |\omega \phi_A \cos(\omega t)| + \right. \\ &\quad \left. + B_3 (\omega \phi_A \cos(\omega t))^3 + \dots \right] \omega \phi_A \cos(\omega t) d\phi = \\ &= \pi \omega \phi_A^2 B_1 + \frac{8}{3\pi} \omega^2 \phi_A^3 B_2 + \frac{3}{4} \omega^4 \phi_A^4 B_3 + \dots \end{aligned} \quad (18)$$

Therefore,

$$B_e(U, \omega, \phi_A) = B_1 + \frac{8}{3\pi} \omega \phi_A B_2 + \frac{3}{4} \omega^2 \phi_A^2 B_3 \quad (19)$$

B_1, B_2 and B_3 are determined from a series of roll amplitude, for a given frequency. Afterwards, the equivalent roll damping is determined using a regression analysis on B_e . An important assumption must be taken into account is that the three damping coefficients are independent from roll amplitude (*Himeno (1981)*).

This procedure is repeated for different frequencies and forward speeds to compute more accurately the damping coefficients.

2.2.3. *Watanabe-Inoue-Takahashi-Formula:*

Watanabe and Takahashi used a data base of model tests and a study of the pressure distribution on the ship's hull caused by roll motion, to derive a formula that predicts the roll damping of ordinary hull forms at zero advance speed.

Takahashi modified this formula to take into account the effect of the advance speed.

The following formula is called the Watanabe-Inoue-Takahashi-Formula:

$$B_e = B_{e0} \left[1 + 0.8 \left\{ 1 - \exp(1 - 10F_n) \right\} \frac{\omega_n^2}{\omega^2} \right] \quad (20)$$

B_{e0} is the equivalent linear damping coefficient at zero advance speed and it can be written as a function of the extinction coefficients:

$$B_{e0} = 2\alpha_e A_\phi = \frac{2}{\pi} \omega_n A_\phi \left(a + \frac{\omega}{\omega_n} b \phi_A \right) \quad (21)$$

Φ_A in degrees

a and b coefficients are computed from the following formulas:

$$N_{10} = \frac{a}{10} + b, \quad N_{20} = \frac{a}{20} + b \quad (22)$$

The terms N10 and N20 represent the drag coefficients of non linear damping at roll amplitude of 10° and 20° and they are given by:

$$\begin{Bmatrix} N_{10} \\ N_{20} \end{Bmatrix} = \begin{Bmatrix} n_{10} \\ n_{20} \end{Bmatrix} + \begin{Bmatrix} 1.5 \\ 1.0 \end{Bmatrix} \frac{A_b}{L^2} \sigma_0 \left[l^3 \left(1 + \frac{d^2}{4l^2} \right) + \frac{fB^4}{64d} \right] \frac{L_d}{W.GM.T_n^2} \quad (23)$$

n10 and n20 are drag coefficients of non linear damping of the naked hull at 10° and 20° :

$$\begin{Bmatrix} n_{10} \\ n_{20} \end{Bmatrix} = \begin{Bmatrix} 0.78 \\ 1.1 \end{Bmatrix} \frac{C_B d}{L} + \begin{Bmatrix} 0.03 \\ 0.02 \end{Bmatrix} \quad (24)$$

C_B ship block coefficient.

L=ship's length

B= ship's beam

D= ship's draft

A_b area of bilge keel at one side of the hull

$l = K_G - d/2$

f is a function of waterline area coefficient C_w given by :

$$f = 1 - \frac{4}{m+1} + \frac{6}{2m+1} - \frac{4}{3m+1} + \frac{1}{4m+1}, \quad m = \frac{C_w}{1-C_w} \quad (25)$$

σ_0 is the efficiency of the bilge keels and it can be determined from watanabe-Inoue method on the figure below:

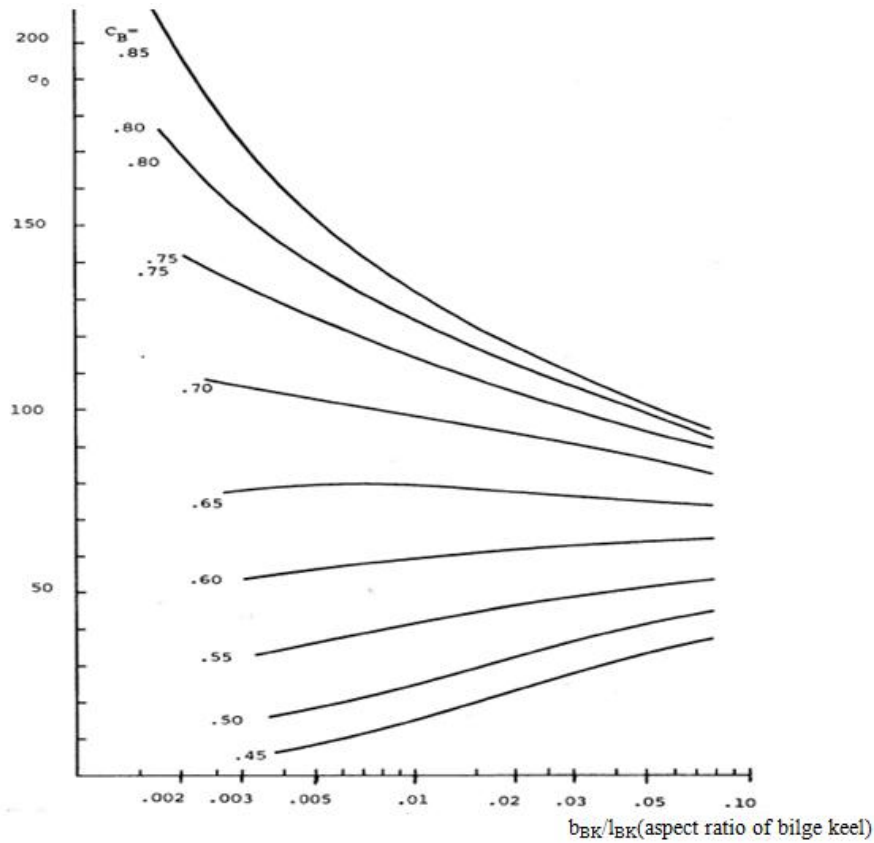


Figure 1 : Bilge-keel efficiency in Watanabe-Inoue method
(Himeno, 1981)

2.2.4. Tasai-Takaki's table:

Tasai-Takaki gathered some experimental results based on forced roll test carried out for four different types of vessels. The aim of the test is to obtain the roll damping by varying the frequency for the same Froude number and roll amplitude. Then, a regression was made to establish an equation that includes three damping coefficients \widehat{B}_1 , \widehat{B}_2 and \widehat{B}_3 in the case of third order approximation as follows:

$$\widehat{B}_e = \widehat{B}_1 + \frac{8}{3\pi} \widehat{\omega} \phi_A \widehat{B}_2 + \frac{3}{4} \widehat{\omega}^2 \phi_A^2 \widehat{B}_3 \quad (26)$$

Table 1: The main characteristics of the four ships tested by Tasai-Takaki

	Container	Cargo ship	Ore Carrier	Tanker
Length L_{pp} (m)	3	3	3	3
Breadth B (m)	0,4354	0,4783	0,493	0,4719
Draft d (m)	0,1628	0,1957	0,194	0,1828
Displacement Δ (Kg)	121,61	199,84	233,4	220,57
C_B	0,5717	0,7119	0,8243	0,8519
C_M	0,97	0,9905	0,9975	0,9946
GM (m)	0,017	0,02174	0,05	0,06077
OB (m)	-0,0425	-0,025	0,089	0,0993
K_L/L_{pp}	0,239	0,2172	0,2356	0,2494
K_B/B	0,382	0,324	0,2602	0,2513
l_{BK}/L_{pp}	0,25	0,25	0,25	0,37
b_{BK}/B	0,0148	0,0159	0,0142	0,00869

(Himeno, 1981)

Table 2: Results for the coefficients \hat{B}_1 , \hat{B}_2 and \hat{B}_3 for different ship types and Froude numbers

Fn	Coef	Ore carrier	Tanker	Container	Cargo ship
0	\hat{B}_1	0,003	0,00209	0,00082	0,00061
	\hat{B}_2	0,03262	0,04168	0,0369	0,04908
	\hat{B}_3	0,127	0,03877	0,08474	0,08994
0,1	\hat{B}_1	0,00359	0,00316		
	\hat{B}_2	0,0411	0,04453		
	\hat{B}_3	0,07783	0,03581		
0,15	\hat{B}_1		0,00344	0,00374	0,00242
	\hat{B}_2		0,04254	0,02531	0,03755
	\hat{B}_3		0,05524	0,09835	0,05226
0,2	\hat{B}_1				0,00332
	\hat{B}_2				0,03551
	\hat{B}_3				0,05226
0,25	\hat{B}_1			0,00628	0,00389
	\hat{B}_2			0,02125	0,04033
	\hat{B}_3			0,03567	0,02206
0,275	\hat{B}_1			0,00671	
	\hat{B}_2			0,01402	
	\hat{B}_3			0,05097	

(Himeno, 1981)

The results given by the Tasai-Takaki method comply with the experimental results and it can be very useful in the preliminary design stage especially for the same ship type as the tested model. However, it's still possible to apply the same method for different ship types by interpolating or extrapolating the existing results.

It's still limited by the prevalent non linear effect due to the presence of the bilge keel.

2.2.5. Component Analysis:

This method is based on the decomposition of the damping coefficient mentioned earlier (hull skin friction damping, hull eddy shedding damping, free surface wave damping, lift force damping, etc...). Each component is predicted separately with a specific formula:

2.2.5.1. Skin Friction Damping:

The skin friction stress on the hull is the origin of the friction damping and it's altered by waves and bilge keel effect:

The prediction of this component is based on the skin friction laws of a flat plate in a steady flow. In fact, Kato's prediction formula (27), was derived from Blasius formula for a laminar flow and Hughes formula for turbulent flow around a cylinder.

$$B_{f0} = \frac{4}{3\pi} \rho S r_e^3 R_0 \omega C_f \quad (27)$$

C_f is the friction coefficient given by:

$$C_f = 1.328 \left[\frac{2\pi v}{3.22 r_e^2 R_0^2 \omega} \right]^{1/2} \quad (28)$$

r_e : effective bilge radius given by:

$$r_e = \frac{1}{\pi} \left[(0.887 + 0.145 C_B) \frac{S}{L} - 2OG \right] \quad (29)$$

ρ : water density

v : kinematic viscosity of water

ω : wave frequency

B : beam,

D : draft,

L : lateral dimension of the ship,

C_B : block coefficient of the ship,

R_0 : amplitude of roll motion (in radians),

U : forward speed (or steady current speed).

OG is the vertical distance from the origin O (still water level) to the roll axis, G , which is measured positive downward ($OG=D-K_G$).

The quantity S is the wetted surface area that can be calculated approximately for a ship by the formula:

$$S = L(1.7D + C_B B) \quad (30)$$

As shown in the Figure2, the skin friction is higher in the model scale compared to the full scale value due to its dependence to the viscosity and to the equivalent Reynolds number ($Re = (reR_0)^2 \omega / \nu$).

Therefore, Froude scaling of C_f is not available.

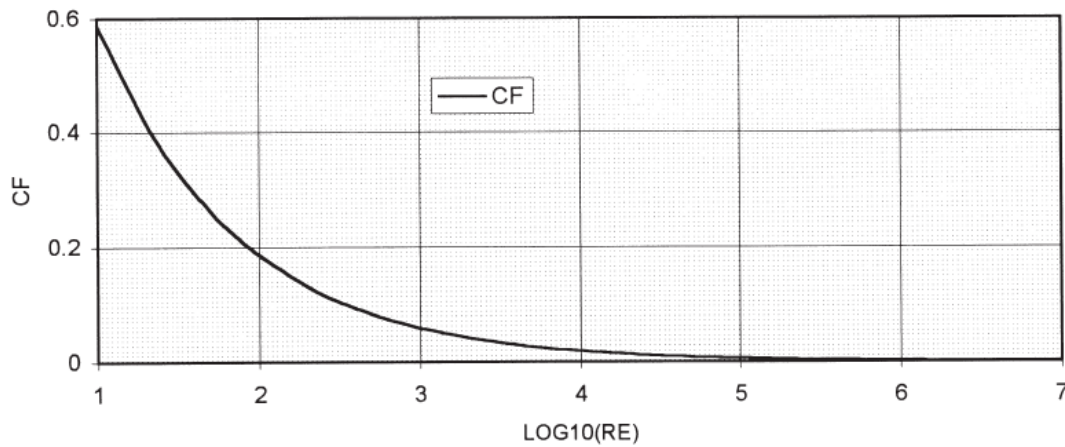


Figure 2 : Variation of C_f with the Reynolds number (Chakrabarti, 2001)

The modified Kato's formula in order to take into account the previously mentioned effect:

$$B_{f_0} = 0.787 \rho S r_e^2 \sqrt{\omega \nu} \left\{ 1 + 0.00814 \left[\frac{r_e^2 R_0^2 \omega}{\nu} \right]^{0.386} \right\} \quad (31)$$

The first term in the bracket gives the result for the case of laminar flow, while the second term gives the modification for turbulent flow by Hughes formula which can be shown in the following figure:

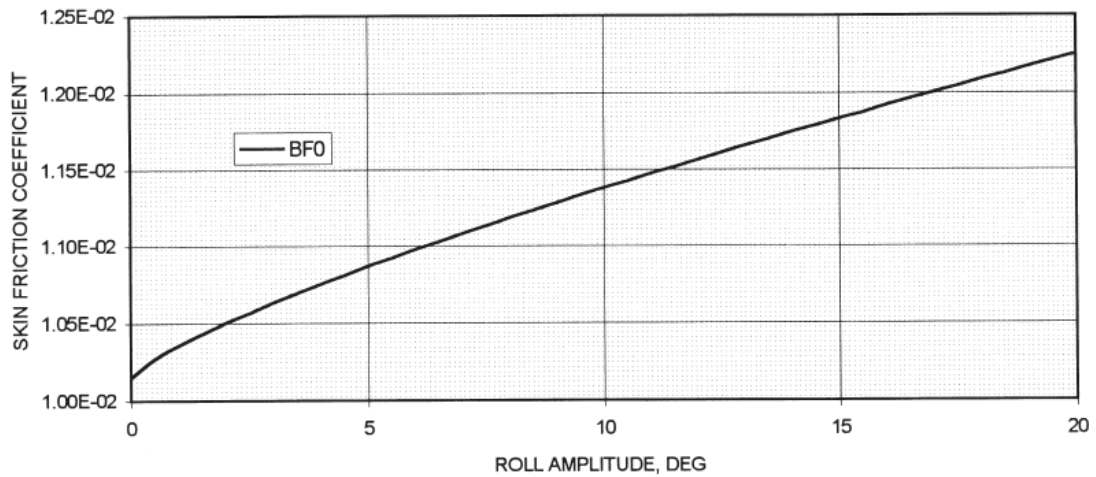


Figure 3: Influence of turbulence on the skin friction roll damping (Chakrabarti, 2001)

Kato's method was confirmed by Ikeda et al, through the measurement of the velocity profile in the boundary layer on two-dimensional cylinders of shiplike sections.

In addition to the previous methods, we can also mention Tamiya's formula based on the analysis of the three-dimensional boundary layer around a rolling cylinder.

$$B_F = B_{F0} \left(1 + 4.1 \frac{U}{\omega L} \right) \quad (32)$$

The coefficient in (32) was deduced from experiments on elongated spheroids in roll motion. B_{F0} is the friction damping coefficient for zero forward speed, determined from Kato's formula.

Tamiya's method was confirmed to be in agreement with Ikeda et al detailed calculations (of the three dimensional boundary layer on the symmetry axis of the body in roll motion), with Kato's formula and with the measurement on an ellipsoid model as shown in the following figure.

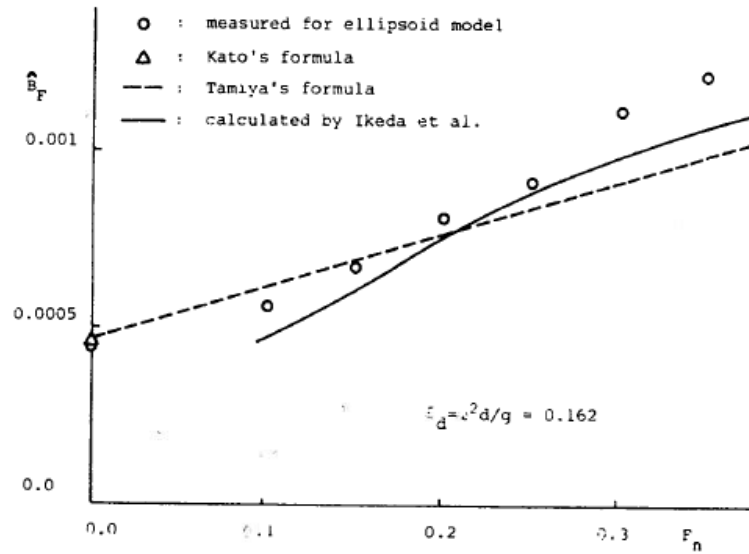


Figure 4: comparison between the different methods
(Himeno, 1981)

2.2.5.2. *Eddy Shedding Damping:*

The viscous eddy damping is due to the vortices coming from the separation of the flow at the sharp corners which causes a pressure variation at the bottom of the ship near the stem and stern and at the bilge circle near the midship.

The eddy-making drag is given by (33) based on the drag coefficient C_e .

$$F = \frac{1}{2} C_e \rho S (r \omega R_0)^2 \quad (33)$$

r is the radial distance from the c.g. of the ship to the corner where eddies are shed (local radius). The drag C_e is obtained from the formula provided for a U shaped or a V shaped hull (Tanaka 1957, 1958).

$$C_e = C_1 (B / KG) C_2 \left(\alpha, \frac{r_e}{D} \right) e^{-\beta r / D} \quad (34)$$

K_G : distance from the keel to the c.g.,

r_e : effective bilge radius defined in this case as follows:

$$\begin{cases} r_e = 0.5B \left[4.12 - 3.69(KG/B) + 0.823(K_G/B)^2 \right] & \text{for } KG/B < 2.1 \\ r_e = 0 & \text{for } KG/B \geq 2.1 \end{cases} \quad (35)$$

The quantity α =angle (deg) between the hull surface at the water line and the vertical, and β =exponential parameter. The value of C_1 (Garrison, 1993) as a function of B/KG is as follows:

Table 3: C_1 as a function of B/KG

B/KG	C_1
0	0,5
0,25	0,61
0,5	0,62
1	0,61
1,5	0,53
2	0,4
2,5	0,35
3	0,32
3,5	0,29
4	0,26

The values of C_2 as a function of α and re/D are given below. The intermediate values may be interpolated from this table

Table 4 : C_2 as a function of α and re/D

α	$re/D=0,0$	$re=0,0571$	$re=0,1142$	$re=0,1713$
0	1	1	1	1
5	0,86	0,75	0,74	0,7
10	0,77	0,67	0,72	0,72
20	0,68	0,75	0,89	1,2
30	0,65	0,92	1,34	1,94

The exponential parameter β is calculated by

$$\beta = 14.1 - 46.7R_0 + 61.7R_0^2 \quad (36)$$

For a rectangular section, e.g., a barge, $C_2=1.0$ and $\beta=0$. Then $C_e=C_1$ and r in the equation for the drag force is the distance from the roll axis to the corner.

For a triangular sectioned ship, the drag coefficient

$$C_e = 0.438 - 0.449(B/K_G) + 0.236(B/K_G)^2 \quad (37)$$

Alternately, the formula for the eddy-making damping per unit ship length is derived empirically by *Ikeda et al.*

$$B_{e0} = \frac{4}{3\pi} \rho D^4 R_0 \omega C_p C_R \quad (38)$$

Where

$$C_p = 0.5 \left[0.87e^{-\gamma} - 4e^{(-0.187\gamma)} + 3 \right] \quad (39)$$

The velocity increment ratio,

$$\gamma = \frac{\sqrt{\pi} f_3}{2[D-OG]\sqrt{H_0\sigma}} \left[r_{\max} + \frac{2M}{H_1} \sqrt{A_1^2 + B_1^2} \right] \quad (40)$$

where

$$\begin{aligned} H_1 &= 1 + a_1^2 + 9a_3^2 + 2a_1(1 - 3a_3)\cos(2\psi) - 6a_3\cos(4\psi) \\ A_1 &= -2a_3\cos(5\psi) + a_1(1 - a_3)\cos(3\psi) - \left[(6 - 3a_1)a_3^2 + a_1(a_1 - 3)a_3 + a_1^2 \right] \cos(\psi) \\ B_1 &= -2a_3\sin(5\psi) + a_1(1 - a_3)\sin(3\psi) - \left[(6 + 3a_1)a_3^2 + a_1(a_1 + 3)a_3 + a_1^2 \right] \sin(\psi) \\ M &= \frac{B}{2(1 + a_1 + a_3)} \end{aligned} \quad (41)$$

C_R is given by:

$$C_R = \left[\frac{r_{\max}}{D} \right]^2 \left[1 - f_1 \frac{R_b}{D} \right] \left[1 - \frac{OG}{D} - f_1 \frac{R_b}{D} \right] + f_2 \left[H_0 - f_1 \frac{R_b}{D} \right]^2 \quad (42)$$

C_R is computed at incremental ship station.

R_b = Bilge radius,

OG = distance (positive downward) from O to G ,

H_0 =half the beam-draft ratio at different stations of the ship (a variable depending on its shape)

$$H_0 = \frac{B}{2D}$$

$$H'_0 = \frac{H_0 D}{D - OG}$$

$$\sigma' = \frac{\sigma D - OG}{D - OG}$$

$$\left\{ \begin{array}{ll} R_b = 2d \sqrt{\frac{H_0(\sigma - 1)}{\pi - 4}} & \text{for } R < D, R < B/2 \\ R_b = D & \text{for } H_0 \geq 1, R/D > 1 \\ R_b = B/2 & \text{for } H_0 \leq 1, R/D > H_0 \end{array} \right.$$

Where s =area coefficient at a cross section along the hull ($\sigma_x = \text{area}/(B_x * D_x)$). The functions, f_1, f_2 , and f_3 are

$$f_1 = 0.5 \left[1 + \tan(h) \{ 20(\sigma - 0.7) \} \right]$$

$$f_2 = 0.5 \left[1 - \cos(\pi\sigma) \right] - 1.5 \left[1 - e^{\{-5(1-\sigma)\}} \right] \sin^2(\pi\sigma)$$

$$f_3 = 1 + 4e^{\{-1.65 \cdot 10^5 (1-\sigma)^2\}}$$

$$\psi = \frac{1}{2} \cos^{-1} \frac{a_1(1+a_3)}{4a_3}$$

The constants a_1, a_2, a_3 are the extinction coefficients derived from fitting the extinction curve in roll with a three degree polynomial in the roll angle.

Ikeda(1984) modified this formula in order to apply it to a rectangular section barge with sharp edges on the corners:

He established his modified formula based on free decay and free roll tests with 2-dimensional models of rectangular cross sections having different breadth to draft ratios.

$$B_{e0} = \frac{2}{\pi} \rho L D^4 (H_0^2 + 1 - OG/D) \left[H_0^2 + (1 - OG/D)^2 \right] R_0 \omega \quad (43)$$

Ikeda(1978a,b) elaborated a formula that takes into account the effect of the forward speed on the eddy damping coefficient:

$$B_e = B_{e0} \left[\frac{(0.04\omega L/U)^2}{1 + (0.04\omega L/U)^2} \right] \quad (44)$$

This formula confirms that the eddy shedding damping decreases with the forward speed.

2.2.5.3. *Lift Damping Coefficient:*

Yumeda et al found a way to express the damping moment by applying the lateral forces formula used in the ship maneuvering field to the roll damping problem.

$$M_L = \frac{1}{2} \rho L d U K_N l_0 l_R \dot{\phi} \quad (45)$$

$$KN = 2\pi \frac{d}{L} + K(4.1B/L - 0.045)$$

$$K = \begin{cases} 0 & \text{for } C_M \leq 0.92 \\ 0.1 & \text{for } 0.92 < C_M \leq 0.97 \\ 0.3 & \text{for } 0.97 < C_M \leq 0.99 \end{cases}$$

C_M is the mid-ship cross-section coefficient (area/BD)c

However *Ikeda et al*, modified the values of the levers l_0 and l_R and proposed the following formula:

$$B_L = 0.5 \rho S_L U k_n l_0 l_R \left\{ 1 - 1.4 \frac{\overline{OG}}{l_R} + 0.7 \frac{\overline{OG}}{l_0 l_R} \right\} \quad (46)$$

Where $l_0 = 0.3 d$ $l_R = 0.5 d$

The lift damping coefficient increases considerably with the forwards speed.

2.2.5.4. *Wave Damping Coefficient:*

Ikeda et al computed the wave damping through an analytical formula derived from the case of a flat plate in current by introducing a pair of doublets at the two longitudinal ends.

$$B_W = B_{W0} \frac{1}{2} \left\{ [(A_2 + 1) + (A_2 - 1) \tan 20(\tau - 0.3)] + (2A_1 - A_2 - 1) e^{(-150[\tau - 0.25])^2} \right\} \quad (47)$$

Where:

$$A_1 = 1 + \xi_d^{-1.2} e^{(-2\xi_d)}$$

$$A_2 = 0.5 + \xi_d^{-1} e^{(-2\xi_d)}$$

$$\xi_d = \omega^2 d / g$$

$$\tau = U \omega / g$$

The previous formula was compared with experimental results as shown in the figure5.

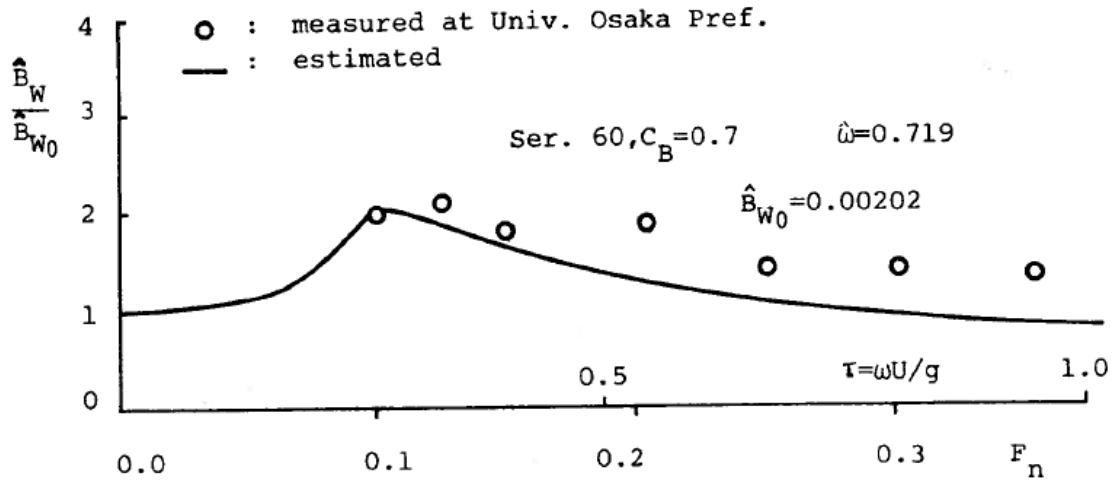


Figure 5: Effect of advance speed on wave component
(Ikeda 1978)

One of the first methods to determine the wave damping was the strip theory. In fact, solving a two dimensional wave problem using strip theory leads to the following formula:

$$B'_{W0} = \rho N_s (l_w - OG)^2 \quad (48)$$

N_s : sway damping coefficient

L_w : the moment lever measured from the point O due to the sway damping force.

2.2.5.5. Bilge Keel Damping:

• Normal force damping of bilge keel:

In the case of zero forward speed, the drag force expression of a body in oscillatory motion can be applied to the problem of the bilge keel drag.

$$F = C_D \frac{1}{2} \rho A |V| |V| \quad (49)$$

Where C_D is the drag coefficient which is known to vary in function of the Keulegan-Carpenter number (VT/D) where V is the max speed $|V_{max}|$, T is the period and D the maximum projected breadth.

By substituting each of the terms of the Keulegan-Carpenter number (V by $\pi r \phi_A$ and T is substituted by $2\pi/\omega$ and D by $2b_{BK}$), Ikeda et al modified the expression of the Keulegan-Carpenter number and proposed a new form of the bilge keel drag.

$$C_D = 22.5 \frac{b_{BK}}{\pi r \phi_A} + 2.4 \quad (50)$$

In order to obtain a good prediction of the normal force damping of the bilge keel, Ikeda et al had to modify the equation (49) by substituting A by b_{BK} per unit length and multiplying the velocity by an empirical coefficient f given by:

$$f = 1 + 0.3e^{\{-160(1-\sigma)\}} \quad (51)$$

The normal force damping of the bilge keel then becomes:

$$B'_{BKN0} = \frac{8}{3\pi} \rho r^2 b_{BK}^2 \omega f^2 \left\{ \frac{22.5}{\pi f} + 2.4 \frac{r\phi_A}{b_{BK}} \right\} \quad (52)$$

This formula showed good agreement with experimental results:

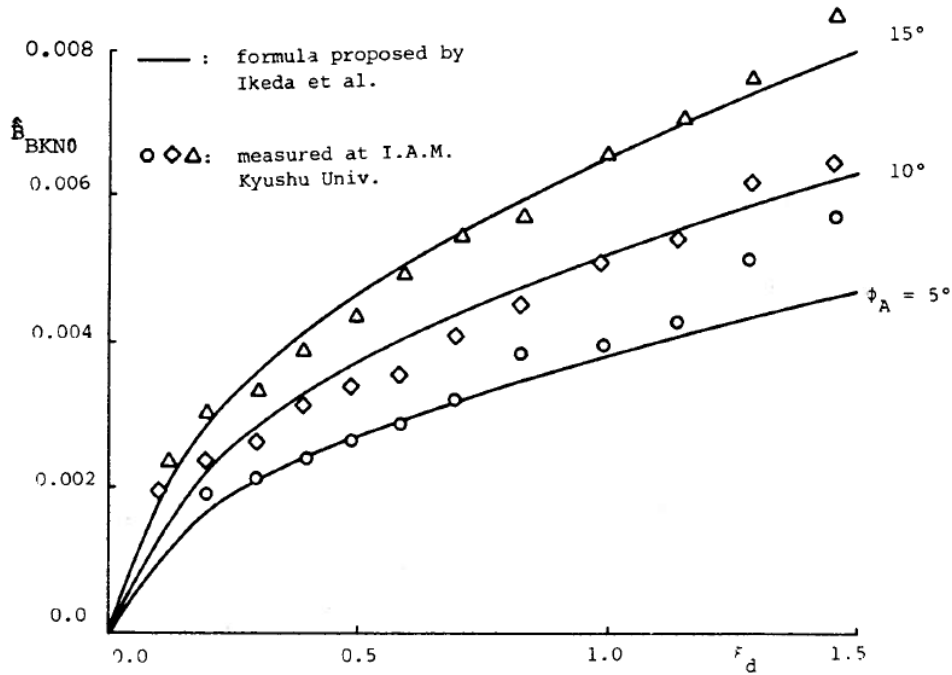


Figure 6 : Comparison of normal force damping of the bilge keel by Ikeda et al and experiments (Ikeda, 1978)

Yuasa et al used the approximation of low-aspect wings to the case of bilge keels then the normal-force damping can be expressed in the form:

$$B_{BKN} = B_{BKN0} + \frac{\pi}{2} \rho b_{BK}^2 r^2 U \quad (53)$$

- **Hull pressure damping due to bilge keels:**

Using a similar methodology as the one used in the previous part concerning the expression of C_D , Ikeda et al expressed the difference in hull pressure between the case with bilge keel and the case without bilge keel as expressed in the formula (54):

$$p = C_p \frac{1}{2} \rho |V_\phi| V_\phi \quad (54)$$

V_ϕ is the instantaneous relative velocity at bilge given by $V_\phi = f r \dot{\phi}$

f is the same coefficient used in the previous section.

C_p was determined experimentally by Ikeda et al in the form of a distribution around the ship hull as shown in figure 7.

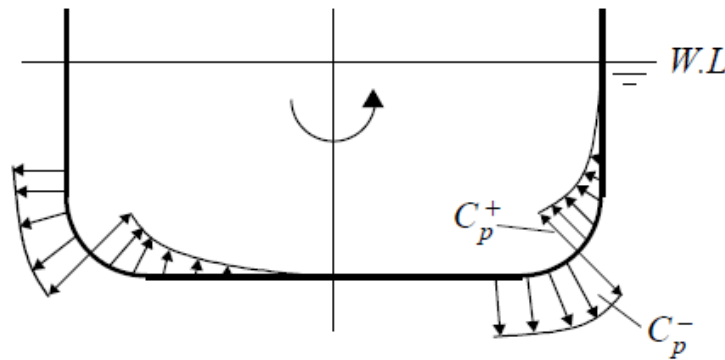


Figure 7: pressure distribution around the hull due to presence of bilge keel
(ITTC – Recommended Procedures 7.5-02-07-04.5, 2011, Page 1 of 33 Numerical Estimation of Roll Damping)

Using the previous distribution, Ikeda et al proposed a formula the pressure damping of the bilge keel.

$$\begin{cases} B_{BKH0} = \frac{4}{3\pi} \rho r^2 d^2 \omega \phi_A f^2 I \\ I = \frac{1}{d^2} \int C_p l_0 ds \end{cases} \quad (55)$$

I is an integration all around the hull circumference

l_0 is the lever moment around the rotation axis.

- **Wave damping of bilge keel:**

Takaki has made a calculation of the contribution of bilge keel on the amplitude of radiation wave but the results showed a huge discrepancy for large roll amplitudes due to the non linear effect of the wave damping.

However, the wave effect of bilge keel can be neglected in case of bilge keels with ordinary breadth of $b_{BK}=B/60$ to $B/80$.

Finally, it's possible to keep only the hull pressure damping due to bilge keel and the normal force damping of bilge keel when dealing with the bilge keel damping.

2.2.6. *Blume Method.*

Blume (1979) method consists on applying time-harmonic exciting roll moment of known frequency and amplitude to a model free in all degrees of freedom and the roll amplitude is measured. Two masses are rotating around a vertical axis in opposite direction with the same frequency of rotation so that the two masses can meet twice per rotation period.

It is required to determine the effective linear roll damping corresponding to the resonance frequency. Therefore the excitation frequency must be varied around the resonance in order to capture the roll resonance frequency ω_ϕ and the corresponding resonance roll amplitude ϕ_{res} .

This procedure is repeated for various amplitudes of the excitation moment and the effective linear roll damping is plotted versus the resonance roll amplitude ϕ_{res} .

A static moment M results in a heel angle $\phi_{stat} = M/C_\phi$, where $C_\phi = \mathbf{m} \mathbf{g} \mathbf{GM}_t$ is the stiffness coefficient and m is the mass displacement. Applying a harmonically oscillating moment $M \sin(\omega_\phi t)$ with the same amplitude M at the resonance frequency $\omega_\phi = \sqrt{C_\phi / I_\phi}$ where I_ϕ is the moment of inertia with respect to the roll axis (including added moment of inertia), can be described by a linearised uncoupled roll equation.

$$\ddot{\phi} + b_{eff} \dot{\phi} + C_\phi \phi = M \sin(\omega_\phi t) \quad (56)$$

Where b_{eff} is the coefficient of the equivalent linear roll damping, and ϕ is the roll angle.

Although the same masses are used to create the static heeling moment M and the harmonically oscillating moment, the amplitude of the harmonically oscillating excitation moment is different from M due to the centrifugal force.

This fact has to be taken into account while performing the experiments and the results must be corrected so that the static heeling moment and the amplitude of the harmonic excitation moment in the previous equation can be assumed equal. (*Blume, 1979*).

2.2.7. Miller method:

Miller et al (1974) developed a method to predict the roll damping of typical naval ships for preliminary design purposes. It is based mainly on the results of a regression analysis of a set of round bottom slender ships of the US Navy.

Miller's method requires two steps to determine the roll damping coefficient. The first step is to determine the zero speed damping ratio according to the following formula:

$$\beta^0(|\bar{\eta}_4|) = 19.25 \left[A_{BK} \sqrt{b_{BK}} + 0.0024 L \cdot B \sqrt{d} \right] d^2 \sqrt{d |\bar{\eta}_4|} / (C_B L \cdot B^3 T) \quad (56)$$

Next step is to compute the critical damping at forward speed:

$$\beta^*(|\bar{\eta}_4|) = \beta^{(0)}(|\bar{\eta}_4|) + 0.00085(L/B) \sqrt{L/\overline{GM}} F \{1 + F + 2F^2\} \quad (57)$$

Where:

A_{BK} is the total area of the bilge keels (port and starboard),

b_{BK} is the width of the bilge keel, C_B is the block coefficient,

d is the distance from the centerline at the load waterline to the turn of the bilge, L , B and T are the ship's length, beam and draft, respectively, is the roll amplitude in radians.

η_4 : Roll amplitude

$F = Fn/C_B$ with F_n is the Froude number.

This method is very easy to use but probably not always available, especially for ships with relatively high block coefficient.

3. THEORY BEHIND THE NUMERICAL TOOLS USED FOR THE ESTIMATION OF ROLL DAMPING:

3.1. Overview Of Roll Motion Analysis Models:

Generally, in seakeeping analysis, potential flow simulation codes are the most commonly used. The reason is that they give satisfactory accuracy at low computational time and they are less expensive in terms of number of CPU and memory required. Nevertheless, this kind of simulation tool needs additional corrections to account for the viscous effect. When it comes to roll prediction, additional explicit roll damping model is added to the code in order to improve the roll motion analysis accuracy.

The application of these potential flow codes in roll damping is generally focused on small and moderate roll amplitudes. In this case, both time domain and frequency domain formulations are available to be used depending on the level of non linearity included and the type of output desired.

Frequency domain method is advantageous to evaluate hydrodynamic and structural concerns involving natural frequency and modal problems. It is usually associated with strip theory which makes it even less computationally intensive but still accurate enough to treat the vessels motion as damped, low amplitude sinusoidal motions. One of the widely used frequency domain roll motion methods is the Ikeda component analysis method.

The main difference between frequency and time domain methods is that for frequency domain methods, the response for a particular frequency is calculated in one step, whereas time domain methods require many thousands of time steps before a regular periodic response is achieved. Hence time domain methods require several orders of magnitude more computing resource than frequency domain methods.

Time domain method allows accounting for the nonlinearities in roll damping and obtaining time histories of ship motion. Generally, forces on the hull are computed by integrating the water pressure and frictional forces on each part of the hull. Roll damping linear and non linear components are usually determined using a data regression analysis namely roll decay or forced roll oscillations. This method does not account for frequency dependence because it requires a large number of tests to capture this frequency dependence.

In the further parts, an example of frequency domain potential theory code will be presented and the theory behind the numerical tools that are used in this study will be detailed.

3.2.Potential Flow Solver Based On Strip Theory: PD strip:

PDSTRIP is an open-source computer program used to calculate the seakeeping of ships and other floating bodies according to the Ordinary Strip Theory of Korvin-Kroukowsky and Jacobs. The program was originally written in FORTRAN 77 by Söding (the program was called STRIP) and then was translated into FORTRAN 90/95 by Bertram and made publicly available in 2006. PDSTRIP includes the features to study the seakeeping of commercial vessels and other particular routines to study the seakeeping of the sailing yachts.

3.2.1. Roll Response Prediction With PDstrip:

Responses in regular waves are given as response amplitude operators, i.e. as ratio between the complex amplitude of a response and the complex amplitude of the wave causing that response. For so-called linear responses this ratio is independent from wave amplitude. PDSTRIP is mainly confined to such linear responses; however, it takes into account a few nonlinear effects.

Responses in natural seaways are given as significant amplitudes. These are defined as the average of the one-third largest positive maxima of the response, neglecting the 2/3 smaller positive maxima.

PDSTRIP can handle unsymmetrical bodies including heeled ships. Forces on fins or sails can be taken into account. The water may be deep or shallow, but the water depth must be constant in space and time. PDSTRIP cannot deal with multi-hulls like catamarans etc.

PDstrip can take into account the effect of the appendages (rudder or bilge keels...) and can introduce their contribution to the roll damping. In fact, all the characteristics of the appendages can be taken into account in the part of the input entitled "fins".

In fact, it's possible to include the desired number of fins, dimensions, their position, and orientation, their motion (fixed or rotating)...Besides, it's possible to include sails in the case of sailing yachts. For only one computation time, PDstrip can give the RAO's of the 6 DOF, taking into consideration, the desired number of wave frequencies and encounter frequencies by giving the possibility to input different ship forward speed and different wave incidence angles.

Regarding the roll motion, PDstrip is an interesting tool that can answer our inquiries about the damping coefficient by providing the RAO in roll for regular or irregular sea.

3.2.2. Strip Method in PDStrip:

3.2.2.1. Fundamental Equations:

Like any potential flow solver the velocity potential has to satisfy the following conditions:

Laplace equation:

Within the fluid region, to enforce the condition of incompressibility:

$$\varphi_{yy} + \varphi_{zz} = 0 \text{ for } z > 0 \text{ outside of the body}$$

(Indices y and z designate partial derivatives with respect to y , z .)

Bottom condition:

For shallow water: $\varphi_z = 0$ at $z = H$

For deep water: $\lim_{z \rightarrow \infty} \varphi_z = 0$

H denotes the water depth.

Free-surface condition:

At the undisturbed free surface, a condition combining the conditions of constant pressure and no flow through the real (wavy) surface, linearized with respect to wave steepness, yields:

$$\varphi_{tt} - g\varphi_z = 0 \text{ at } z = 0$$

Hull boundary condition:

There is no flow through the (submerged part of the) hull contour:

$$\nabla\varphi \cdot \vec{n} = \vec{v} \cdot \vec{n} \text{ along the contour}$$

\vec{v} is the motion velocity of the body at the respective contour point, and \vec{n} is the (inward)unit normal on the contour.

Radiation condition:

Waves created by the hull propagate away from the hull. To formulate this as a boundary condition, the formula for linear shallow-water (Airy) waves is applied:

$$\phi = \text{Re} \left[\frac{-ic\hat{\zeta}}{\sinh(kH)} \cosh(k[z-H]) e^{i(\omega t \mp ky)} \right] \quad (58)$$

In the argument of the exponential function the $-$ sign holds for waves running in $+y$ direction, and the $+$ sign for waves running in opposite direction. Thus the two signs hold for the sides $y > 0$ and $y < 0$ of the body, respectively.

In order to obtain the numerical solution a patch method is used (*Soeding (1993), Bertram (2000)*). This method is very advantageous the way it computes the forces more accurately than a traditional panel method. The patch method approximates the potential $\hat{\phi}$ as a superposition of point sources.

$$\hat{\phi}(y, z) = \sum_{i=1}^n q_i \frac{1}{2} \ln \left[(y - y_i)^2 + (z - z_i)^2 \right] \quad (59)$$

where q_i are the source strengths of the n sources at locations (y_i, z_i) . This satisfies the Laplace equation everywhere except at the location of the sources (y_i, z_i) which are therefore located within the section contour or above the line $z = 0$.

Near the midpoint between every two offset point that define the section contour, one source is generated. This source is shifted from the midpoint to the interior of the section by 1/20 of the segment length. Along the average water surface $z = 0$ grid points are generated automatically. Near to the body, their distance is equal to 1.5 of the offset point distance on the contour at the waterline. Farther to the sides, the distance increases by a factor of 1.5 from one segment to the next, until a maximum distance of 1/12 of a wavelength (of the waves generated by the body oscillations) is attained.

Whereas in the panel method the boundary conditions are, usually, satisfied at a ‘collocation point’ in the middle of each segment, in the patch method the integral of the boundary condition over each segment has to be used.

The linear equation system resulting from the boundary conditions is solved for the complex amplitudes of all source strengths. The flow potential follows then from (15). According to Bernoulli’s equation, the complex amplitude of the pressure is:

$$p = -\rho\phi_t$$

This pressure amplitude is integrated over the section contour to give the complex amplitudes of horizontal force, vertical force and x (roll) moment, each for horizontal, vertical and rolling motion of the section with unit amplitude. (BERTRAM, SÖDING (2006)).

3.2.2.2. *Determination Of the Response Amplitude Operator RAO*

PDStrip is based on the fundamental equation of motion written in frequency domain as follows:

$$(-\omega_e M - B + S)\hat{u} = \hat{F}_e \quad (60)$$

Where

$u = \{u_1, u_2, u_3, u_4, u_5, u_6\}^T$ is the response in the six degrees of freedom, (surge u_1 , sway u_2 , heave u_3 , roll u_4 , pitch u_5 , yaw u_6),

$\omega_e = \omega - kv \cos \mu$ is the encounter frequency.

$k = 2\pi/\lambda$ is the wave number,

ω the wave frequency,

v the ship speed and μ the wave direction.

The $\hat{\cdot}$ symbol indicates generally a complex amplitude. M is the real mass matrix of the ship, S is the real matrix due to hydrostatics, B is the complex matrix due to ship motions (added mass and damping) and \hat{F}_e are the excitation forces due to the incident wave and its diffraction. In general B is calculated from 2D hydrodynamic forces exerted from the water on a sectional strip moving periodically. The 3-component motion amplitude vector

of the strip $\hat{u}_x = \{\hat{u}_2, \hat{u}_3, \hat{u}_4\}^T$ is related to the respective force vector $\hat{f}_x = \{\hat{f}_2, \hat{f}_3, \hat{f}_4\}^T$ by:

$$\hat{f}_x = \begin{pmatrix} \bar{m}_{22} & \bar{m}_{23} & \bar{m}_{24} \\ \bar{m}_{32} & \bar{m}_{33} & \bar{m}_{34} \\ \bar{m}_{42} & \bar{m}_{43} & \bar{m}_{44} \end{pmatrix} \omega_e^2 \hat{u}_x \quad (61)$$

The elements of the complex added mass matrix in (61) can be interpreted as real value added masses m_{ij} and damping n_{ij} :

$$\bar{m}_{ij} = m_{ij} + \frac{n_{ij}}{i\omega_e} \quad (62)$$

This illustrates the relation between complex added mass, real added mass and damping. A corresponding relation holds for the complex added mass matrix, the real added mass matrix and the real damping matrix, which result from combining the 3 forces due to 3 motions within a 3×3 matrix.

The desired motion amplitude can be calculated by solving the above equation once the matrices B and S are computed in parallel with the exciting forces and the fin forces. (BERTRAM, SÖDING (2006)).

3.2.3. Inputs:

PDstrip requires the implementation of two input files, a geometry input file and a data input file. In the geometry file details about each section has to be provided. For instance, the number of sections, whether the hull is symmetric or not, the number of offsets per section and the coordinates of each offset point.

The data input file includes details about the required output data, the characteristics of the ship (mass, the center of gravity position, the different gyration radii and moments of inertia), details about the dimensions and locations of the different fins and appendages, details about the location and dimensions of the sails and the conditions of the simulation (Wave steepness, wave height, different wave lengths, forward speed and the wave heading angles).

3.2.4. Outputs:

The following responses are computed and are presented in different output files.

- Translations in directions x, y, z of the ship-fixed coordinate origin
- Rotations around the three coordinate axes
- The translation of specified points on the body in 3 coordinates directions
- The relative translation between these points and the water. Here the water is assumed to be disturbed by the incident waves, but not by the ship.
- The acceleration at these points; if required, after weighing with a function of motion frequency (encounter frequency)
- The pressure at a specified number of points on each offset section
- Sectional force (3 components) and moment (3 components) in cross sections (x = constant) of the body.
- Longitudinal and transverse drift force on the body
- Water drift velocity in a specified height.

3.3. Component Analysis Programs:

3.3.1. IKEDA Roll Damping Prediction Computer Program: RDPM: (Ikeda 1978)

It is a code written in FORTRAN77. The theory behind it is the component discrete type roll damping prediction method described in the previous chapter. This program was developed in Osaka Prefecture University. The advantage brought by this code compared to potential theory code is the fact that it is able to predict the viscous effect which affects significantly the roll motion amplitude. This prediction relies on empirical estimation method developed for general cargo type of ships.

This method is based mainly on the computation of five components which are friction component, wave making component, eddy making component, lift component and bilge-keel component. Since these components were described earlier, the following part will only contain a brief explanation of how each component was implemented in this code.

- **Frictional Component :**

Here Ikeda used the modified Kato's formula at $F_n=0$; (different from the Kato's formula stated in the previous chapter) and he accounted for the forward speed effect using the Tamiya advanced speed modification.

$$B_F = \frac{4}{3\pi} \rho S_f r_f^3 \phi_0 \omega C_f \left(1 + 4.1 \frac{U}{\omega L} \right) \quad (63)$$

C_f (the equivalent flat plate frictional coefficient), r_f (the equivalent radius), S_f (the surface area) are presented in the following equations.

$$C_f = 1.328 \left(3.22 \frac{r_f^2 \phi_0^2}{T \nu} \right)^{-0.5}$$

$$r_f = \frac{(0.887 + 0.145 C_b)(1.7d + C_b B) - 2\overline{OG}}{\pi}$$

$$S_f = L(1.75d + C_b B)$$

Where ν is the coefficient of kinematic viscosity, T is roll period, \overline{OG} is distance from the water surface to the center of gravity (down ward +).

Generally, this component represents 8 to 10% of the total roll damping and it is sensitive to Reynolds effect (scale effect).

- **Wave Making Component**

This method does not give any estimation formula for this component but it can be calculated at $F_n=0$ and inserted as an input value B_{w0} . The effect of forward speed is taken into account using the following modification equation:

$$\frac{B_w}{B_{w0}} = 0.5 \left[(A_2 + 1) + (A_2 - 1) \tanh 20(\Omega - 0.3) \right] + (2A_1 - A_2 - 1) \exp \left\{ -150(\Omega - 0.25)^2 \right\} \quad (64)$$

$$A_1 = 1 + \xi_d^{-1.2} \exp(-2\xi_d)$$

$$A_2 = 0.5 + \xi_d^{-1.0} \exp(-2\xi_d)$$

$$\xi_d = \frac{\omega^2 d}{g}, \quad \Omega = \frac{\omega U}{g}$$

This component represents 5 to 30 % of the total roll damping and it could be greater for shallow draught and large section vessels.

- **Eddy Making Component by Naked Hull**

A first order equation is derived from the measured results of the two dimensional models with various shapes of cross-sections in order to approximate the pressure distribution on the hull caused by eddies.

$$B_E = \frac{4}{3\pi} \rho L d^2 r_m^2 \phi_0 \omega \left\{ \left(1 - f_1 \frac{R}{d} \right) \left(1 - \frac{OG}{d} - f_1 \frac{R}{d} \right) + f_2 \left(H_0 - f_1 \frac{R}{d} \right)^2 \right\} C_p \quad (65)$$

$$f_1 = 0.5[1 + \tanh\{20(\sigma - 0.7)\}]$$

$$f_2 = 0.5(1 - \cos \pi\sigma) - 1.5[1 - \exp\{-5(1 - \sigma)\}]\sin^2 \pi\sigma$$

$$C_p = 0.5\{0.87 \exp(-\gamma) - 4 \exp(-0.187\gamma) + 3\}$$

γ in the previous equation is the ratio of the maximum current velocity and mean velocity on the hull surface. This can be obtained by the calculation for the Lewes form section. The eddy making component decreases quickly with the increment of forward speed. The forward speed effect is approximately expressed with the following equation.

$$\frac{B_E}{B_{E0}} = 0.5 \frac{(0.04K)}{\{(0.04K)^2 + 1\}} \quad \text{Where, } K = \frac{L\omega}{U}$$

- **Lift Component by Naked Hull**

The lift component is given by:

$$B_L = 0.5 \rho S_L U k_n l_0 l_R \left\{ 1 - 1.4 \frac{\overline{OG}}{l_R} + 0.7 \frac{\overline{OG}}{l_0 l_R} \right\} \quad (66)$$

$$\text{where } l_0 = 0.3d, \quad l_R = 0.5d$$

K_n is the lift gradient used in maneuverability calculations given by:

$$k_n = 2\pi \frac{d}{L} + \kappa \left(4.1 \frac{B}{L} - 0.045 \right) \quad (67)$$

The previous equation for lift component is only available for bare hull. We can proceed the same way to calculate the lift coming from large bilge keels or skeg and so on.

- **Bilge Keel Component :**

Only two parts of the bilge keel component are considered in this Ikeda prediction code: the hull surface pressure component and the normal pressure component on bilge keel. The normal pressure component on the bilge keel is given by the following equation.

$$B_N = \frac{4}{3\pi} \rho r^3 l_{BK} b_{BK} \phi_0 \omega f^2 \left(22.5 \frac{b_{BK}}{r\pi f \phi_0} + 2.4 \right) \quad (68)$$

f is the modification coefficient about a bilge radius:

$$f = 1 + 0.3 \exp\{-160(1 - \sigma)\}$$

Where, r is the distance from the center of rolling to the bilge-keel, b_{BK} and l_{BK} are the width and length of a bilge keel, ϕ_0 is roll amplitude. .

In this code two types of algorithms can be chosen (1) is the simplified estimation method. (2) is the method that the attachment condition of a bilge keel can be more correctly taken into consideration. The algorithm (2) is recommended for fine ship type.

- **INPUT DATA & OUTPUT DATA**

The input file name of the following program is "OSM.RDP", an output file name is "OSMB44.CSV", and both files are text files. The input file is written the calculated conditions which are:

Hull data (for each section the coordinates of each offset point are given, L_{pp}, T, B , number of cross sections, number of midship sections)

Bilge keel dimension and position

Forward speed

Roll amplitude,

Wave period and wave direction (roll period).

Position of the center of gravity.

In the output file, the conditions of calculation, the calculated roll damping coefficient and its components are written.

3.3.2. *Ikeda Simple Formulas Program for the Prediction Of Roll Damping.*(Ikeda 2010)

Ikeda original prediction method built according to the strip theory procedure seems to be complicated in the simple design stage of a ship. Therefore, a simple prediction method was developed on the basis of this original method using a (Kawahara et al 2008) regression analysis.

The simplicity of this method resides on the use of the basic ship dimensions and aspect ratios of the hull form and bilge keel.

This method proposes a simple prediction formula for only four components: the frictional, the wave, the eddy and the bilge keel components at zero advance speed.

The nondimensionalization of the roll damping coefficient (B_{44}) and circular frequency ($\omega=2\pi/T_\omega$) are defined as follows:

$$\hat{B}_{44} = \frac{B_{44}}{\rho \nabla B^2} \sqrt{\frac{B}{2g}}$$

$$\hat{\omega} = \omega \sqrt{\frac{B}{2g}}$$

Where ρ denotes water density, ∇ displacement volume, B beam and g is gravity acceleration, respectively.

The relationship between B_{44} and N coefficient (Bertin) is as follows.

$$N = \hat{B}_{44} \frac{\pi B \hat{\omega}}{GM \varphi_a}$$

- **Frictional Component (B_F) :**

The frictional component is computed the same way as the original Ikeda prediction method as detailed in the previous part.

- **Wave component (B_W) :**

The proposed formula for the wave component is the following:

$$x_1 = B/d, x_2 = C_b, x_3 = C_m, x_4 = 1 - OG/d, x_5 = \hat{\omega}$$

$$\hat{B}_W = A_1/x_5 \cdot \exp(-A_2(\text{LOG}(x_5) - A_3)^2/1.44)$$

$$A_1 = (A_{11}x_4^2 + A_{12}x_4 + A_{13})AA_1$$

$$A_2 = -1.402x_4^3 + 7.189x_4^2 - 10.993x_4 + 9.45$$

$$A_3 = A_{31}x_4^6 + A_{32}x_4^5 + A_{33}x_4^4 + A_{34}x_4^3 + A_{35}x_4^2 + A_{36}x_4 + A_{37} + AA_3$$

$$x_6 = x_4 - AA_2$$

$$AA_1 = (AA_{11}x_3 + AA_{12}) \times (1 - x_4) + 1.0$$

$$AA_3 = AA_{31}(-1.05584x_6^9 + 12.688x_6^8 - 63.70534x_6^7 +$$

$$172.84571x_6^6 - 274.05701x_6^5 + 257.68705x_6^4 - 141.40915x_6^3$$

$$+ 44.13177x_6^2 - 7.1654x_6 - 0.0495x_1^2 + 0.4518x_1 - 0.61655)$$

$$AA_{31} = (-0.3767x_1^3 + 3.39x_1^2 - 10.356x_1 + 11.588) \cdot AA_{311}$$

$$AA_{32} = -0.0727x_1^2 + 0.7x_1 - 1.2818$$

$$AA_{311} = (-17.102x_2^3 + 41.495x_2^2 - 33.234x_2 + 8.8007) \cdot x_4 +$$

$$36.566x_2^3 - 89.203x_2^2 + 71.8x_2 - 18.108$$

$$A_{31} = -7686.0287x_2^6 + 30131.5678x_2^5 - 49048.9664x_2^4 +$$

$$42480.7709x_2^3 - 20665.147x_2^2 + 5355.2035x_2 - 577.8827$$

$$A_{32} = 61639.9103x_2^6 - 241201.0598x_2^5 + 392579.5937x_2^4 -$$

$$340629.4699x_2^3 + 166348.6917x_2^2 - 43358.7938x_2 + 4714.7918$$

$$A_{33} = -130677.4903x_2^6 + 507996.2604x_2^5 - 826728.7127x_2^4$$

$$+ 722677.104x_2^3 - 358360.7392x_2^2$$

$$+ 95501.4948x_2 - 10682.8619$$

$$A_{34} = -110034.6584x_2^6 + 446051.22x_2^5 - 724186.4643x_2^4$$

$$+ 599411.9264x_2^3 - 264294.7189x_2^2$$

$$+ 58039.7328x_2 - 4774.6414$$

$$A_{35} = 709672.0656x_2^6 - 2803850.2395x_2^5 + 4553780.5017x_2^4$$

$$- 3888378.9905x_2^3 + 1839829.259x_2^2$$

$$- 457313.6939x_2 + 46600.823$$

$$A_{36} = -822735.9289x_2^6 + 3238899.7308x_2^5 - 5256636.5472x_2^4$$

$$+ 4500543.147x_2^3 - 2143487.3508x_2^2$$

$$+ 538548.1194x_2 - 55751.1528$$

(Ikeda 2010)

$$\begin{aligned}
A_{37} &= 299122.8727x_2^6 - 1175773.1606x_2^5 + 1907356.1357x_2^4 \\
&\quad - 1634256.8172x_2^3 + 780020.9393x_2^2 \\
&\quad - 196679.7143x_2 + 20467.0904 \\
AA_{11} &= AA_{111}x_2^2 + AA_{112}x_2 + AA_{113} \\
AA_{12} &= AA_{121}x_2^2 + AA_{122}x_2 + AA_{123} \\
AA_{111} &= 17.945x_1^3 - 166.294x_1^2 + 489.799x_1 - 493.142 \\
AA_{112} &= -25.507x_1^3 + 236.275x_1^2 - 698.683x_1 + 701.494 \\
AA_{113} &= 9.077x_1^3 - 84.332x_1^2 + 249.983x_1 - 250.787 \\
AA_{121} &= -16.872x_1^3 + 156.399x_1^2 - 460.689x_1 + 463.848 \\
AA_{122} &= 24.015x_1^3 - 222.507x_1^2 + 658.027x_1 - 660.665 \\
AA_{123} &= -8.56x_1^3 + 79.549x_1^2 - 235.827x_1 + 236.579 \\
A_{11} &= A_{111}x_2^2 + A_{112}x_2 + A_{113} \\
A_{12} &= A_{121}x_2^3 + A_{122}x_2^2 + A_{123}x_2 + A_{124} \\
A_{13} &= A_{131}x_2^3 + A_{132}x_2^2 + A_{133}x_2 + A_{134} \\
A_{111} &= -0.002222x_1^3 + 0.040871x_1^2 - 0.286866x_1 + 0.599424 \\
A_{112} &= 0.010185x_1^3 - 0.161176x_1^2 + 0.904989x_1 - 1.641389 \\
A_{113} &= -0.015422x_1^3 + 0.220371x_1^2 - 1.084987x_1 + 1.834167 \\
A_{121} &= -0.0628667x_1^4 + 0.4989259x_1^3 + 0.52735x_1^2 \\
&\quad - 10.7918672x_1 + 16.616327 \\
A_{122} &= 0.1140667x_1^4 - 0.8108963x_1^3 - 2.2186833x_1^2 \\
&\quad + 25.1269741x_1 - 37.7729778 \\
A_{123} &= -0.0589333x_1^4 + 0.2639704x_1^3 + 3.1949667x_1^2 \\
&\quad - 21.8126569x_1 + 31.4113508 \\
A_{124} &= 0.0107667x_1^4 + 0.0018704x_1^3 - 1.2494083x_1^2 \\
&\quad + 6.9427931x_1 - 10.2018992 \\
A_{131} &= 0.192207x_1^3 - 2.787462x_1^2 + 12.507855x_1 - 14.764856 \\
A_{132} &= -0.350563x_1^3 + 5.222348x_1^2 - 23.974852x_1 + 29.007851 \\
A_{133} &= 0.237096x_1^3 - 3.535062x_1^2 + 16.368376x_1 - 20.539908 \\
A_{134} &= -0.067119x_1^3 + 0.966362x_1^2 - 4.407535x_1 + 5.894703 \\
&\quad \left(\begin{array}{l} 0.5 \leq C_b \leq 0.85, \quad 2.5 \leq B/d \leq 4.5, \quad \hat{\omega} \leq 1.0 \\ -1.5 \leq OG/d \leq 0.2, \quad 0.9 \leq C_m \leq 0.99 \end{array} \right)
\end{aligned}$$

(Ikeda 2010)

- **Eddy Component (B_E)**

The formula proposed by this method to determine the roll damping is the following:

$$\begin{aligned}
 x_1 &= B/d, x_2 = C_b, x_3 = C_m, x_4 = OG/d \\
 \hat{B}_E &= \frac{4 L_{pp} d^4 \hat{\omega} \varphi_a}{3 \pi \nabla B^2} C_R = \frac{4 \hat{\omega} \varphi_a}{3 \pi x_2 \cdot x_1^3} C_R \\
 C_R &= A_E \cdot \exp(B_{E1} + B_{E2} \cdot x_3^{B_{E3}}) \\
 A_E &= (-0.0182x_2 + 0.0155) \cdot (x_1 - 1.8)^3 - 79.414x_2^4 \\
 &\quad + 215.695x_2^3 - 215.883x_2^2 + 93.894x_2 - 14.848 \\
 B_{E1} &= (-0.2x_1 + 1.6) \cdot (3.98x_2 - 5.1525) \cdot x_4 \\
 &\quad \cdot \left\{ (0.9717x_2^2 - 1.55x_2 + 0.723) \cdot x_4 + (0.04567x_2 + 0.9408) \right\} \\
 B_{E2} &= (0.25x_4 + 0.95) \cdot x_4 \\
 &\quad - 219.2x_2^3 + 443.7x_2^2 - 283.3x_2 + 59.6 \\
 B_{E3} &= (46.5 - 15x_1) \cdot x_2 + 11.2x_1 - 28.6 \\
 &\quad \left(\begin{array}{l} 0.5 \leq C_b \leq 0.85, \quad 2.5 \leq B/d \leq 4.5 \\ -1.5 \leq OG/d \leq 0.2, \quad 0.9 \leq C_m \leq 0.99 \end{array} \right)
 \end{aligned}$$

(Ikeda 2010)

- **Bilge Keel component :**

$$\begin{aligned}
 x_1 &= B/d, x_2 = C_b, x_3 = C_m, x_4 = OG/d, x_5 = \hat{\omega} \\
 x_6 &= \varphi_a \text{ (deg)}, x_7 = b_{BK}/B, x_8 = l_{BK}/L_{pp} \\
 \hat{B}_{BK} &= A_{BK} \cdot \exp(B_{BK1} + B_{BK2} \cdot x_3^{B_{BK3}}) \cdot x_5 \\
 A_{BK} &= f_1(x_1, x_2) \cdot f_2(x_6) \cdot f_3(x_7, x_8) \\
 f_1 &= (-0.3651x_2 + 0.3907) \cdot (x_1 - 2.83)^2 - 2.21x_2 + 2.632 \\
 f_2 &= 0.00255x_6^2 + 0.122x_6 + 0.4794 \\
 f_3 &= (-0.8913x_7^2 - 0.0733x_7) \cdot x_8^2 \\
 &\quad + (5.2857x_7^2 - 0.01185x_7 + 0.00189) \cdot x_8 \\
 B_{BK1} &= \{5x_7 + 0.3x_1 - 0.2x_8 \\
 &\quad + 0.00125x_6^2 - 0.0425x_6 - 1.86\} \cdot x_4 \\
 B_{BK2} &= -15x_7 + 1.2x_2 - 0.1x_1 \\
 &\quad - 0.0657x_4^2 + 0.0586x_4 + 1.6164 \\
 B_{BK3} &= 2.5x_4 + 15.75 \\
 &\quad \left(\begin{array}{l} 0.5 \leq C_b \leq 0.85, \quad 2.5 \leq B/d \leq 4.5 \\ -1.5 \leq OG/d \leq 0.2, \quad 0.9 \leq C_m \leq 0.99 \\ 0.01 \leq b_{BK}/B \leq 0.06, \quad 0.05 \leq l_{BK}/L_{pp} \leq 0.4 \end{array} \right)
 \end{aligned}$$

(Ikeda 2010)

- **How the hull form is implemented only from the ship dimensions?**

Depending on the inputted values of the length, beam, draft, midship sectional coefficient and longitudinal prismatic coefficient, the hull shape is changed methodically according to the following formula which is based on the Taylor Standard Series.

$$y_1 = Q(x) + C_p P(x) + f_{11} t T(x) + n N(x) + f_{12} F(x)$$

$$y_2 = Q(x) + C_w P(x) + f_{21} t T(x) + n N(x) + f_{22} F(x)$$

where

$$Q(x) = -30x^2 + 100x^3 - 105x^4 + 36x^5$$

$$P(x) = 60x^2 - 180x^3 + 180x^4 - 60x^5$$

$$T(x) = x - 6x^2 + 12x^3 - 10x^4 + 3x^5$$

$$N(x) = -0.5x^2 + 2x^3 - 2.5x^4 + x^5$$

$$F(x) = -26.562x^6 + 105.74x^5 - 162.71x^4$$

$$+ 116.58x^3 - 34.532x^2 + 0.6998x + 0.7923$$

$$t = -3969.7C_p^6 + 16664.6C_p^5 - 28230C_p^4$$

$$+ 24951C_p^3 - 12205C_p^2 + 3147.7C_p - 335.67$$

(at stern side and $C_p < 0.73$)

$$t = 113.64C_p^2 - 149.68C_p + 50.221$$

(at stern side and $C_p \geq 0.73$)

$$t = 96.339C_p^5 - 173.59C_p^4 + 159.75C_p^3$$

$$- 113.4C_p^2 + 54.123C_p - 10.686$$

(at bow side and $C_p < 0.72$)

$$t = 41.667C_p^2 - 49.167C_p + 14.9$$

(at bow side and $C_p \geq 0.72$)

$$n = 5.7035C_p^3 - 30.16C_p^2 + 33.471C_p - 10.606$$

(at stern side and $C_p < 0.74$)

$$n = -10.417C_p^2 + 13.458C_p - 4.305$$

(at stern side and $C_p \geq 0.74$)

$$n = -1664.6C_p^5 + 5596.7C_p^4 - 7413.2C_p^3$$

$$+ 4815.6C_p^2 - 1525.3C_p + 186.79$$

(at bow side and $C_p < 0.73$)

$$n = 0.625C_p + 0.4312$$

(at bow side and $C_p \geq 0.73$)

(Ikeda 2010)

- **Inputs:**

Length between perpendiculars (L_{pp})

Length / breadth ratio (L_{pp}/B)

Breadth / draft ratio (B/d)

Block coefficient (C_b)

Midship section coefficient (C_m)

Center of gravity / draft ratio (OG/d): OG is plus when the center of gravity is below the calm water surface.

Roll amplitude

Wave period (T_w)

Bilge keel length / L_{pp} ratio (l_{BK}/L_{pp})

Bilge keel breadth / B ratio (b_{BK}/B)

- **Output:**

Non-dimensional frictional damping coefficient (B_F)

non-dimensional wave damping coefficient (B_W)

non-dimensional eddy damping coefficient (B_E)

non-dimensional bilge keel damping coefficient (B_{BK})

non-dimensional roll damping coefficient (B_{44})

Important:

It is noticeable from the output of this method that compared to the previous methods all the components are calculated except the lift component. In fact, all the components at zero forward speed, and at forward speed, the lift (B_L) is added and the forward speed corrections are applied (as well as the Tamyia's formula for the friction component).

3.4. "2DRoll Program": A Flume Software

Any normal up to date seakeeping software, is generally able to predict the ship motion in heave and pitch with a satisfactory accuracy. Whereas, when it comes to lateral plane motions the same accuracy is difficult to reach and significant errors might be obtained.

Therefore a tool adapted with the roll motion analysis is needed to predict the roll RAO. According to the following demonstration it is possible to use 2DRoll to estimate the roll damping from the amplitude of the roll response at the resonance.

In frequency domain, the roll motion equation without any coupling with sway and yaw can be written as follows:

$$\eta_4 = \left[\frac{\omega_0^2 - \omega^2 q + 2in\omega_0\omega}{\omega_0^2 - \omega^2 + 2in\omega_0\omega} \right] \bar{\zeta} e^{i\omega t}$$

Where:

$$\omega_0 = \left(\frac{C_{44}}{A_{44} + I_4} \right)^{1/2}$$

Is the roll natural frequency:

$$q = \frac{A_{44}}{(I_4 + A_{44})}$$

Is the ratio of hydrodynamic moment of inertia to total moment of inertia:

$$n = \frac{B_{44}}{2\omega_0(A_{44} + I_4)} = \frac{\omega_0 B_{44}}{2C_{44}}$$

Is the roll decay coefficient.

At resonance ($\omega = \omega_0$), the previous roll motion equation can be written as:

$$\frac{\eta_4}{\bar{\zeta}} = \left(\frac{1 - q + 2in}{2in} \right) e^{i\omega t}$$

This equation confirms that it is possible to calculate the roll damping which is proportional to (n: roll decay coefficient) once the peak response in resonance is well predicted.

(Schmitke 1978)

4. OBSERVATIONS AND ANALYSIS OF THE NUMERICAL SIMULATIONS USED TO PREDICT THE ROLL DAMPING COMPONENT

4.1. Overview:

Numerical investigation was carried out for three different ships. Three main open source codes were used based on the theoretical methods detailed in the previous chapter. The aim of this numerical study is to examine the efficiency of each numerical tool when it comes to roll damping estimation and to discuss the limitation of each one with regard to the characteristics of each ship and each seakeeping test condition.

The roll motion response, analysed with PDstrip for each ship, for a certain loading condition and different test conditions, is finally exploited to evaluate the quantity of damping that was used to dissipate the roll energy. The test conditions were inspired from the details of the seakeeping test report related to roll decay or forced roll test or model test in regular waves. Furthermore, a direct estimation of the roll damping was carried out by two different Ikeda methods and the results were interpreted and compared.

The results are finally discussed with regard to the ability of the seakeeping tools to predict the real ship motion and the roll damping and their efficiency to include all the nonlinearities surrounding the roll motion. The limitations of each method are highlighted referring to every kind of discrepancy obtained.

4.2. Numerical Simulations for an 8000-9000 TEU container Ship

4.2.1. Estimation of roll damping using IKEDA simple prediction formula

4.2.1.1. Details and conditions of the computation.

This container ship has the following particulars:

$L_{pp}=319\text{m}$

$B=42.8$

$T=15\text{m}$

$GM=2.14$

$LCG=152.31\text{m}$

$\Delta=141428\text{ t}$

Bilge keels: $L_{BK}=101.08\text{ m}$

$H_{BK}=0.4\text{ m}$

Bilge keel aspect ratio= $5.92\text{ e-}3$

Similarly to the forced roll and roll decay tests of an 8000-9000 TEU ship, the Ikeda simple prediction method was carried out in the following conditions:

GM= 2.14 m

Forward speed= 20 Kts

Wave heading: 90° Beam seas.

Roll amplitudes: 1.4°, 3.4°, 4.6°, 7.3°, 13.1°

The forced roll test was carried out around the ship roll natural circular frequency $\omega_n=0.267$ rad/s.

4.2.1.2. Results:

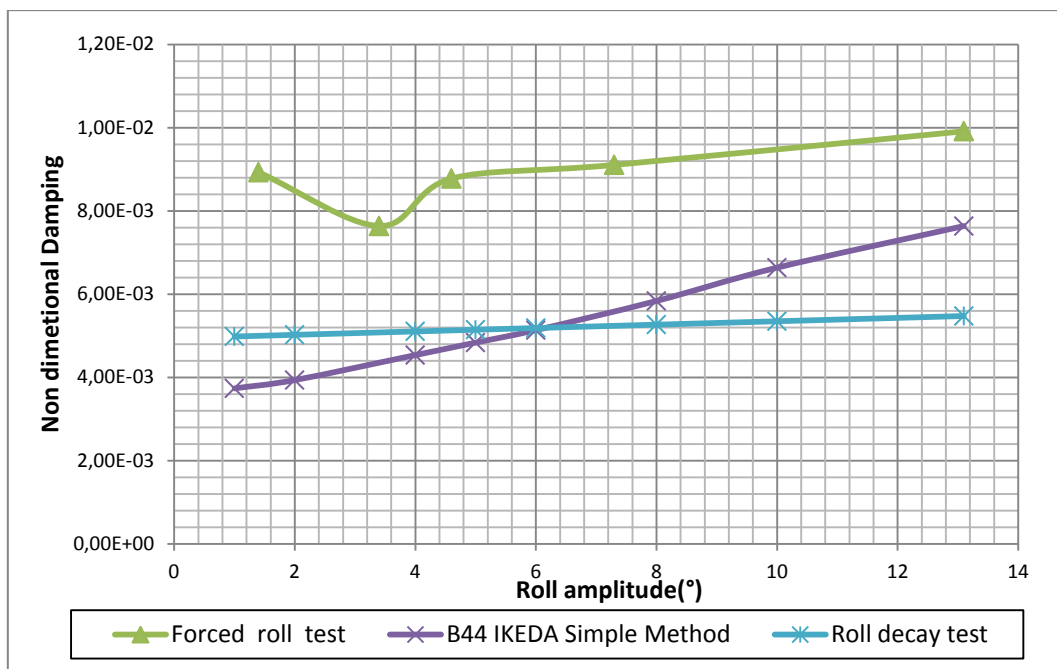


Figure 8: Non dimensional Roll damping coefficient VS Roll amplitude obtained with Roll decay test, Forced roll test and Ikeda simple formulas. FW speed=20Kts, GM=2,14m, 90° Beam seas

Table 5: non dimensional roll damping using forced roll, roll decay test and Ikeda simple formulation

Forced roll test	
Roll Amp	\hat{B}_{44}
1,40E+00	8,93E-03
3,40E+00	7,64E-03
4,60E+00	8,78E-03
7,30E+00	9,11E-03
1,31E+01	9,91E-03

Ikeda Simple Formula	
Roll Amp	\hat{B}_{44}
1	0,003734
2	0,003934
4	0,004534
5	0,004834
6	0,005134
8	0,005834
10	0.006634
13.1	0.007634

Roll decay test	
Roll amp	B44Hat
1	0,00498
2	0,005
4	0,0051
5	0,00514
6	0,005263
8	0,005347
10	0,005473
13,1	0,005473

The damping components given by this method at zero speed are the friction component, the eddy component, the wave component and the bilge keel component. The lift component is added from the Ikeda original method in order to account for the forward speed effect on the roll damping. In this case the added value of the non dimensional lift component obtained from Ikeda original method is $B_L=0,002633799$.

To be able to compare the experimental nondimensional values of the roll damping \hat{B}_{44} , the nondimensionalization convention presented by IKEDA is used to nondimensionalize both the results of forced roll and roll decay test.

$$\hat{B}_{44} = \frac{B_{44}}{\rho \Delta B^2} \sqrt{\frac{B}{2g}}$$

$$\hat{\omega} = \omega \sqrt{\frac{B}{2g}}$$

4.2.1.3. *Interpretation of the results:*

It is obvious that the roll damping obtained by the Ikeda simple formula is underestimated compared to the forced roll test results. However it is still in the same range of the Roll decay test results. This may be reflected by the fact that the Ikeda method is derived from an experimental data base composed mainly of roll decay tests.

Generally, the accuracy of the Ikeda simple method is affected by the position of the center of gravity. A very high position of the center of gravity leads to more discrepancy with the experimental results. This fact will be detailed the further sections.

A forced roll test is carried out in a constant known roll forcing moment, while the presented roll decay test was based on a random initial inclination angle. The initial inclination angle has a big influence on the whole range of roll damping coefficients obtained and this might lead to different results with the forced roll test. This influence will be proved in the case of the third test case (DTMB 5415) roll decay analysis.

Another suspected reason for this disagreement with the forced roll test results is that whenever the roll natural period is long, the wave component basically and many other components particularly are quite low. In fact, large container ship with flat hull shape always have longer natural roll period and it is the case for this 8000-9000 TEU container ship. A relatively high roll period means that the moment due to the waves radiated when the ship rolls is low compared to the moment corresponding to a lower period. This could result in a lower wave damping component.

4.2.2. Prediction Using Ikeda Computer Program :

4.2.2.1. Details And Conditions Of the computation.

The following conditions were set in the input file of the Ikeda Program:

GM= 2.14 m

Froud number $F_n= 0.179$ corresponding to a Forward speed= 20 Kts

Wave heading: 90° Beam seas.

Roll amplitudes: 1.4°, 3.4°, 4.6°, 7.3°, 13.1°

The ratio wave length/ $L_{pp}= 2.6$ which corresponds to the natural frequency $\omega_n=0.267$ rad/s

In this method the loading condition is to be inputted by fixing the corresponding draft (in this case $T=15$ m). The displacement is then calculated by integrating the waterline area through the sections.

4.2.2.2. Results:

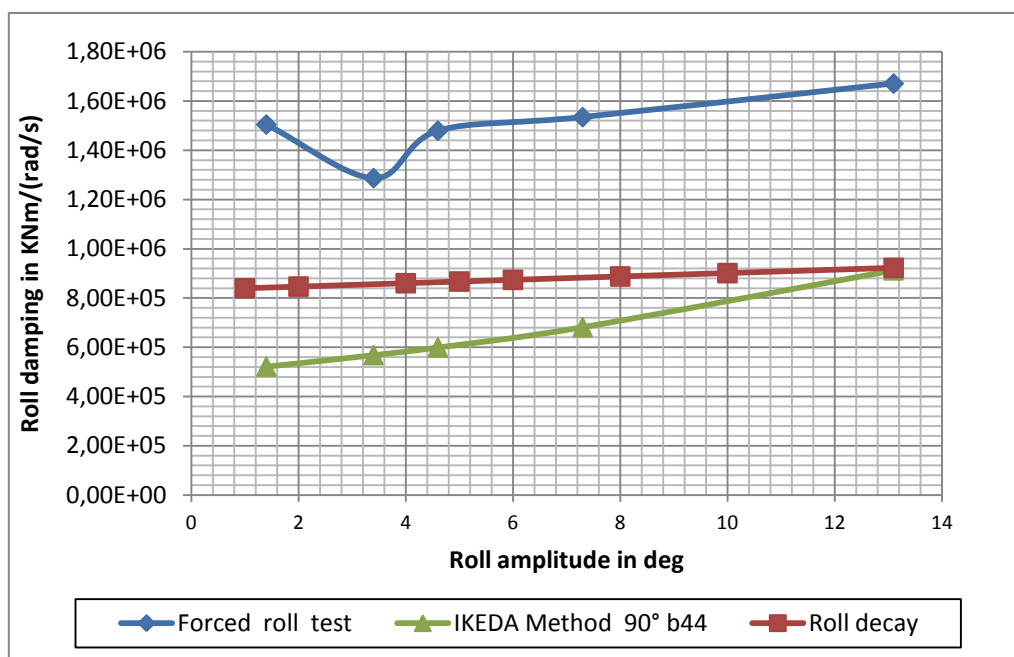


Figure 9: Dimensional roll damping component B44 VS Roll Amplitude, 20Kts, 90° beam seas, GM=2.14m

Table 6: Ikeda program numerical values:

8000-9000 TEU CS 20 Kts, 90° Beam seas			
Forced roll test		IKEDA Method	
Roll Amp	B44	Roll Amp	B44
1,40E+00	1,50E+06	1,40E+00	521536,6
3,40E+00	1,29E+06	3,40E+00	568.341
4,60E+00	1,48E+06	4,60E+00	599502,1
7,30E+00	1,53E+06	7,30E+00	681763
1,31E+01	1,67E+06	1,31E+01	912.516

4.2.2.3. *Interpretation of the Results*

The values of the total damping are close to the roll decay test results for the same reason presented in the previous section. In fact, Ikeda simple prediction method was built on the basis of the original method using mainly the same roll decay data base. Therefore, the results are closer to the roll decay case.

The investigation of the bilge keel component in the output file shows that it is more accurately determined with the Ikeda original method due to the use of an integration method that considers the transversal attachment distance of the bilge keel and does not present any sensitivity to the position of the center of gravity. Nevertheless, it is still underestimated due to the fact that it is difficult to account for the contribution of the bilge keel to the vortex shedding, the wave radiation and to the alteration of the pressure distribution.

IKEDA program provides all the components (the friction component, the eddy component, the lift component and the bilge keel component). It is recommended to evaluate the wave component at zero forward speed separately using an accurate potential flow solver or using Ikeda simple prediction formula for wave component. It is possible then to insert this value as a user defined constant in the source code of the program and it will account for the forward speed effect according to the following formula:

$$\frac{B_w}{B_{w0}} = 0.5 \left[\left\{ (A_2 + 1) + (A_2 - 1) \tanh 20(\Omega - 0.3) \right\} + (2A_1 - A_2 - 1) \exp \left\{ -150(\Omega - 0.25)^2 \right\} \right]$$

$$A_1 = 1 + \xi_d^{-1.2} \exp(-2\xi_d)$$

$$A_2 = 0.5 + \xi_d^{-1.0} \exp(-2\xi_d)$$

$$\xi_d = \frac{\omega^2 d}{g}, \quad \Omega = \frac{\omega U}{g}$$

B_{w0} : Wave component at zero forward speed

In this case the added value of wave component was evaluated by Ikeda simple formula and it is equal to $B_w=33704.635$ in (KN.m/(rad/s)).

4.2.3. Calculation Using Miller Method:

4.2.3.1. Details And Conditions Of the Computation:

Miller method parameters related to the 8000-9000TEU container ship are detailed in the following table:

Table 7: Miller method's parameters for the 8000-9000TEU container ship:

Container 8000-9000 TEU	
Miller Parameters	
b_{BK}	0,4
a_{BK}	101,08
A_{BK}	40,432
C_B	0,672
d	20,2
L	319
B	42,8
T	15
GM	2,41
F	0,27

A_{BK} is the total area of the bilge keels (port and starboard),

b_{BK} is the width of the bilge keel, C_B is the block coefficient,

d is the distance from the centerline at the load waterline to the turn of the bilge, L , B and T are the ship's length, beam and draft, respectively, is the roll amplitude in radians.

η_4 : Roll amplitude

$F = Fn/C_B$ with Fn is the Froude number.

The values of the zero speed and forward speed damping ratios are presented in the following table:

Table 8 : Roll damping ratio for 8000-9000TEU container at 20 Kts Forward speed, $T=15m$

Container 8000-9000 TEU		
η_4 (Roll amp)	$\beta_0(\eta_4)$	$\beta(\eta_4)$
1	0,02420363	0,05206602
2	0,03422911	0,06209149
3	0,04192192	0,06978431
4	0,04840727	0,07626965
5	0,05412097	0,08198336
6	0,05928655	0,08714894
7	0,06403679	0,09189918
8	0,06845821	0,0963206
9	0,0726109	0,10047329
10	0,07653861	0,104401
11	0,08027437	0,10813676
12	0,08384384	0,11170623
13,25	0,08810255	0,11596494

4.2.3.2. Results:

When the aim is to compare the results with Ikeda method or the experimental results shown previously, it is always recommended to convert the results using the nondimensionalisation convention presented by Ikeda method:

$$\hat{B}_{44} = \frac{B_{44}}{\rho \Delta B^2} \sqrt{\frac{B}{2g}}$$

$$\hat{\omega} = \omega \sqrt{\frac{B}{2g}}$$

The results are plotted in function of the roll amplitude and compared to the experimental results:

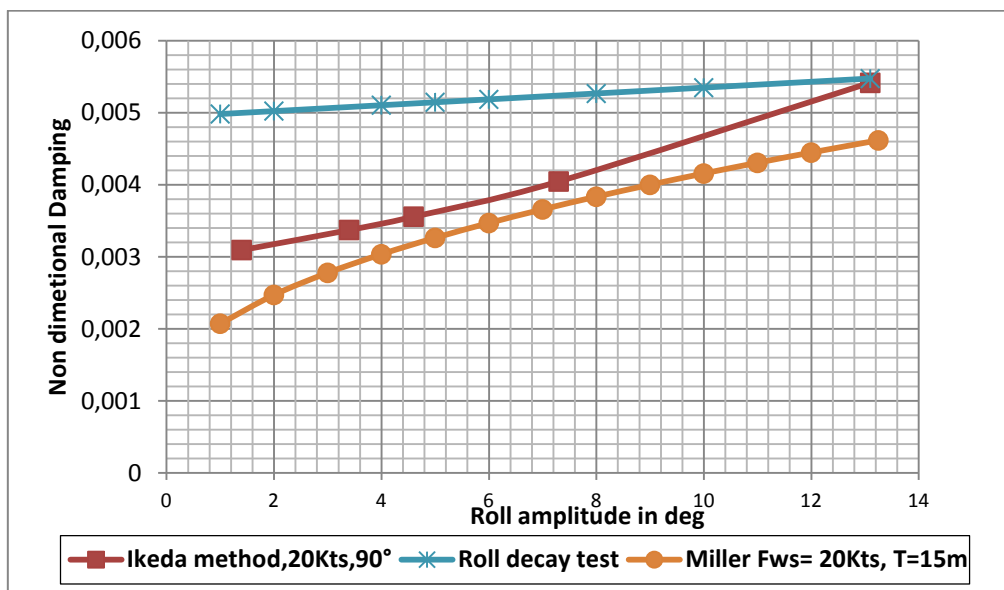


Figure 10 : Miller Nondimensional Damping ratio Vs roll amplitude, 20Kts & T=15m

Table 9 : Miller Damping coefficient after Ikeda nondimensionalisation

Miller results for 8000-9000TEU CS	
Roll ampl	\hat{B}_{44}
1	0,002072353
2	0,002471391
3	0,002777583
4	0,003035715
5	0,003263134
6	0,003468737
7	0,003657808
8	0,003833791
9	0,003999078
10	0,00415541
11	0,004304103
12	0,004446176
13,25	0,004615683

4.2.3.3. *Interpretation of the Results:*

First thing to be noticed is that Miller method curve has nearly the same trend as the Ikeda original method which confirms the similarity of the methods regarding the regression process based on the experimental data base and proves as well the same dependence of the roll damping coefficient on the roll amplitude.

As stated in the presentation of Miller method in the first chapter, the method should be used with caution when it comes to commercial ships with high block coefficient. In fact, this is the case, the 8000-9000 TEU Container ship has the highest block coefficient among the three tested vessels and this is the most suspected reason of the obtained discrepancy with the experimental roll decay test results.

4.2.4. *Prediction of Roll Damping from Roll Response Using PDstrip:*

4.2.4.1. *Details and Conditions Of the Computation:*

The roll motion of the 8000-9000TEU container ship is investigated in regular waves through the determination of the roll transfer function in stern quartering seas. The results of the simulation with PDstrip are compared to the tests in regular seas. The wave height was 4m, the heading was 35 deg from astern and the speed was 20 Kts. The tests are assumed to be in deep water condition.

In the input file, the following parameters are inserted:

- $g=9.81 \text{ ms}^{-2}$
- $T=15\text{m}$
- Heading =35°
- Displacement= 141428 t
- Cg position (0, 0, 18.6): As recommended in PDstrip the roll motion is sensitive to the value of GM. Therefore, the center of gravity position has to be adjusted in order to have the exact value of GM=2.14m. In order to highlight this fact, a sensitivity analysis was carried out with regard to the position of center of gravity and its influence on the resonance frequency value.
- Max wave height =4m
- Wave steepness: the chosen value is 0.1, recommended in the PDstrip manual, to be able to take into account the certain nonlinear effects on the RAOs: resistive forces and moments on the body cross sections, nonlinear forces on fins; and the possibility of surf-riding.

- $(k_{XX})^2=250.77 \text{ m}^2$; $(k_{YY})^2= 6360.0625 \text{ m}^2$; $(k_{ZZ})^2= 6368.04 \text{ m}^2$ (Respectively: Roll gyration radius, Pitch gyration radius, Yaw gyration radius).
- The simulation included different wave lengths (in m): 1540.95; 833.13;684.86, 385.23; 246.55;171.216;125.79; 96.309; 85.31; 76.096.
- Forward speed (in m/s)= 10.288 m/s

4.2.4.2. Results:

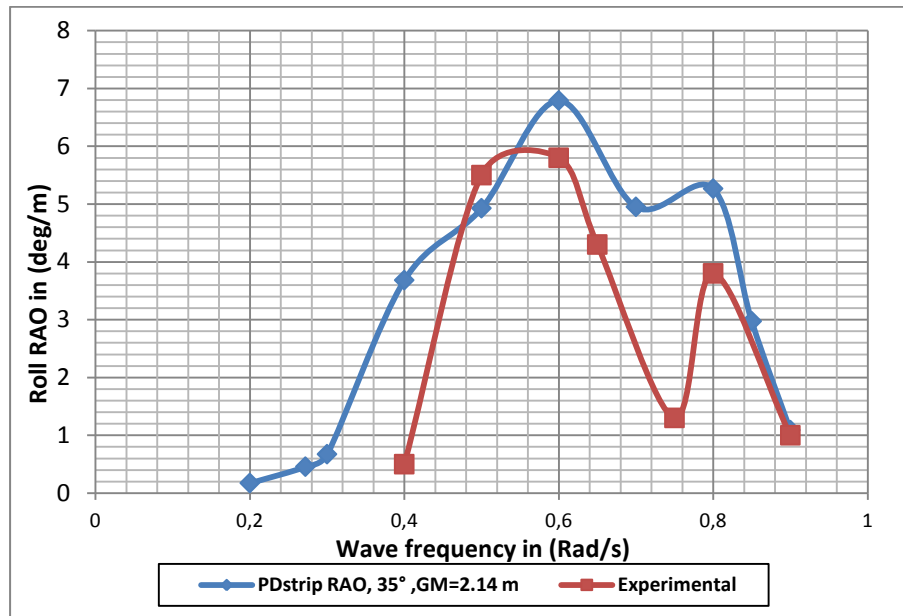


Figure 11 : RAO in (°/m) VS Wave frequency in (rad/s), 35°: Stern quartering seas, 20Kts: Forward Speed, GM=2.14m

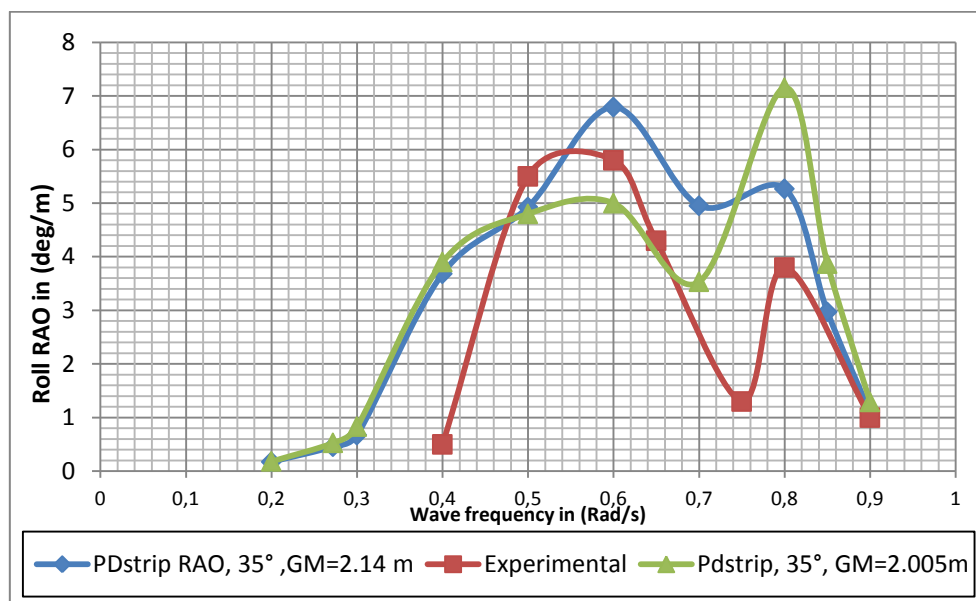


Figure 12 : Sensitivity analysis for the PDstrip RAO regarding the GM value

4.2.4.3. Evaluation Of the Damping Coefficient Using 2DRoll a Flume Software:

A 2Droll regression for the hull form of the 8000-9000 TEU vessel has been made and the corresponding value of the roll damping was used to predict the RAO using the spring mass system equation implemented in the 2Droll program. The chosen value of the damping coefficient $F_{\text{hull}}=0.075$.

The stern quartering seas RAO has approximately the same value of peak as the RAO obtained by PDstrip. Given that the experimental (Roll decay and Forced roll test) are generally simulated by a beam seas roll response, this Value ($F_{\text{hull}}=0.075 \Rightarrow B_{44}=0.005$) cannot be considered for a comparison with the experimental results.

4.2.4.4. Interpretation Of the Results:

The RAO values are provided in the output file in rad/m (η_4 / kA). In order to have the same nondimensionlization convention as in the experimental results, the output file values are multiplied by the wave number $k=2\pi/\lambda$ then by the conversion ratio from radian to degree (57.295). Thus we obtain RAO values in (deg/m).

The vortex damping part is coming from the contribution of the sway motion coupled with roll, and to take it into consideration, the following values (0.6; 0.8) were assigned to the resistance coefficients in the input file.

The friction part of the damping is accounted for by simulating the flow separation at the end of the ship. Therefore, all the flow separation coefficients have to be equal to 1 in the input file except after the location where the flow separates.

Concerning the bilge keel, only the quadratic bilge keel damping component is considered. Therefore the roll motion reduction is not so realistic but the contribution of the bilge keel is still important in all other aspects of roll response.

The shape of the RAO obtained is similar to the RAO determined by regular wave experiments. The resonance period is well detected by PDstrip as shown in the graph but the amplitude is still a bit overestimated.

The experimental RAO presents two peaks. In stern quartering seas, one encounter frequency can correspond to two wave frequencies. In this case, two different wave frequencies corresponding to the same encounter wave frequency which is close to the natural roll frequency of the ship, have led to the two peaks of the response observed in the RAO obtained by PDstrip in 35° stern quartering seas.

4.3. Numerical Simulations For an 16000-18000 TEU Container Ship:

4.3.1. Prediction of Roll Damping Using IKEDA Simple Prediction Formula

4.3.1.1. Details and Conditions Of the Computation.

Ikeda simple prediction method requires the following main particulars of the ship:

$$L_{pp}=375.9\text{m}$$

$$B=59\text{m}$$

$$T=14.5\text{m}$$

$$\Delta=228162.672\text{ t}$$

$$\text{Bilge keel: in two parts: } L_{BK1}=41.52\text{m}$$

$$H_{BK1}=0.4\text{m}$$

$$L_{BK2}=41.52\text{m}$$

$$H_{BK2}=0.8\text{m}$$

$$\text{Bilge keel aspect ratio}=4.49 \text{ e-}3$$

The chosen roll period is the resonance period: $T=34.6\text{ s}$

All the input parameters were kept constant except the roll angle that varied, and for each of the following values of the roll angle the nondimensional value of the roll damping \hat{B}_{44} is recorded.

Roll angles: 1; 2; 4 ; 5 ; 6 ; 8 ; 10

4.3.1.2. Results:

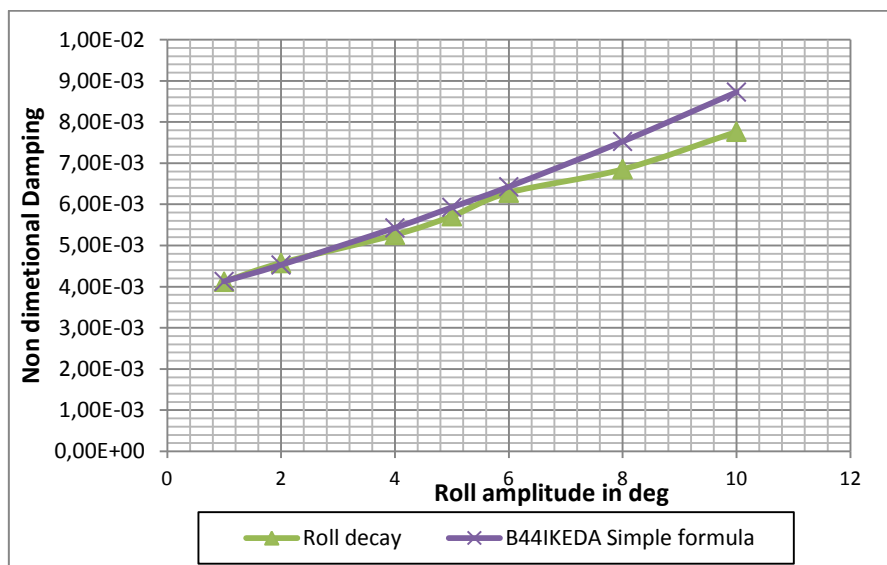


Figure 13 : Non Dimensional Damping Coefficient VS Roll Amplitude
90° heading, 21Kts FW speed, GM=2,9m

Table 10 : IKEDA Simple Prediction Formula numerical values for a 16000-18000 TEU Container Ship

Container 16000-18000TEU			
90°, 21 Kts			
Ikeda Simple Formula		Roll Decay Test	
Roll Amp	B44Hat	Roll Amp	B44Hat
1	4,13E-03	1	4,12E-03
2	4,53E-03	2	4,57E-03
4	5,43E-03	4	5,26E-03
5	5,93E-03	5	5,71E-03
6	6,43E-03	6	6,28E-03
8	7,53E-03	8	6,85E-03
10	8,70E-03	10	7,76E-03

4.3.1.3. Interpretation Of the Results:

The components given by this method at zero forward speed are the friction component, the eddy component, the wave component and the bilge keel component. The non dimensional lift component ($B_L=0.002726$) is added from the Ikeda original method to take into account the effect of the ship forward speed.

The results given by the simple method are in good agreement with the roll decay values especially for lower values of the roll amplitude. This confirms that this method is available for low and medium roll angles. Other methods should be used when it comes to larger roll angles namely EFD and CFD.

4.3.2. Prediction of Roll Damping Using Ikeda Computer Program

4.3.2.1. Details and Conditions Of the Computation.

The simulation input details were set up as follows:

GM= 2.9 m

Froude number $F_n= 0.177$ corresponding to a Forward speed= 21 Kts

Wave heading: 90° Beam seas.

Wave amplitudes: 1°, 2°, 4°, 5°, 6°, 8, 10°

The ratio wave length/ $L_{pp}= 4.146$ which corresponds to the natural frequency $\omega_n=0.181$ rad/s

In this method the loading condition is to be inputted by fixing the corresponding draft (in this case $T=14.5$ m). The displacement is then calculated by integrating the waterline area through the sections.

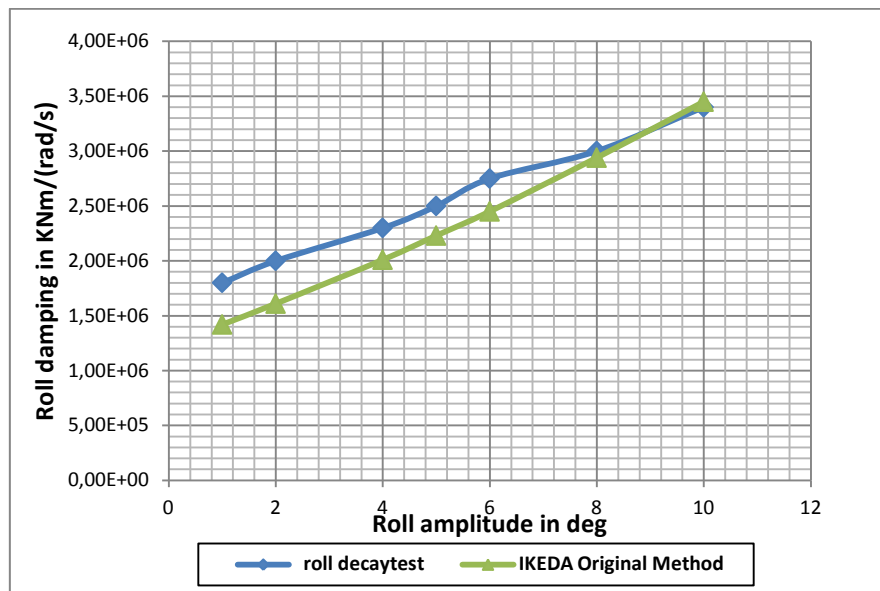


Figure 14 : Dimensional roll damping component B44 VS Roll Amplitude
21Kts, 90° beam seas, GM=2.9 m

Table 11 : IKEDA Computer program numerical values for an 16000-18000 TEU Container Ship

16000-18000TEU CS 21 Kts, 90° Beam Seas			
roll decaytest		IKEDA Original Method	
Roll Amp	b44	Roll Amp	b44
1,00E+00	1,80E+06	1,00E+00	1,42E+06
2,00E+00	2,00E+06	2,00E+00	1,61E+06
4,00E+00	2,30E+06	4,00E+00	2,01E+06
5,00E+00	2,50E+06	5,00E+00	2,23E+06
6,00E+00	2,75E+06	6,00E+00	2,45E+06
8,00E+00	3,00E+06	8,00E+00	2,94E+06
1,00E+01	3,40E+06	1,00E+01	3,45E+06

4.3.2.2. Interpretation Of the Results:

Following the same procedure as for the previous ship, the wave component evaluated according to the Ikeda simple formula is added to the sum of the other components obtained by the current method.

The results of the original method are in good agreement with the roll decay test. But they are still slightly lower. The small difference is due to the adopted value of the wave component which was taken from the IKEDA wave component formula. However, a more accurate prediction of the wave damping component could be obtained from the evaluation of the wave radiation force using a potential flow solver.

Similar container ships have high roll period, therefore Ikeda uses Takaki formula to account for the decrease of bilge keel drag in case of high roll period or high roll amplitudes.

Nevertheless, this consideration might not be very realistic and might have led to the underestimation of the bilge keel damping component.

4.3.3. Calculation Using Miller Method :

4.3.3.1. Details and Conditions Of the Computation:

The input parameters of the Miller method in the case of the 16000-18000TEU container ship are specified in the following table:

Table 12 : Miller method parameters for the 16000-18000TEU container ship

Container 16000-18000TEU	
Miller Parameters	
bBK	0,6
aBK	41,52
ABK	24,912
CB	0,657
d	27
L	379,5
B	59
T	10,5
GM	2,9
F	0,27

A_{BK} is the total area of the bilge keels (port and starboard),

b_{BK} is the width of the bilge keel, C_B is the block coefficient,

d is the distance from the centerline at the load waterline to the turn of the bilge, L , B and T are the ship's length, beam and draft, respectively, η_4 is the roll amplitude in radians.

η_4 : Roll amplitude

$F = F_n / C_B$ with F_n is the Froude number.

The values of the zero speed and forward speed damping ratios are presented in the following table:

Table 13 : Roll damping ratio for 8000-9000TEU container at 20 Kts Forward speed, T=15m

Container 16000-18000TEU		
fi4(Roll amp)	Beta0	beta(nu4)
1	0,04048518	0,06439362
2	0,05725469	0,08116313
3	0,07012239	0,09403083
4	0,08097036	0,1048788
5	0,09052762	0,11443606
6	0,09916804	0,12307648
7	0,10711372	0,13102216
8	0,11450939	0,13841783
9	0,12145554	0,14536399
10	0,12802538	0,15193383
11	0,13427416	0,1581826
12	0,14024478	0,16415322
13,25	0,14736828	0,17127673

4.3.3.2. Results:

The damping ratios obtained by Miller for the 16000-18000TEU container were converted using the Ikeda nondimensionalisation process then plotted in function of the roll amplitude and compared to the experimental results:

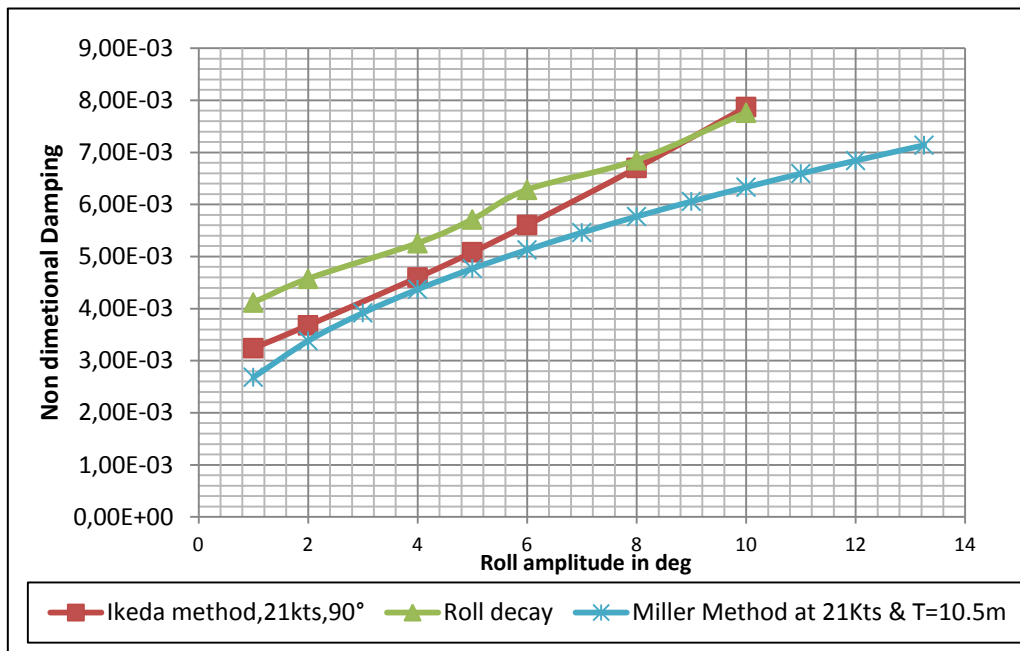


Figure 15 : Miller Nondimensional Damping ratio Vs roll amplitude, 20Kts & T=15m

Table 14 : Miller damping coefficient after Ikeda nondimensionalisation:

Miller results for 16000-18000TEU	
Roll amplitude	B44
1	0,00268413
2	0,00338314
3	0,0039195
4	0,00437168
5	0,00477006
6	0,00513022
7	0,00546142
8	0,00576969
9	0,00605923
10	0,00633308
11	0,00659355
12	0,00684242
13,25	0,00713935

4.3.3.3. *Interpretation Of the Results:*

Even though this ship has a relatively high block coefficient, the results obtained from Miller method is close enough to the experimental results as a preliminary design method.

The discrepancy appears then grows more for large roll angles which proves that this method is also not so efficient for large roll angles.

4.3.4. *Prediction of Roll Damping from Roll Response Using PDstrip:*

4.3.4.1. *Details and Conditions Of the Computation:*

The roll motion of the 16000-18000 TEU container ship is investigated in regular waves through the determination of the roll transfer function in stern quartering seas and beam seas. The results of the simulation with PDstrip are compared to the tests in regular seas.

First Simulation: Stern Quartering Seas:

The wave height was 7.5 m, the heading was 45 deg from astern and the speed was 21 Kts. The tests are assumed to be in deep water condition.

In the input file, the following parameters are inserted:

- $g=9.81 \text{ ms}^{-2}$
- $T=10.5\text{m}$
- Heading =45°
- Displacement= 156737.672 t
- Cg position (0, 0, 23.281): As recommended in PDstrip the roll motion is sensitive to the value of GM. Therefore, the center of gravity position has to be adjusted in order to have the exact value of GM=9m. In order to highlight this fact, a sensitivity analysis was carried out with regard to the position of center of gravity and its influence on the resonance frequency value as shown in the figure 16.
- Max wave height =7.6 m
- Wave steepness: the chosen value is 0.1, recommended in the PDstrip manual, to be able to take into account the certain nonlinear effects on the RAOs: resistive forces and moments on the body cross sections, nonlinear forces on fins; and the possibility of surf-riding.
- $(k_{XX})^2=590.49 \text{ m}^2$; $(k_{YY})^2= 9594.2025 \text{ m}^2$; $(k_{ZZ})^2= 9594.2025 \text{ m}^2$ (Respectively: Roll gyration radius, Pitch gyration radius, Yaw gyration radius).

- The simulation included different wave lengths (in m): 1540.95, 833.13, 684.86, 385.23, 246.55, 171.216, 125.79, 96.309, 85.31, 76.096.
- Forward speed (in m/s)= 10.8024m/s

Results:

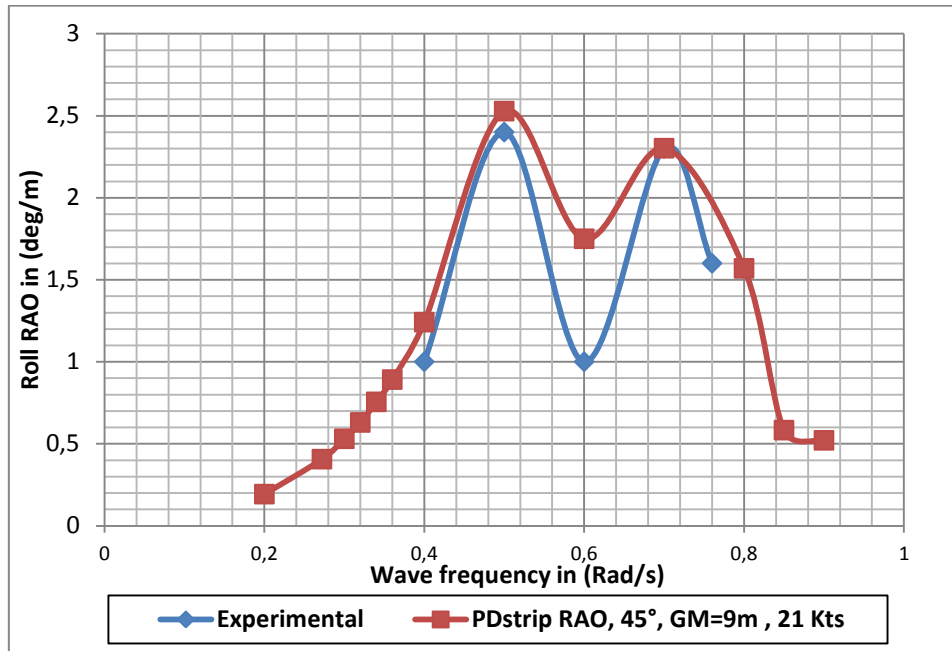


Figure 16 : RAO in ($^{\circ}$ /m) VS Wave frequency in (rad/s)
Stern quartering 45° , 21 kts

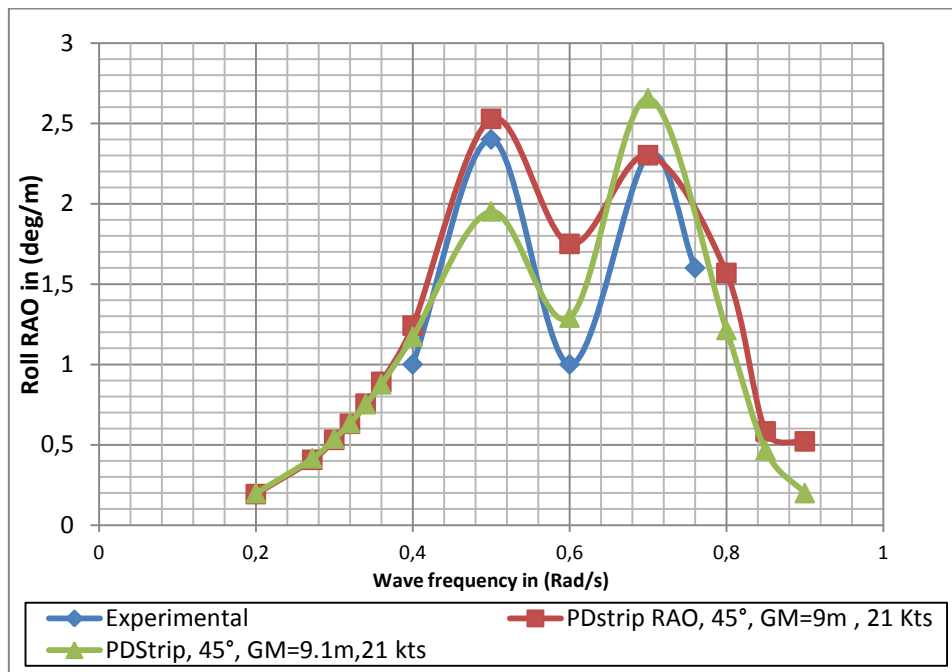


Figure 17 : Sensitivity analysis regarding the value of GM

- **second simulation: Beam seas:**

The wave height was 7.6 m, the heading was 90 deg Beam seas and the speed was 0 Kts. The tests are assumed to be in deep water condition.

In the input file, the following parameters are inserted:

- $g=9.81 \text{ ms}^{-2}$
- $T=10.5\text{m}$
- Heading =90°
- Displacement= 156737.672 t
- Cg position (0,0, 23.281) : As recommended in PDstrip the roll motion is sensitive to the value of GM. Therefore, the center of gravity position has to be adjusted in order to have the exact value of GM=9m. In order to highlight this fact, a sensitivity analysis was carried out with regard to the position of center of gravity and its influence on the resonance frequency value.
- Max wave height =7.6m
- Wave steepness: the chosen value is 0.1, recommended in the PDstrip manual, to be able to take into account the certain nonlinear effects on the RAOs: resistive forces and moments on the body cross sections, nonlinear forces on fins; and the possibility of surf-riding.
- $(k_{XX})^2=590.49 \text{ m}^2$; $(k_{YY})^2= 9594.2025 \text{ m}^2$; $(k_{ZZ})^2= 9594.2025 \text{ m}^2$ (Respectively: Roll gyration radius, Pitch gyration radius, Yaw gyration radius).
- The simulation included different wave lengths (in m): 1540.95, 833.13, 684.86, 385.23, 246.55, 171.216, 125.79, 96.309, 85.31, 76.096.
- Forward speed (in m/s)= 0 m/s

Results:

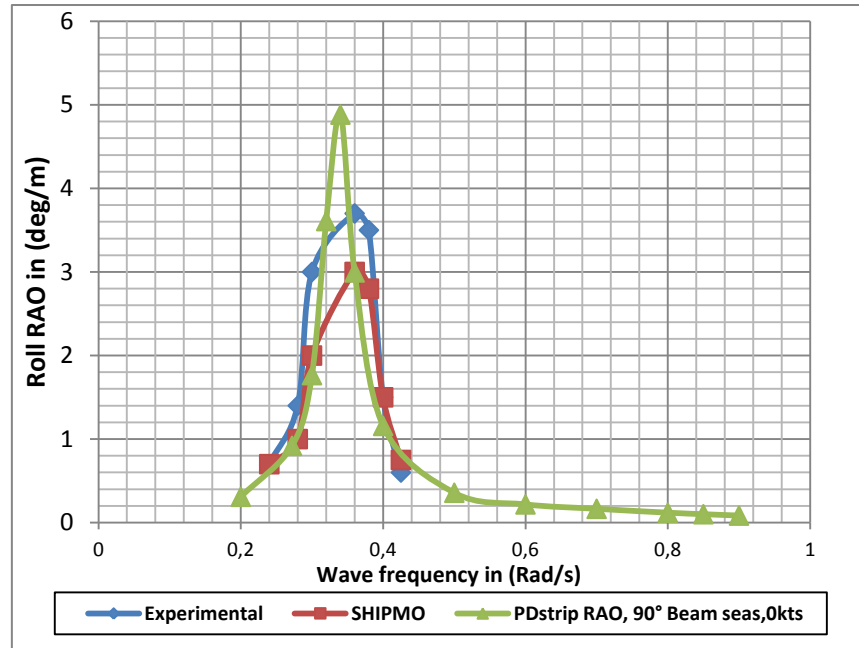


Figure 18: RAO in ($^{\circ}$ /m) VS Wave frequency in (rad/s)

Beam seas, 0 kts

4.3.4.2. Evaluation Of the Damping Coefficient Using 2DRoll a Flume Software:

In order to obtain the same roll response for the beam seas calculation using 2DRoll, a regression analysis has to be made based on similar body plans. Finally, the chosen roll damping ratio F_{hull} was equal to 0.06 and based on the ship characteristics and the sea conditions, the RAO was computed.

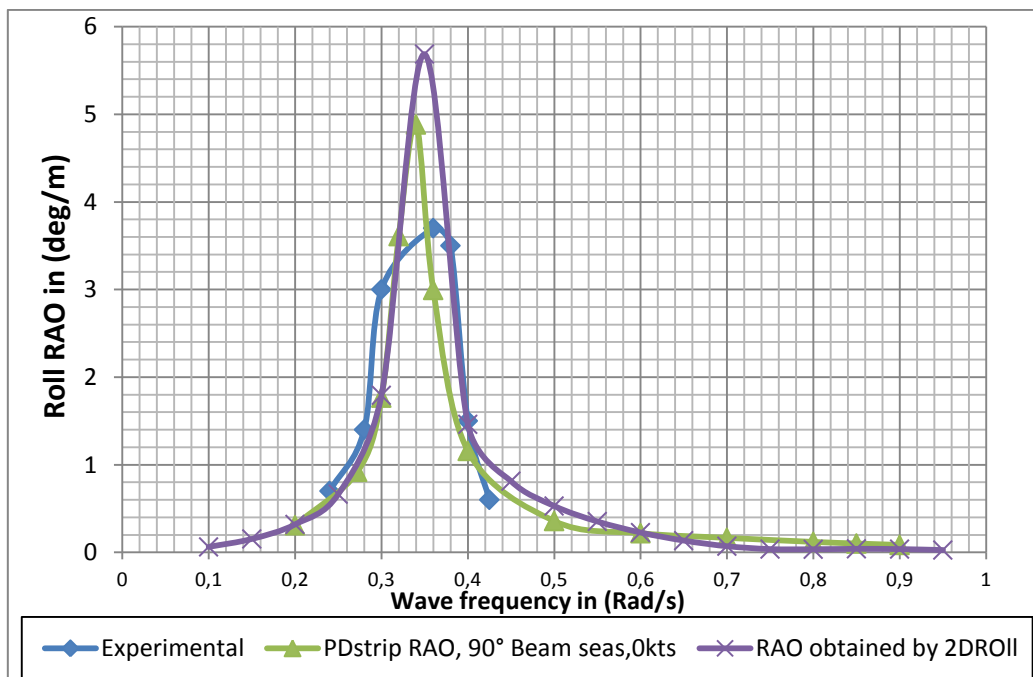


Figure 19: Roll RAO obtained from 2DRoll at 90° & 21 Kts

The value of the RAO at the resonance frequency is similar to the one obtained by PDstrip in the previous plot. Therefore, it is possible to consider the chosen value of the roll damping ratio ($F_{hull}=0.06$). After conversion using Ikeda nondimensionalisation formula we obtain the coefficient $\hat{B}_{44}=0.0025$ which matches very well the average value of the \hat{B}_{44} obtained experimentally.

4.3.4.3. Interpretation of The results:

The Roll response for beam seas and stern quartering seas seem to follow well the trend of the experimental roll response. However, it is obvious that the RAOs presented, are missing, in some cases, some important details about the characteristic roll response due to the lack of measurement points in some frequency ranges. For instance, in beam seas, the maximum response is obtained near the natural roll frequency of the ship while the experimental RAO presents a lower value in that area and the maximum response is obtained for a further frequency range.

Concerning the stern quartering seas test case, the response obtained by PDstrip sticks well with the experimental roll RAO especially the peak values. This means that the viscous contribution to the roll damping was taken accurately into account thanks to a good choice of the so called resistance coefficients ($C_y=0.8$, $C_z=0.6$). Those values are more suitable for well-rounded base which is obviously the case for this vessel.

The contribution of the bilge keel seems also very realistic due to its relatively big dimensions and especially the breadth (0.8m).

4.4. Numerical Simulations For DTMB 5415:

4.4.1. Post Processing of the Roll Decay Test Measurements Performed by the University of IOWA:

4.4.1.1. Roll Decay Test Experimental Conditions

The experiments are performed in the IIHR—Hydroscience & Engineering at the University of IOWA towing tank. The tank is 100 m long, 3.048 m wide and 3.048 m deep, and is equipped with a drive carriage, plunger wavemaker and wave dampener system. There are two coordinate systems referenced in these experiments. The global coordinate system, origin at model VCG, is a right-handed Cartesian coordinate system (x, y, z) used to reference motions, force and moment measurements. The $x, y,$ and z axes are directed aft, to starboard and upward respectively. The local coordinate system, origin at model forward perpendicular (FP, $x = 0$), is a right-handed Cartesian coordinate system (x, y, z) used to reference flow-field and wave-field measurements. The $x, y,$ and z axes are directed aft, to starboard and upward respectively.

The geometry of interest is DTMB model 5512, which is a 1/46.6 scale geosym of DTMB model 5415. The full scale is the DDG-51 ARLEIGH BURKE-class destroyer, with $L=3.048$ m and block coefficient, $CB = 0.506$. The model is unappended (no shafts, struts, rudders or propulsors) except for the use of bilge keels as noted. The DTMB model 5512 and full-scale particulars are summarized in the following table.



Figure 20: Model 5512 suspended in air from the IIHR towing tank carriage

Table 15 : Summary of DTMB model 5512 and fullscale particulars:

	DTMB 5512	Full-Scale
Length, L	3.048 m	142.04 m
Beam, B	0.386 m	17.99 m
Draft, T	0.214 m	9.97 m
Wetted Surface Area, S	1.371 m ²	2977 m ²
Block Coefficient, CB	0.506	0.506

The IIHR—Hydroscience & Engineering at the University of IOWA performed different roll decay test for different initial inclination angles. The measured results were recorded and published in the IIHR website. Only enough high initial inclination angle tests are of importance for this study. Therefore, $\phi_0=15^\circ$ and $\phi_0=20^\circ$ were studied and compared.

4.4.1.2. Roll Decay Test For $\phi_0=15^\circ$

- **Roll Decay Time History :**

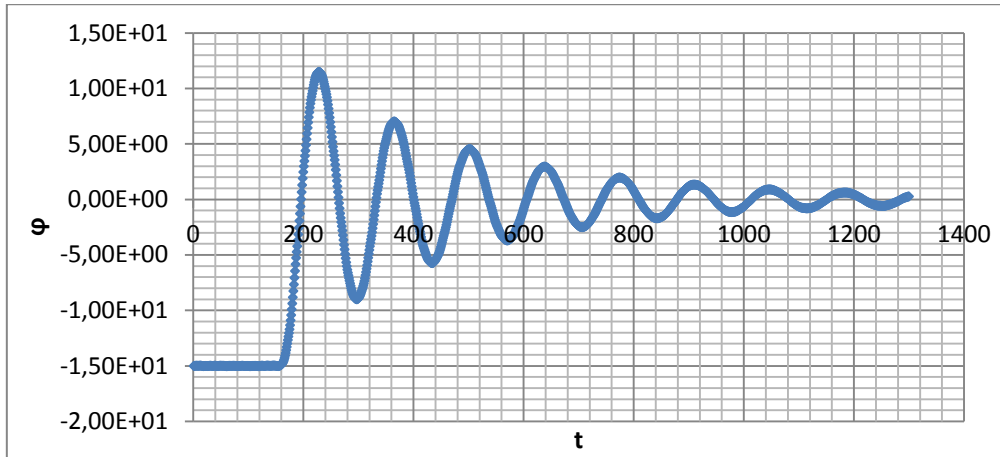


Figure 21: Roll decay time history for initial inclination angle $\phi_0=15^\circ$

In order to obtain the extinction coefficients, a decrement analysis was performed and roll decrement curve was plotted. This procedure has been explained in the first chapter.

- **Roll Decrement Analysis :**

Table 16 : Roll decrement table

ϕ_m	$\Delta\phi$	$\Delta\phi/\phi_m$
13,25	3,5	0,26415094
10,25	2,5	0,24390244
8	2	0,25
5,75	2,5	0,43478261
4	1	0,25
3,25	0,5	0,15384615
2,75	0,5	0,18181818
2,25	0,5	0,22222222
1,875	0,25	0,13333333
1,54	0,42	0,27272727
1,215	0,23	0,18930041
0,95	0,3	0,31578947
0,7	0,2	0,28571429

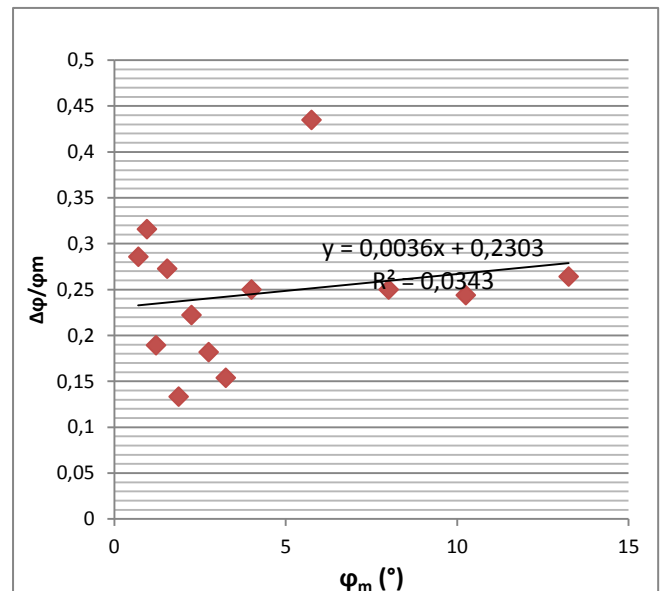


Figure 22: Roll decrement curve $\Delta\phi/\phi_m$ VS ϕ_m
for $\phi_0=15^\circ$

Table 17 : Roll decay coefficients:

a	b
0,23	0,003

B1	B2
0,72493516	0,00273032

φ_m	Be	Behat
13,25	0,87253627	0,00989321
10,25	0,83911715	0,00951429
8	0,81405281	0,0092301
5,75	0,78898847	0,00894591
4	0,76949399	0,00872487
3,25	0,76113921	0,00863014
2,75	0,75556935	0,00856699
2,25	0,7499995	0,00850383
1,875	0,74582211	0,00845647
1,54	0,74209031	0,00841416
1,215	0,73846991	0,00837311
0,95	0,73551788	0,00833963
0,7	0,73273296	0,00830806

Using the ITTC recommended procedure “Numerical estimation of the roll damping”, the equivalent roll damping coefficient was extracted from the linear and the quadratic damping B1 and B2 coefficient for each mean roll angle based on the quick formula:

$$B_{\varphi_e} = B_{\varphi_1} + \omega_E \varphi_a B_{\varphi_2}$$

4.4.1.3. Roll decay test for $\phi_0=20^\circ$

- Roll decay time history :

Similarly to the above section, the roll decay time history was plotted from the measurements of the IIHR.

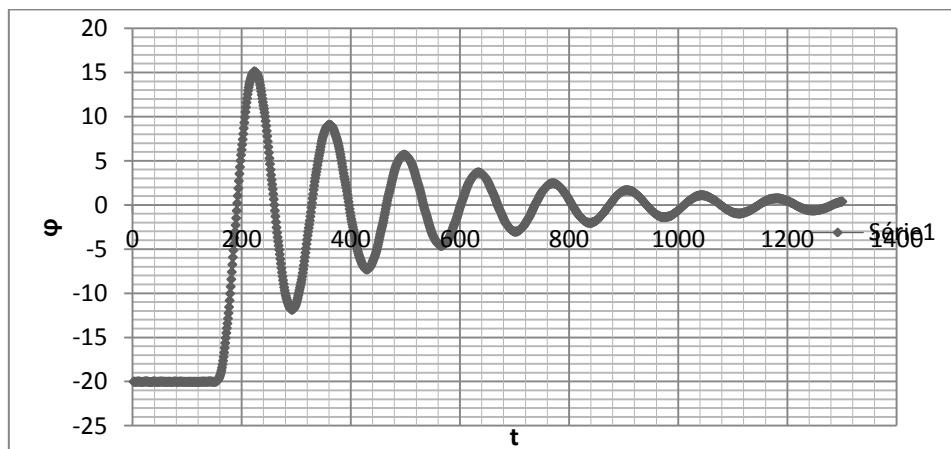
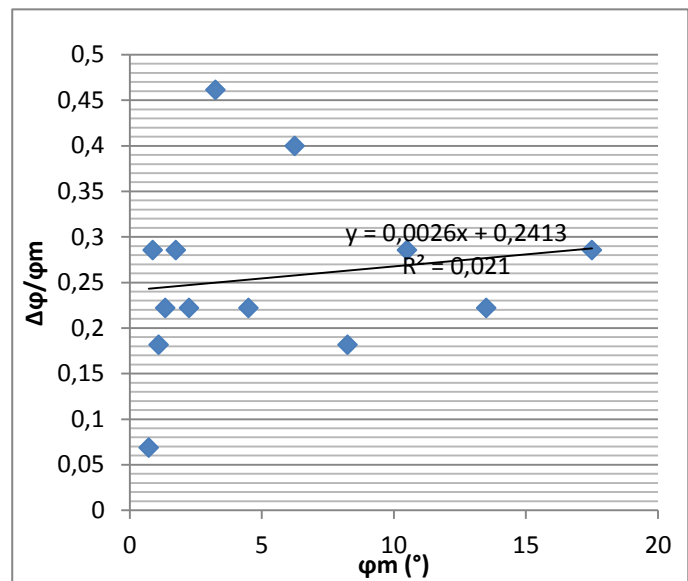
Figure 23: Roll decay time history for $\phi_0=20$

Table 18 : Roll decrement table:

ϕ_m	$\Delta\phi$	$\Delta\phi/\phi_m$
17,5	5	0,28571429
13,5	3	0,22222222
10,5	3	0,28571429
8,25	1,5	0,18181818
6,25	2,5	0,4
4,5	1	0,22222222
3,25	1,5	0,46153846
2,25	0,5	0,22222222
1,75	0,5	0,28571429
1,35	0,3	0,22222222
1,1	0,2	0,18181818
0,875	0,25	0,28571429
0,725	0,05	0,06896552

Figure 24: Roll decrement curve $\Delta\phi/\phi_m$ VS ϕ_m
for $\phi_0=20^\circ$

Roll extinction coefficients were determined from the decrement analysis for $\phi_0=20^\circ$.

Table 19 : Roll decay coefficients:

a	b
0,241	0,002

B_1	B_2
0,75960775	0,00182022

ϕ_m	Be	\hat{B}_e
17,5	0,88957129	0,01008636
13,5	0,85986534	0,00974954
10,5	0,83758587	0,00949693
8,25	0,82087628	0,00930747
6,25	0,8060233	0,00913906
4,5	0,79302695	0,0089917
3,25	0,78374384	0,00888644
2,25	0,77631735	0,00880224
1,75	0,7726041	0,00876014
1,35	0,76963351	0,00872645
1,1	0,76777689	0,0087054
0,875	0,76610593	0,00868646
0,725	0,76499195	0,00867383

Finally, the roll damping coefficient was extracted from the extinction coefficients for each mean roll angle.

⇒ In the rest of the sections, those non dimensional coefficients will be compared to the nondimensional damping coefficients corresponding to another model with a different scale of the same ship (DDG-51).

4.4.2. Estimation of Roll Damping of the DTMB 5415 Using Component Analysis Method: Ikeda Program as an Example

4.4.2.1. Details and Conditions of the Computation.

In the input file 24 sections were inserted with enough offset points per section.

The ration $(\text{Draft}-K_G)/\text{Draft}$ is set to 0.22

Froud number $Fn= 0.28$ exactly as in the roll decay test conditions

Wave heading: 90° Beam seas.

Wave amplitudes: $1^\circ, 2^\circ, 4^\circ, 5^\circ, 6^\circ, 8^\circ, 10^\circ, 13.5^\circ$ and 17.5° .

The ratio wave length/ $L_{pp}= 1.22$ which corresponds to the natural roll period of the full scale ship $T_n=10.5$ s.

The scaled width of the bilge keel is 0.016, located between $0.373 L_{pp}$ and $0.705 L_{pp}$.

The ship is considered as slender, therefore the algorithm of the bilge keel attachment is chosen by setting the parameter Type_BK to the value 2. The integration method is then chosen and the bilge keel attachment locations will be accurately taken into account.

Therefore the following scaled values of the bilge keel attachment transverse position were detailed in the input file:

0.253; 0.259; 0.267; 0.272; 0.264; 0.258; 0.250; 0.248; 0.24

4.4.2.2. Results of The Simulation:

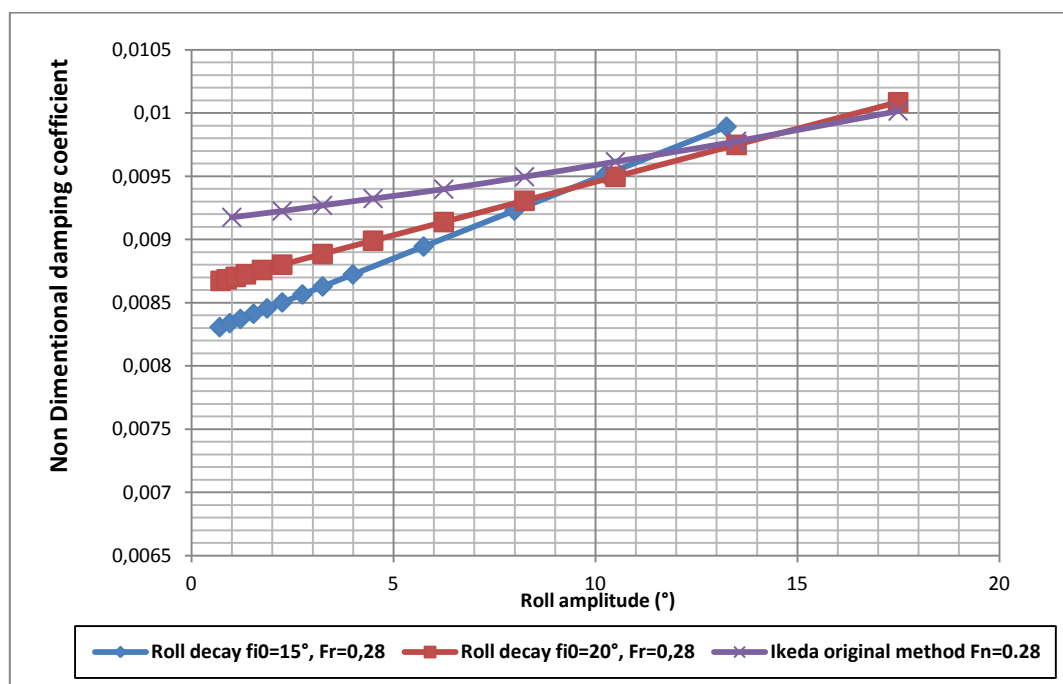


Figure 25: Comparison of Ikeda original method results for DTMB 5415 with roll decay test results for two different initial inclination angles at $Fn=0.28$.

Table 20: Roll damping numerical values for DTMB 5415:

DTMB 5415		Roll decay $\varphi_0=15^\circ$, $F_n=0,28$			Roll decay $\varphi_0=20^\circ$, $F_n=0,28$		
Ikeda original method, $F_n=0,28$		φ_m	Be	\hat{B}_{44}	φ_m	Be	\hat{B}_{44}
Roll amp	B44						
1	0,009176672	0,7	0,73273467	0,008308078	0,725	0,76499195	0,00867383
2,25	0,009226627	0,95	0,7355196	0,008339654	0,875	0,76610593	0,00868646
3,25	0,009270953	1,215	0,73847163	0,008373126	1,1	0,76777689	0,0087054
4,5	0,009325023	1,54	0,74209204	0,008414176	1,35	0,76963351	0,00872645
6,25	0,009399147	1,875	0,74582385	0,008456489	1,75	0,7726041	0,00876014
8,25	0,009497779	2,25	0,75000125	0,008503854	2,25	0,77631735	0,00880224
10,5	0,009616767	2,75	0,75557112	0,008567008	3,25	0,78374384	0,00888644
13,5	0,009777853	3,25	0,76114099	0,008630161	4,5	0,79302695	0,0089917
17,5	0,010016977	4	0,76949579	0,008724892	6,25	0,8060233	0,00913906
		5,75	0,78899032	0,00894593	8,25	0,82087628	0,00930747
		8	0,81405471	0,009230121	10,5	0,83758587	0,00949693
		10,25	0,83911911	0,009514312	13,5	0,85986534	0,00974954
		13,25	0,87253831	0,009893234	17,5	0,88957129	0,01008636

4.4.2.3. Interpretation of the Results:

Obviously, the initial roll angle has an influence on the damping coefficient. For the higher initial roll angle (here 20°) the roll decay coefficients are slightly higher and the error percentage is lower. The roll damping coefficients obtained from the Ikeda original method are in good agreement with roll decay test results. It seems that the Ikeda original method works well with this type of slender ships rather than the previous two container ships which are fuller and have buttock flow and streamlines.

Investigating the damping components in the output file, we can notice that the lift damping is predominant which reflects the effect of the slenderness of the ship and the aspect ratio that figures in the formula of the lift component.

Contrarily to what everyone might expect, the test case is a fast vessel and at the test speed the viscous effect might prevail. In fact, the eddy damping component decreases drastically with the forward speed especially for similar fast ships.

The scale effect was not present in this test case due to the fact that the ship geometry and test data were both available for the model scale.

4.4.3. Miller Method Calculation:

4.4.3.1. Details and Conditions Of the Calculation.

The following table summarizes all the inputs of the Miller method related to the DTMB 5415:

Table 21: Miller method parameters for the DTMB 5415:

DTMB 5512	
Miller Parameters	
b_{BK}	0,4
a_{BK}	47,302
A_{BK}	18,92
C_B	0,506
d	6,4
L	142
B	18
T	9,97
GM	1,7
F	0,5533

Table 22: The values of the zero speed and forward speed damping ratios are presented

DTMB 5415		
φ_4	β_0	$\beta(\eta_4)$
1	0,01312275	0,08655549
2	0,01855837	0,09199111
3	0,02272927	0,09616201
4	0,0262455	0,09967824
5	0,02934336	0,1027761
6	0,03214404	0,10557678
7	0,03471953	0,10815227
8	0,03711674	0,11054948
9	0,03936825	0,11280099
10	0,04149778	0,11493052
11	0,04352324	0,11695598
12	0,04545854	0,11889128
13,25	0,04776753	0,12120027

4.4.3.2. Results Of the Calculation:

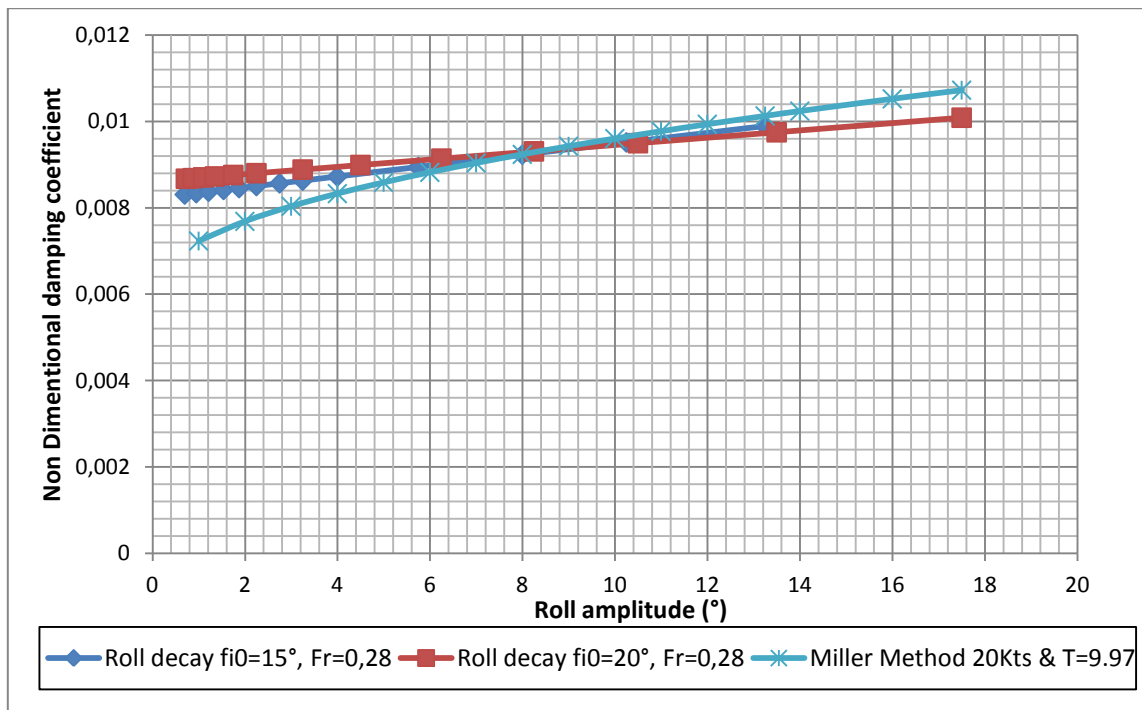


Figure 26: Nondimensional damping coefficient for DTMB 5415 Compared to the roll decay test results

Table 23: Miller damping coefficient after the Ikeda nondimensionalisation

DTMB 5415	
Roll amp	B_{44}
1	0,00723273
2	0,007686941
3	0,008035468
4	0,008329291
5	0,008588154
6	0,008822183
7	0,009037396
8	0,009237711
9	0,009425851
10	0,009603798
11	0,009773049
12	0,009934767
13,25	0,01012771
14	0,010239123
16	0,010522411
17,5	0,010723411

4.4.3.3. *Interpretation of the Results:*

The results of Miller method stick very well to the roll decay damping coefficients especially for moderate range of roll angles. This could confirm the fact that Miller built his regression analysis on a similar type of Navy slender round bottomed ship.

4.4.4. *Simulation of Roll Motion Using PDstrip :*

4.4.4.1. *Details and Conditions Of the Simulation.*

A potential theory computation was performed using PDstrip in the same conditions as those of the stationary regular wave test carried out the Kelvin Hydrodynamic Laboratory University of Strathclyde Glasgow using a 1/100 scale model of the DDG-51 US Navy destroyer. The wave characteristics of each run are described in the following table:

Table 24: Summary of the experimental wave condition of the stationary beam seas test of the model DTMB 5415

omega	Wave length	λ/L	Steepness	Hsea
1,17747824	44,42	0,3128169	0,02	0,8884
0,99651374	62,018	0,43674648	0,02	1,24036
0,92677328	71,703	0,5049507	0,02	1,43406
0,81995572	91,6017	0,64508239	0,02	1,832034
0,72005393	118,783	0,8365	0,02	2,37566
0,64843706	146,47	1,03147887	0,02	2,9294
0,55983181	196,503	1,38382394	0,02	3,93006
0,48003752	267,26	1,88211268	0,02	5,3452
0,44673485	308,592	2,1731831	0,02	6,17184
0,4052657	374,977	2,6406831	0,02	7,49954
0,36002658	475,133	3,34600704	0,02	9,50266

The corresponding full scale conditions used in motion numerical calculation are described in the PDstrip input file:

- Deep water condition, Beam seas
- Displacement: 8635.01 t
- Draft: T=6.15m
- GM= 1.993m, LCG=70.408m, KG=7.566m
- $(k_{XX})^2=48.052 \text{ m}^2$; $(k_{YY})^2= 1354.39 \text{ m}^2$; $(k_{ZZ})^2= 1354.39 \text{ m}^2$ (Respectively: Roll gyration radius, Pitch gyration radius, Yaw gyration radius).
- The steepness is chosen to be equal to the steepness of the experimental test, steep=0.2
- The maximum wave height is chosen to be higher than all the wave height of the test in order to consider the different real wave amplitudes used in each test.
- The following values of the wave lengths were fixed as an input: 44.42, 62.018, 71.703, 91.6017, 118.783, 146.47, 196.503, 267.26, 308.592, 374.977, 475.133.
- The test is stationary, therefore the forward speed is equal to zero.

4.4.4.2. Results:

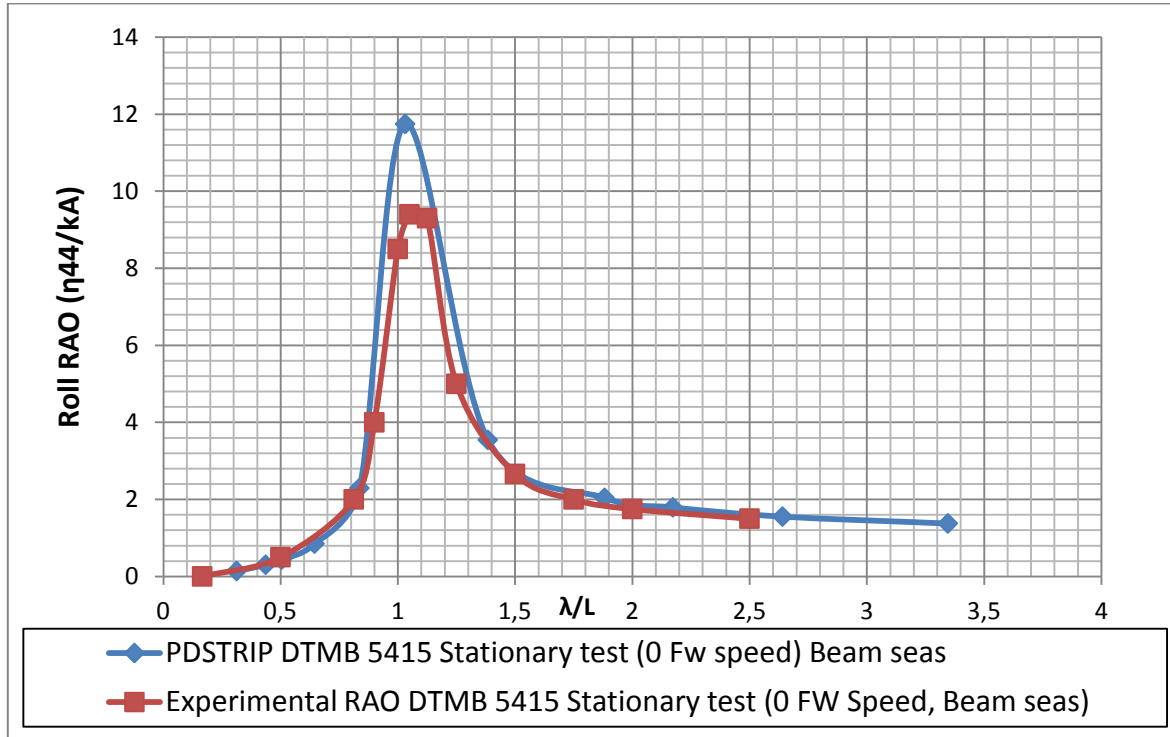


Figure 27: Roll RAO (η_{44}/kA) VS (λ/L) for the DTMB 5415 at 0 Forward speed & T=6.15 m PDStrip VS Experimental

Table 25: Table of Roll RAO VS λ/L for the DTMB 5415 :

DTMB 5415 Stationary test (0 Fw speed) Beam seas	
λ/L	Roll RAO
0,312821851	0,14
0,436746957	0,303
0,504954461	0,436
0,645082456	0,851
0,836502068	2,292
1,031518115	11,744
1,38382396	3,544
1,882129652	2,039
2,17318677	1,792
2,640686375	1,553
3,34600827	1,374

4.4.4.3. Evaluation Of the Damping Coefficient Using 2DRoll a Flume Software

The regression analysis based on the body plan shape contributed to a chosen roll damping ratio ($F_{hull} = 0.095$). This value was inserted as an input for the 2DRoll spring mass system calculation in addition to the ship characteristic and the sea conditions then the identical RAO obtained was plotted.

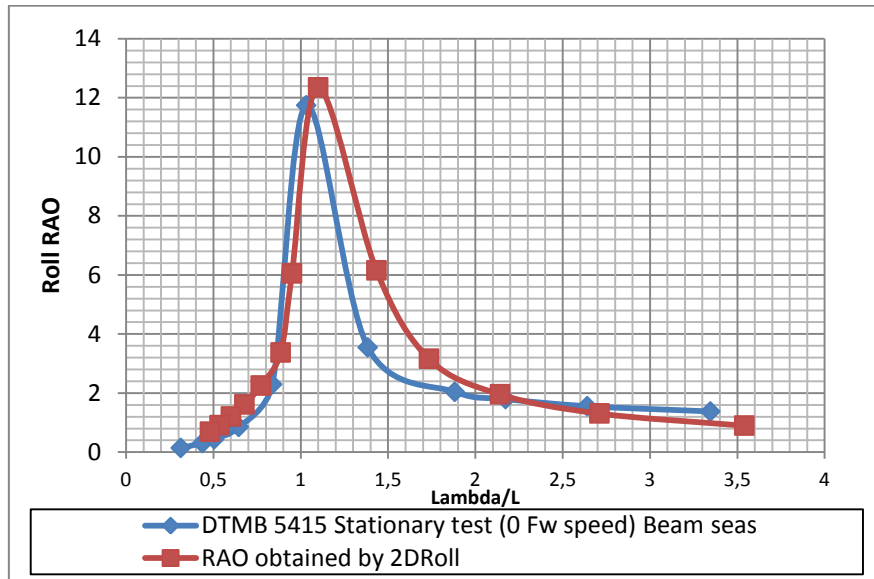


Figure 28: Roll RAO obtained by 2DRoll FLUME Software

Due to the obvious similarity of the obtained RAOs, the roll damping ratio chosen in this 2DRoll Calculation was valid and was then converted to a roll damping non dimensional coefficient $B_{44} = 0.0079$ which matches very well the average value of the nondimensional roll damping coefficient coming from the roll decay test.

4.4.4.4. Interpretation Of the Results:

Obviously, PDstrip estimated accurately the resonance frequency of the DTMB 5415 at ($\lambda/L=1$). The trend of the RAO is identical to the trend of the towing tank test RAO. It seems that the response at the resonance frequency is a bit overestimated by PDstrip compared to the experimental one. This fact could be due to the underestimation of the linear term of the bilge keel component. The gradient of the lift coefficient of the bilge keel which is a user defined parameter in the input file could not correspond to the real condition of the test. It is evident that PDstrip is a potential flow solver which is still unable to predict correctly the viscous damping component even with the corrections that account for the vortices generated on the keel and the bilge keel due to the sway and roll motion coupling.

In fact, the good choice of the so called resistance coefficients determines the accurate prediction of the viscous roll component.

Here, it is probably the case since the resistance coefficients in the input file were ($C_y=0.8$, $C_z=0.6$). It could be more useful to choose $C_y=1.2$ to account for the vortices generated in the sharp keel of the DTMB 5415 especially in the stem and stern as seen in the figure below.

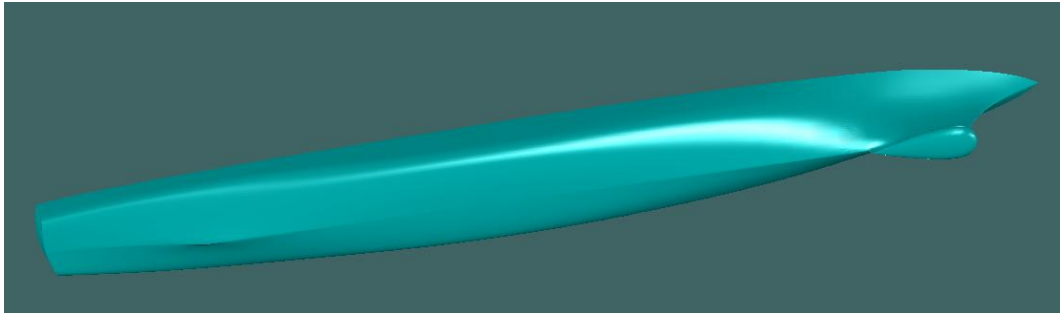


Figure 29: Shape of the bottom of the DTMB 5415

The eddy damping component is strongly dependant on the cross sectional area σ . The more σ is high the more the eddy component prevails in that area. In fact, high cross sectional area in a certain zone of a ship creates sharp corners in the high rake zones like bow and stern. It is the case in this ship, where the eddy damping component is generally considerable in these areas.

4.5.Comparative Analysis Of the Used Simulation Tools:

4.5.1. Comparison of the tools used for the 8000-9000 TEU Container Vessel:

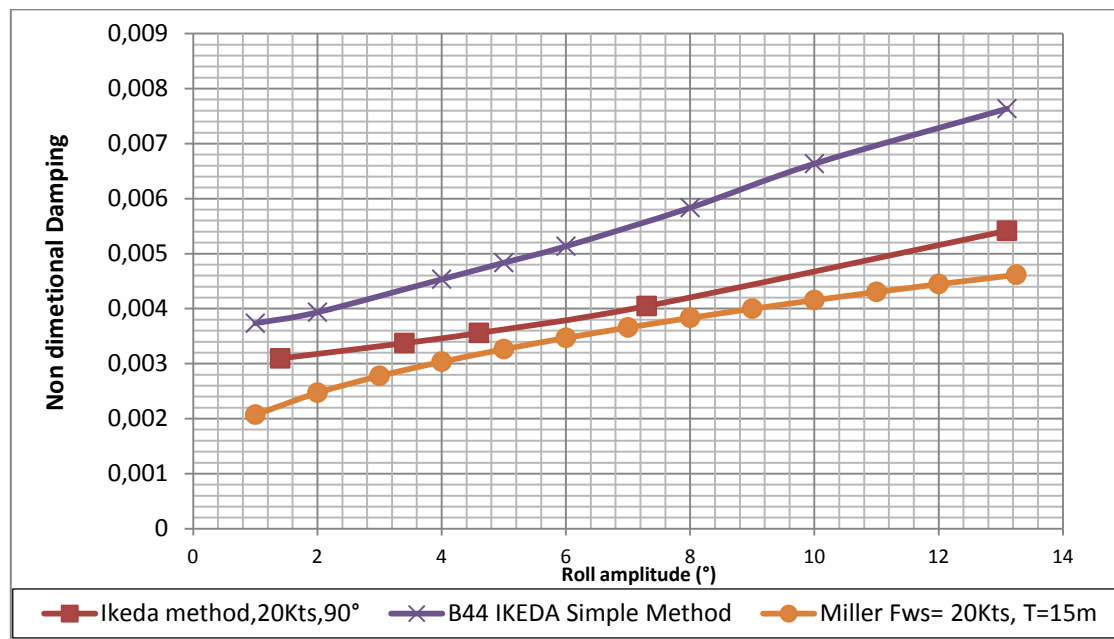


Figure 30: Comparison of the nondimensional roll damping coefficient obtained with the different numerical tools used for the 8000-9000 TEU Container ship: FwSpeed= 20Kts, GM=2.14m

As concluded earlier, both the results of the two Ikeda methods presented are in enough agreement with the experimental results. However, the difference between the two methods is obvious. We could have had even more difference if the wave component was derived from a potential flow solver for the original method and from the Ikeda proposed formula for the simple method. Therefore, we chose to equate the wave component for both of the methods to investigate the other reasons of discrepancy.

4.5.2. Comparison of the tools used for the 16000-18000 TEU Container Vessel:

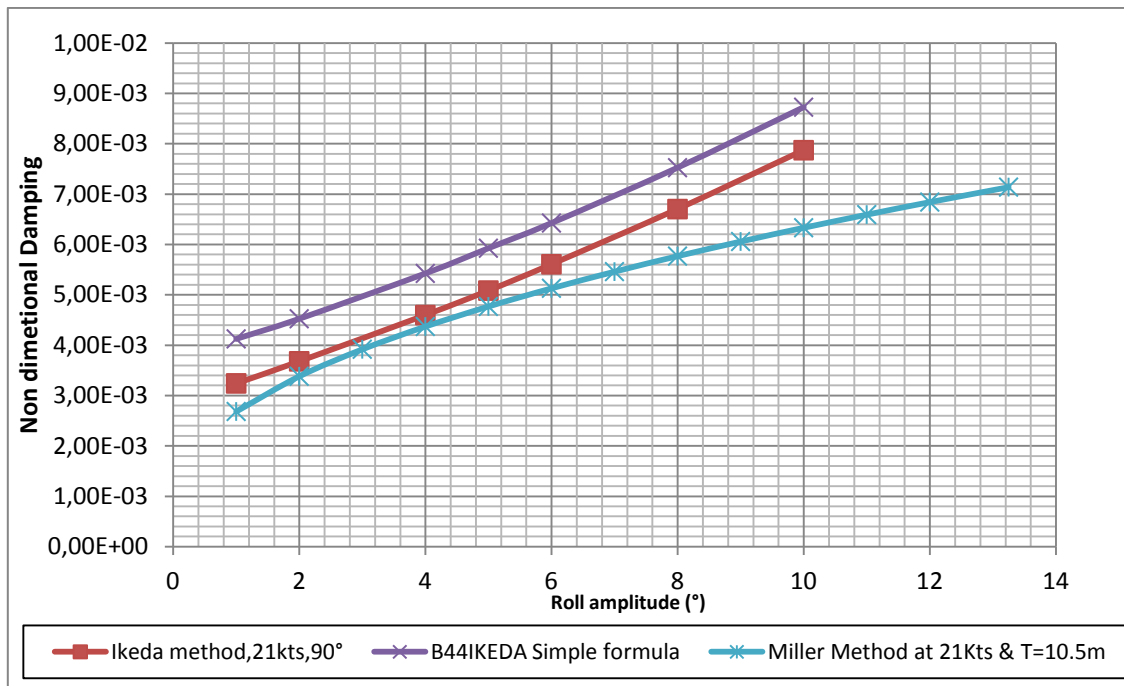


Figure 31: Comparison of the nondimensional roll damping coefficient obtained with the different numerical tools used for the 16000-18000 TEU Container ship: FWS= 21Kts, GM=2.9m

Similarly to the previous case, the same wave component is added to the damping obtained from both methods. The values of the damping coefficients obtained from both the methods are very close and the two curves almost follow the same slope.

4.5.3. Comparison of the tools used for the DTMB 5415:

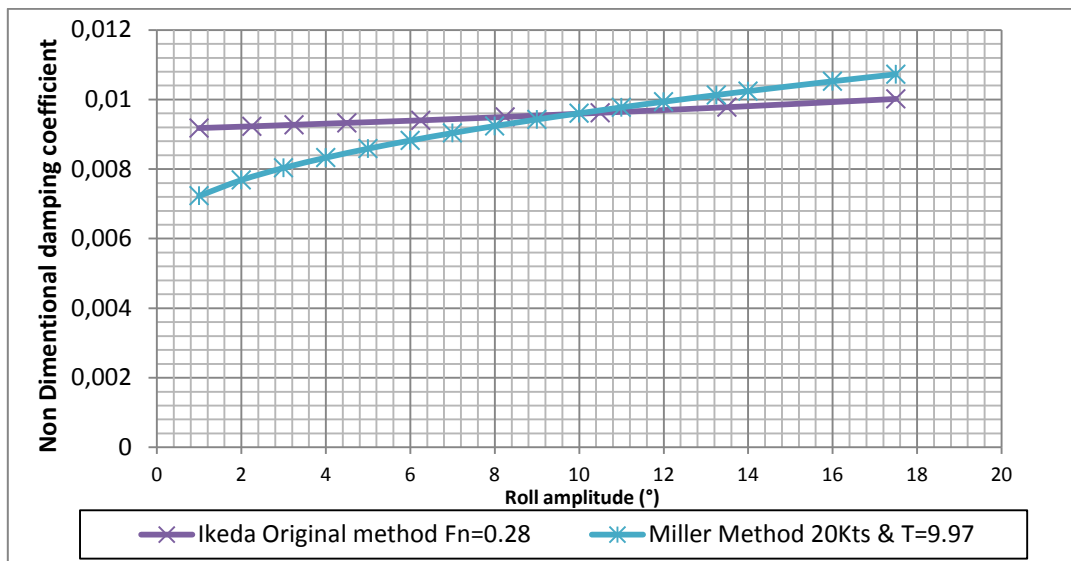


Figure 32: Comparison of the nondimensional roll damping coefficient obtained with the different numerical tools used for the 16000-18000 TEU Container ship: FW= 20Kts, T=2.9m

Both methods used in this test case are in good agreement and in the same range as the experimental results. Concerning Miller method the dependency to roll amplitude seems to be clear while the slope of the curve obtained by Ikeda program implemented based on Ikeda original method is low. Miller method is able to show more non linearity of the roll damping coefficient while the shape of the curve obtained by Ikeda original method confirms the fact that this method is based on linearized form of the roll damping coefficient.

5. CONCLUSION:

5.1. Summary:

This dissertation consists of testing and analysing different numerical and empirical roll prediction models that are supposed to be able to substitute the experimental decay or forced roll tests, at least in a preliminary design stage of the stabilisation equipments.

Among all the methods presented in the state of art, those that were well supported in the literature and that were converted into numerical programs have been chosen to be tested regarding their efficiency to assess all the damping components and to capture all the physical features related to them.

Any study that seeks to predict the roll damping coefficient of a ship should start with analysing the roll motion of the considered ship in the sea conditions that are judged critical. For this aim, the open source code PDstrip has been used to detect all the special behaviours, in different wave headings, of the three tested ships. PDStrip was very successful when it comes to detecting correctly the resonance zone of each ship. In addition, the RAOs obtained follow well the trend of the experimental RAOs. This makes it very easy and advantageous to combine PDStrip with the in house software of FLUME (2DRoll). However, in order to obtain an accurate value of the maximum response, it is necessary to insert all the user defined parameters correctly. In fact, the value of the RAO at resonance is affected mainly by the good estimation of the viscous and lift component and their nonlinearity.

Generally, both Ikeda methods results are closer to the roll decay test damping values. It is very likely to happen, because the formulas defining each damping component were the result of a regression analysis of roll decay experimental data base which is more abundant and less expensive than forced roll experiments. In the fourth section, it has been proven that the wave damping component at zero forward speed which is an input parameter for Ikeda program, can be obtained whether from the simple Ikeda formula of the wave damping or by integrating the wave damping component for each strip provided in the hydrodynamic components matrix in the section result output file of PDstrip. This shows a very useful complementarity between those different used methods. This complementarity could be a remedy for the limitation of each tool. It is also the case for the lift component missing in the simple formula of Ikeda and provided by the original Ikeda method.

Analysing the results of the DTMB 5415, confirmed the influence of the initial inclination angle on the slope of the curve $B_{44}=f(\text{wave amplitude})$. It showed, as well, that Ikeda methods are more suitable for similar slender ships while they show some discrepancy for full ships with buttock flow. The examination of the roll damping values given by Ikeda in the case of the DTMB 5415 in 20 kts forward speed proves the decrease of eddy damping

coefficient with the forward speed as it was predictable by the theory. The component analysis method allows examining every roll damping component separately and interpreting it according to the sea conditions. This fact, helps to better understand for which conditions and for which ships, this method is more suitable.

This work confirmed that the treatment of roll damping requires some more special considerations compared to analysing other degrees of freedom. Every discrepancy obtained is generally due to neglecting one of those considerations.

The reason of the small disagreement of the two Ikeda methods is that a high position of the center of gravity represents a limitation for the accuracy of the simple prediction formula proposed by IKEDA. In fact the center of gravity positions for 8000-9000 TEU vessel characterized by the ratio $\frac{D-K_G}{D} = -0.216$ is higher than the water line which is traduced by the negative sign of the $\frac{D-K_G}{D}$ ratio.

This limitation was highlighted by IKEDA et al when he presented the simple formulation method and the different approaches to predict each component separately.

IKEDA Compared his original method and the proposed simple one for a ship with the following particulars ($L/B=6.0$ $B/d=4.0$, $C_b=0.65$, $C_m=0.98$, $\phi_a=10^\circ$, $b_{BK}/B=0.025$ and $l_{BK}/L_{pp}=0.2$.) and he plotted the damping coefficient of this ship for two different positions of the center of gravity (OG denotes the distance between water surface and center of gravity, and defined plus when the center of gravity is below water surface $\overline{OG} = D - K_G$).

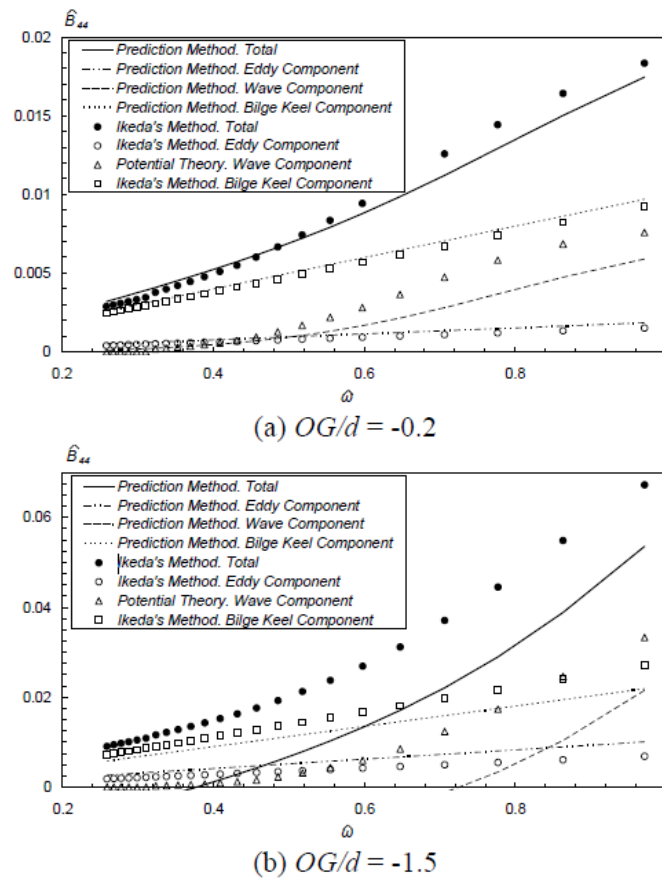


Figure 33: Comparison of Ikeda methods for different center of gravity positions.

This study elaborated by Ikeda confirms our previous conclusion and explanation. If we want to investigate which component is more sensitive to the position of the center of gravity, we can notice that the bilge keel component is more sensitive. In fact, the more the center of roll is higher, the more vortices are generated around the bilge keel.

In addition, the input of the simple method itself fixes a limitation for the OG/D distance inserted value to an interval of $[-1.5, 0.2]$ and this was the reason why the results of Ikeda simple method for the DTMB 5512 was not considered. In fact, the position of the center of gravity of the DTMB was out of this range $OG/D = 0.35$.

The difficulties encountered during the prediction of the roll damping are mainly the effect of the viscosity and the induced flow separations especially around the bilge keel. This effect associated to the dependency to ship forward speed and to the roll amplitude contributes to the non linearity of this damping coefficient.

5.2.Areas of Future Work:

During this study, it was noticeable that the nonlinearity of the obtained roll damping coefficients increases for large roll angles which led to deviation from the trend of the experimental results. Therefore, focusing on different tools that might be able to account for

this high non linearity and that might analyse the different phenomena leading to it, is required.

Moreover, it is important to investigate the reliability of URANS simulations when dealing with roll motion analysis and how far this method can match the expectation of industry regarding computational time and cost.

Due to the complexity of the bilge keel damping component and the interaction of this component with the eddy damping, the lift and the wave radiation effect, it is necessary to treat this part of the damping separately and multiply the effort to reach more accuracy during the evaluation of this term. Similarly, the rudder contribution to roll damping is very important and has to be incorporated separately in any method aiming the determination of roll damping.

This work has been elaborated in the frame of an industrial project supported by FLUME stabilization systems (Hoppe Marine) and seeking to develop its ability to predict roll damping and to broaden the database of FLUME with modern results in order to improve the regression analysis carried out during the design of the stabilisation equipments. After the complementarity of all the used models has been proved, it can be very useful to incorporate them in one single module of the FLUME Software.

6. ACKNOWLEDGEMENTS

First of all I would like to extend my gratitude to Mr Stefan Winkler, Sales Manager of FLUME Stabilization Systems, for being my mentor, for his encouragement and for providing me with the necessary research environment at Hoppe Marine. I would also like to thank Mr Alessandro Castagna, R&D engineer at Hoppe Marine for his patience and constant help. I am really grateful to every employee in Hoppe Marine, especially those who made me feel part of their team.

Professor Kornev has been my supervisor in University of Rostock and I appreciate his valuable guidance.

I would like to express my deep appreciation to Professor Bronsart for the warm welcome in the shipbuilding department of University of Rostock, for providing all the circumstances of a comfortable stay in Rostock.

I would also like to extend all my respect and recognition to Professor Rigo for his support and special care from the moment I took part of this master program until its achievement.

I would also like to recognize and express my appreciation to my family, to my friends and all those who have place in my heart (MDMV).

In particular, I would like to thank the following people for their specific contributions and support of this work:

Professor Lionel Gentaz, Professor Pierre-emmanuel guillerm and the entire hydrodynamic department team of Ecole Centrale de Nantes.

Professor Heinrich Söding and Dipl.-Ing. Sven Handschel from Fluid Dynamics and Ship Theory Department in Hamburg University of Technology (TUHH) for their warm welcome in their offices and their valuable guidance regarding PDstrip program.

This thesis was developed in the frame of the European Master Course in “Integrated Advanced Ship Design” named “EMSHIP” for “European Education in Advanced Ship Design”, Ref.:159652-1-2009-1-BE-ERAMUNDUS-EMMC.

7. REFERENCES:

- M. Irvine, J. Longo, and F. Stern, (August 2004), “*Towing-Tank Tests for Surface Combatant for Free Roll Decay and Coupled Pitch and Heave Motions*”, 25th Symposium on Naval Hydrodynamics.
- Yuki KAWAHARA, Kazuya MAEKAWA, Yoshiho IKEDA, (2010), “*A Simple Prediction Formula of Roll Damping of Conventional Cargo Ships on the Basis of Ikeda’s Method and Its Limitation*”
- Yoshiho Ikeda, Yoji Himeno and Norio Tanaka: (May 1978), Journal of the Society of Naval Architects of Japan. “*Component of Roll Damping of Ship at Forward Speed.*”
- Yoshiho Ikeda, Yoji Himeno and Norio Tanaka: (Nov. 1977). “*On Eddy Making Component of Roll Damping Force on Naked Hull*”. Journal of the Society of Naval Architects of Japan No.142. p.59-69
- Robert V. Wilson *, Pablo M. Carrica, Fred Stern, (July 2005). “*Unsteady RANS method for ship motions with application to roll for a surface combatant*”.
- Schmitke, R.T., (1978). “*Ship Sway, Roll and Yaw Motions in Oblique Seas*”. Transactions Society of Naval Arch and Marine Eng. 86.
- Subrata Chakrabarti, 2001, “*Empirical calculation of roll damping for ships and barges*”. Ocean Engineering, p915–932.
- Himeno, Y., 1981. “*Prediction of ship roll damping — state of the art*”. Report No. 239. Department of Naval Architecture and Marine Engineering. The University of Michigan, Ann Arbor, MI. September.
- BERTRAM, V.; SÖDING, H.; GRAF, K. (2006), “*PDSTRIP –A strip method for ship and yacht seakeeping*”, 9th Numerical Towing Tank Symp., Le Croisic
- BERTRAM, V. (2000), “*Practical Ship Hydrodynamics*”, Butterworth&Heinemann, Oxford
- ITTC – Recommended Procedures 7.5-02-07-04.5, (2011), “*Numerical Estimation of Roll Damping.*” Page 1 of 33.
- Ould el Moctar, Vladimir Shigunov & Tobias Zorn, (2012), “*Duisburg Test Case: Post-Panamax Container Ship for Benchmarking*”, p 55-56
- The Society of Naval Architects and Marine Engineers. “*Principles of Naval Architecture Second Revision. Volume III · Motions in Waves and Controllability.*”

8. APPENDIX

8.1.PDstrip Simulation for the 8000-9000 TEU Container Ship:

Input file:

```

0 t t f
9.81 1.025 15 -1e6 999.
1 35
8400geomet.out
f
141428 -2.7 0.0 18.15 250.77 6360.0625 6368.04 0.0 0.0 0.0

1 1 1 1 1
1 1 1 1 1
1 1 1 1 1
1 1 1 1 1
1 1 1 1 1
0 0 0 0 0

0 flow separation
0.1 4.0 wave steepness; max wave height
0.8 0.6 0.8 0.6 0.8 0.6 0.8 0.6 0.8 0.6
0.8 0.6 0.8 0.6 0.8 0.6 0.8 0.6 0.8 0.6
0.8 0.6 0.8 0.6 0.8 0.6 0.8 0.6 0.8 0.6
0.8 0.6 0.8 0.6 0.8 0.6 0.8 0.6 0.8 0.6
0.8 0.6 0.8 0.6 0.8 0.6 0.8 0.6 0.8 0.6
0.8 0.6 0.8 0.6 0.8 0.6 0.8 0.6 0.8 0.6
0.8 0.6 Cy Cz

2 fin
-33.15 21.3 2.0 0.95 0.0 0.05 0.0 0.0 0.0 0.0 0.0 0.0 0.6 101.08 0.1 0.155 1.2 0.6 20
-33.15 -21.3 2.0 0.95 0.0 0.05 0.0 0.0 0.0 0.0 0.0 0.0 0.6 101.08 0.1 0.155 1.2 0.6 20

0 sails

0 forces depending on motions
0.0 0.0 0.0 0.0 0.0 suspended weight
0 motion points

10
1540.95 833.13 684.86 385.23 246.55 171.216 125.79 96.309 85.31 76.096 wave
length

1
10.288 t 1 speed
0/

```

8.2.PDstrip simulation for the 16000-18000 TEU container Ship:***Input file:***

```

0 t t f
Containter ship 18000TEU August 2013
9.81 1.025 10.5 -1e6 999.
1 45
18000geomet.out

f
156737.672 -7.434 0.0 23.281 590.49 9594.2025 9594.2025 0.0 0.0 0.0

1 1 1 1 1
1 1 1 1 1
1 1 1 1 1
1 1 1 1 1
0 0 flow separation

0.1 7.6 wave steepness; max wave height
0.8 0.6 0.8 0.6 0.8 0.6 0.8 0.6 0.8 0.6
0.8 0.6 0.8 0.6 0.8 0.6 0.8 0.6 0.8 0.6
0.8 0.6 0.8 0.6 0.8 0.6 0.8 0.6 0.8 0.6
0.8 0.6 0.8 0.6 0.8 0.6 0.8 0.6 0.8 0.6
0.8 0.6 0.8 0.6 Cy Cz
4 fin
-80.575 28.154 1.908 0.95 0.0 0.05 0.0 0.0 0.0 0.0 0.0 0.0 0.8 41.52 0.1 0.01 1.2 0.6 20
-80.575 -28.154 1.908 0.95 0.0 0.05 0.0 0.0 0.0 0.0 0.0 0.0 0.8 41.52 0.1 0.01 1.2 0.6 20
28.067 28.154 1.908 0.95 0.0 0.05 0.0 0.0 0.0 0.0 0.0 0.0 0.8 41.52 0.1 0.01 1.2 0.6 20
28.067 -28.154 1.908 0.95 0.0 0.05 0.0 0.0 0.0 0.0 0.0 0.0 0.8 41.52 0.1 0.01 1.2 0.6 20

0 sails

0 forces depending on motions

0.0 0.0 0.0 0.0 0.0 suspended weight

0 motion points

13
1540.95 833.13 684.86 601.93 533.2 475.6 385.23 246.55 171.216 125.79 96.309 85.31
76.096 wave length

1
10.8024 t 1 speed

0/

```

8.3.PDstrip simulation for the DTMB 5415:**Input file:**

0 t t f

US Combattant DTMB5415 september 2013

9.81 1.025 6.15 -1e6 999.

1 90

DTMB5415geomet.out

f

8635.01 -0.752 0.0 7.56 48.052 1354.39 1354.39 0.0 0.0 0.0

0 0 0 0 0

0 0 0 0 0

0 0 0 0 0

0 0 0 0 0

0 0 flow separation

0.02 6.0 wave steepness; max wave height

0.8 0.6 0.8 0.6 0.8 0.6 0.8 0.6 0.8 0.6

0.8 0.6 0.8 0.6 0.8 0.6 0.8 0.6 0.8 0.6

0.8 0.6 0.8 0.6 0.8 0.6 0.8 0.6 0.8 0.6

0.8 0.6 0.8 0.6 0.8 0.6 0.8 0.6 0.8 0.6

0.8 0.6 0.8 0.6 Cy Cz

0 fin

0 sails

0 forces depending on motions

0.0 0.0 0.0 0.0 0.0 suspended weight

0 motion points

11

44.42 62.018 71.703 91.6017 118.783 146.47 196.503 267.26 308.592 374.977 475.133

wave length

1

0.0 t 1 speed

0/